DYE-SENSITIZATION OF SEMICONDUCTOR ELECTRODES IN ELECTROCHEMICAL PHOTOCELLS

Michio MATSUMURA
Faculty of Engineering Science
Osaka University
1979

Contents

Preface

The technology and manufacturing industry in the world have been developing with an ever increasing speed. Recently, however, people became conscious that the fossil fuel, i.e., petroleum, coal, etc., on which their civilization has depended, will be exhausted. Many alternative energy sources have been proposed and are being investigated, solar energy being one of them.

From far before the history of man, the plants on the land and algae in the sea have been utilizing the solar energy with the aid of their photosynthetic organs, producing chemical energy and oxygen. Man and animals have owed their activity to the products of the photosynthesis. The total amount of the solar energy incident on the earth is ca. 5.5×10^{24} J per year, which is greater than the total energy consumed in the world by a factor of 10,000. Solar energy is unexhaustible and can be used without polluting the environments. Therefore, it has been considered to be one of the most preferable energy sources.

On the other hand, the difficulty in the utilization of solar energy comes from the low energy density on the earth, ca. 1.4 kJ m^{-2} s^{-1}. Therefore, large area is necessary to get a sufficient amount of energy. For instance, in order to obtain electric power now consumed in Japan by use of the solid state solar cell with an efficiency of 10 %, the solar cell must be extended on the land as large as Kanagawa Pre-

fecture (2.4×10^{10} m^2). From the practical point of view, the development of low cost devices of the solar cell is one of the most important subjects.

The electrochemical solar cell has attracted attention in recent years, since it has the possibility of generating chemical energy, e.g. hydrogen, directly. In addition, the junction part of the photocell can be made relatively easily; the immersion of the semiconductor electrode in a solution usually causes an excellent junction. The potential profile at semiconductor/solution interface is analogous to that of semiconductor/metal interface. The photovoltaic effect in such cells arises essentially from the generation of electrons and holes in the illuminated semiconductor and their efficient separation by the built-in electric field inside the space charge layer of the semiconductor electrode.

The semiconductor electrode to be used in an electrochemical solar cell must satisfy the following requirements: (1) the electrode is resistible against corrosion and dissolution, (2) the energy of the band-gap is small enough ($<$ 2 eV) to absorb the solar light efficiently, etc. Very few systems have been known, which satisfy the above requirements.

The feasibility of dye-sensitization is one of the most interesting and important characteristics of the electrochemical photocells. The colorless semiconductors dipped in soluitons containing organic dyes, e.g. xanthene dyes, some-

times cause photocurrents under the visible light. By utilizing this effect, efficient solar cells are expected to be attained from large-band-gap semiconductors. The present thesis is on the study of dye-sensitization of electrochemical photocells.

The fundamental properties of the dye-sensitization effect on the semiconductor electrodes will be reviewed in chapter 1. Chapters 2 to 5 give results of the study on some fundamental mechanisms of the dye-sensitized photocurrent, i.e., decay of the photocurrent during the illumination (chapter 2), relation between the dye adsorption and the photocurrent (chapter 3), effect of the surface treatment of the electrode on the photocurrent (chapter 4), and effect of chelating dyes on the photocurrent (chapter 5). In the last chapter the application of the dye-sensitized photocurrent to the photocell system will be described.

The dye-sensitization is interesting in relation to the photosynthesis in plants. The effect of the sensitizing dye on semiconductors can be compared with that of chlorophyll. The elucidation of the dye-sensitized photocell, therefore, will give us important suggestions to the understanding of the mechanisms of the photosynthesis, e.g., energy transfer in the antenna chlorophyll, electron-transport steps, etc. The dye-sensitization effect is related with other brances of science such as photochemistry, surface chemistry,

heterogeneous catalysis, electrochemistry, and electrophotography. It is hoped that the present work may contribute to clarify such variety of scientific and technological problems.

CHAPTER 1

Fundamental Properties of the Dye-sensitization Effect on the Semiconductor Photo-electrodes.

Introduction

The photovoltages arising from the interfaces between semiconductors and aqueous solutions have been studied in detail by many authors, and the origin of the photovoltage has been fairly well understood.[1-3] The spectral sensitization of the photocurrents by dyes has also been studied by some groups.[4-8] In most cases of the semiconductors studied to date, the photocurrent is accompanied by chemical reactions involving the electrode material. In the case of n-type semiconductors, such as zinc oxide and cadmium sulfide, the reaction is the anodic dissolution of the metal ion into an aqueous solution. In the case of gallium phosphide, silicon and germanium, the reaction is oxide formation. These reactions cause either material loss at the electrode or the formation of an opaque or insulating layer on the surface of the electrode; these effects are obviously undesirable for solar energy conversion.

Fujishima and Honda[9] reported in 1972 that n-type

titanium oxide (TiO_2) single crystals show a photovoltaic effect in aqueous solution without experiencing such corroding reactions; instead they cause decomposition of water into hydrogen and oxygen. Recently, this phenomenon has received much attention as the basis for a system to convert solar energy directly into storable fuels.

However, the efficiency of energy conversion of TiO_2 photocell is very small, due to the position of the flat band potential of TiO_2 relative to the reduction potential of water.[10] The flat band potential means the potential at which the potential gradient in the semiconductor electrode disappears, agreeing nearly with the lower limit of the conduction band at the surface. The use of TiO_2 semiconductor has another disadvantage in that its sensitive spectral region lies mainly at short wavelengths ($\lambda < 400$ nm). As the solar energy in this region is only 4 % of the total, no better efficiency than 4 % can be expected even if no further losses occur.

One direction to improve the properties of the photoelectrochemical cell is to use sensitizing dyes for expanding the spectral responses of the semiconductor electrodes into the visible region. In this chapter, the fundamental properties of the dye-sensitization effect on the semidonductor electrodes will be reviewed from our preliminary experiments.

Experimental

The electrode materials used were single crystal of titanium dioxide (rutile) purchased from Nakazumi Crystal Co., and zinc oxide (ZnO) sinter. Most specimens for the latter were donated by Matsushita Electric Industries Co.

The crystal of TiO_2 were polished with silicon carbide and alumina, and etched in hydrochloric acid; they were then thermally treated in vacuum to render them n-type. One of the surfaces of each of the specimens was indium-coated by vacuum evaporation in order to provide an ohmic contact and a copper wire was attached with silver paste. Finally, all surfaces except the one which faces the solution were covered with epoxy resin to prevent their contact with the solution (Fig. 1). In the case of ZnO, the sintered specimens show n-type characteristics, and the procedure to make the electrode was the same as that of TiO_2.

As a general experimental set-up, the electrode was placed in a glass cell having a flat plate window and the cell filled with an electrolyte solution. In all experiments a platinum counter electrode was used. The potential of the semiconductor electrode was controlled by use of a Hokutodenko potentiostat against the saturated calomel electrode (SCE). The light sources used were a 500 W high pressure Xe lamp combined with a small monochromator, and a 500 W high pressure Hg lamp.

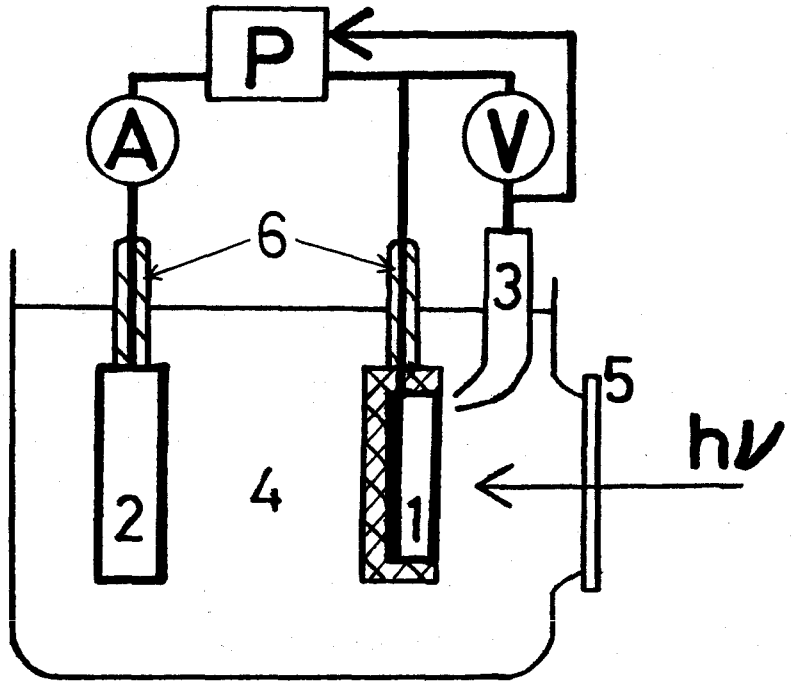

Fig. 1 Schematic diagram of the photocell: 1, semiconductor electrode; 2, Pt electrode; 3, saturated calomel electrode; 4, electrolyte solution; 5, quartz window; 6, glass rods; V, voltmeter; P, potentiostat.

Results and Discussion

The Mechanism of the Dye-sensitized Photocurrent.

When an organic dye is dissolved in an aqueous electrolyte solution of a wet photo-cell (Fig. 1), a photocurrent is generated by illumination in the region of the absorption spectra of the dye as well as in the region of semiconductor absorption. Fig. 2 gives, as an example, the photocurrent action spectrum of a < zinc oxide|aq. electrolyte|platinum > photocell, with rose bengal as a sensitizer. It can be seen that the photocurrent action spectrum is quite similar to the absorption spectrum of the dye, except for a slight shift to longer wavelengths. The significance of this shift will be discussed later.

There are two theories concerning the origin of the dye-sensitized photocurrent. They are (1) the electron transfer mechanism and (2) the energy transfer mechanism. When an n-type electrode is anodically biased (i.e. sufficient positive potential is applied to the electrode so that an anodic photocurrent will flow), the electronic energy band of the semiconductor is bent near the surface as shown in Fig. 3. In the first of the two mechanisms, the electron in the dye is photo-excited from the ground state to the first singlet (or triplet) excited state. It is then transferred into the conduction band of the semiconductor and moves into the interior under the influence of the electric field in the space

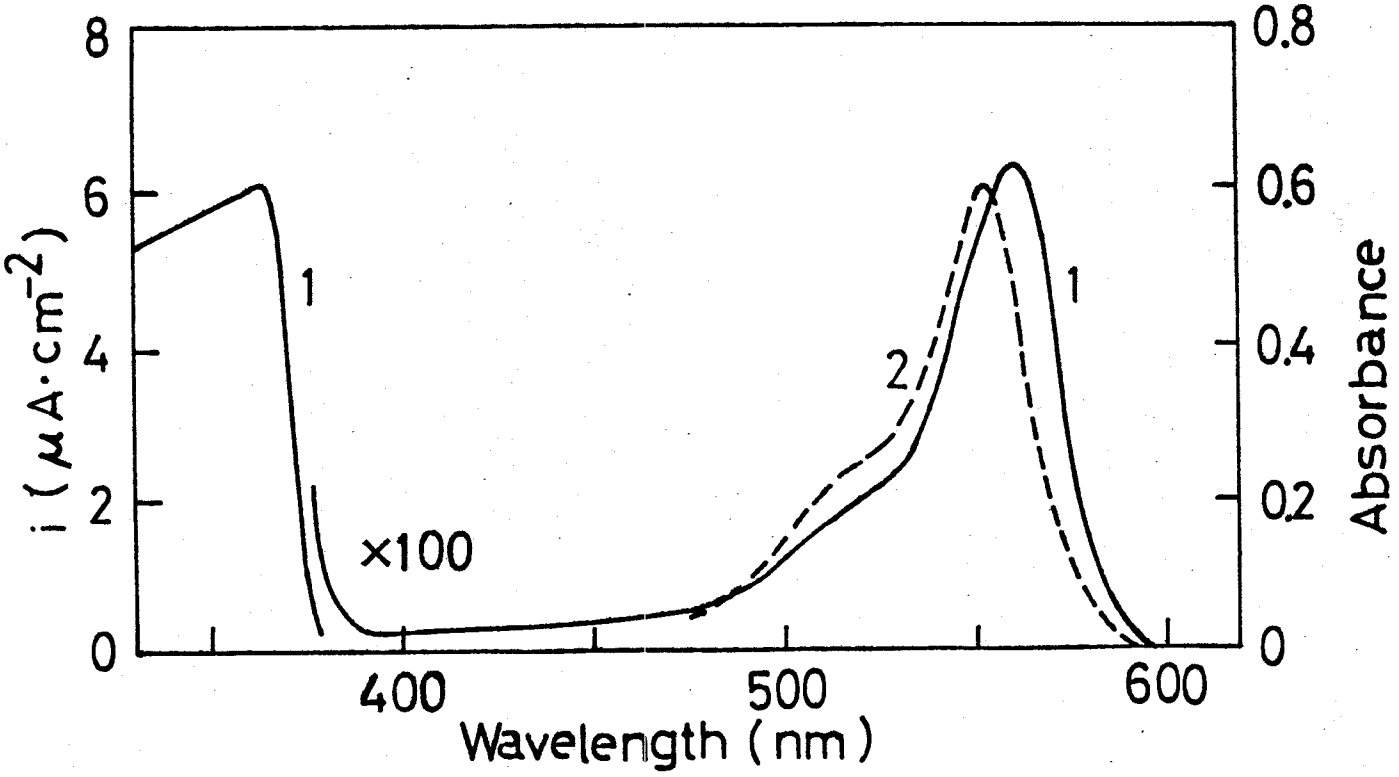

Fig. 2 Curve (1) is the photocurrent action spectrum of <ZnO|rose bengal| Pt> in a solution of 2.4 x 10^{-6} mol/l rose bengal and 0.2 mol/l Na_2SO_4 at an anodic bias of 0.5 V (vs. SCE), for the illumination by 4.7 x 10^{14} photons/cm^2 s. Curve (2) is the absorption spectrum of the dye obtained from 6 x 10^{-6} mol/l aqueous solution.

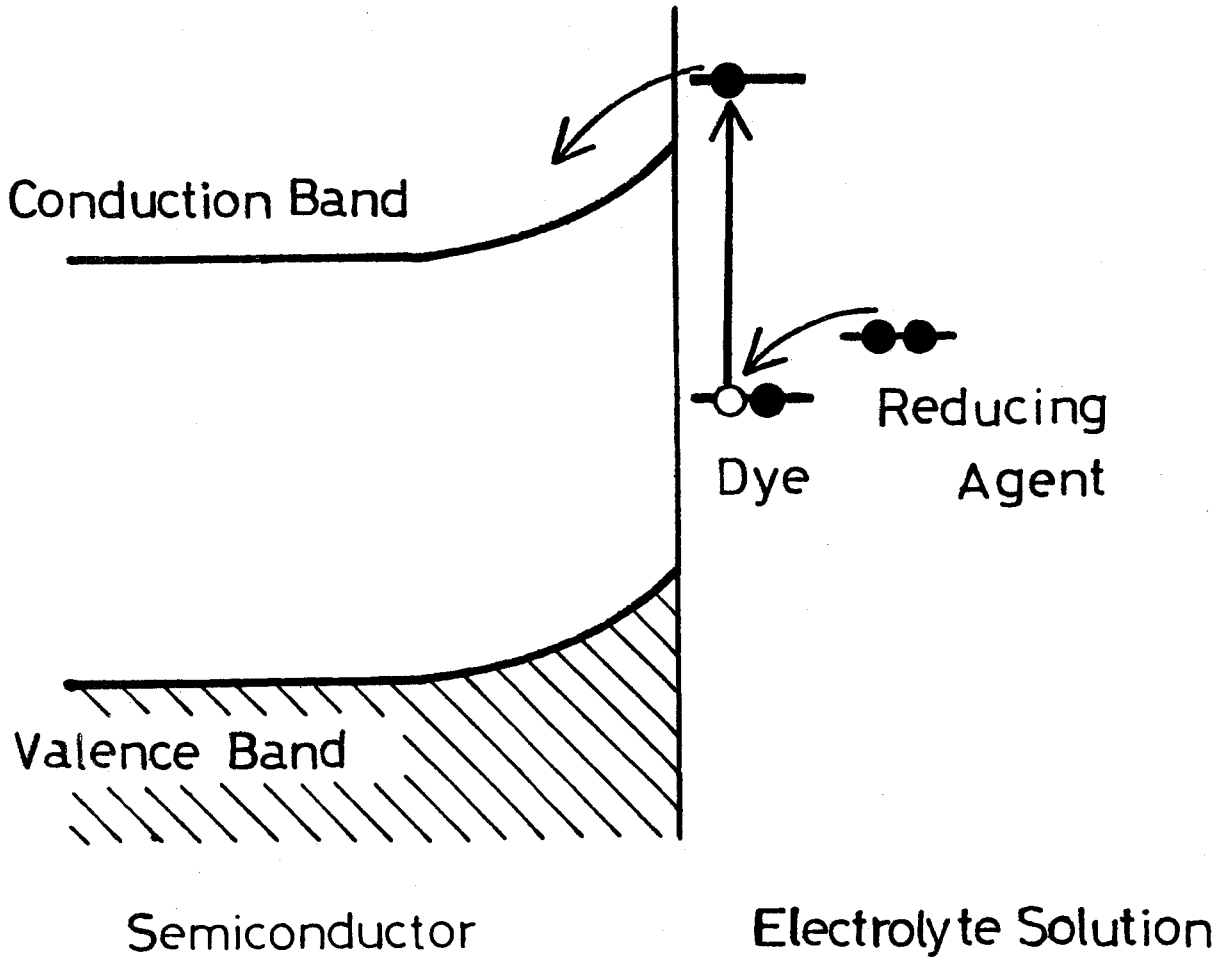

Fig. 3 Electron transfer mechanism of dye-sensitized anodic photocurrent at the solid-liquid interface.

charge layer. In this mechanism, the energy of the excited state of the dye must be higher than the energy of the conduction band of the semiconductor.

The second mechanism, the energy transfer mechanism, implies that the energy of the excited dye is transferred to the semiconductor, exciting electrons from some "impurity" levels (associated with defects near the surface of the semiconductor) to the conduction band. The electron flows into the interior as before. The electron in the dye, or other species in the solution, is transferred into the hole thus created. In this mechanism, the sole requirement is that the excitation energy of the dye be higher than the energy difference between the bottom of the conduction band and the "impurity" level.

The correlation between the energy levels of the semiconductor conduction bands and those of the excited states of the dyes is graphically shown in Fig. 4, using available data on work functions and excitation energies of semiconductors and crystalline dyes, together with the presence or absence of the photocurrents of the photo-cells <semiconductor|aq. electrolyte-dye solution|Pt> at sufficiently high anodic bias.

The results show that the photocurrent flows when the excited state of the dye is high (rhodamine B), but does not flow when it is low (crystal violet and others). The energies

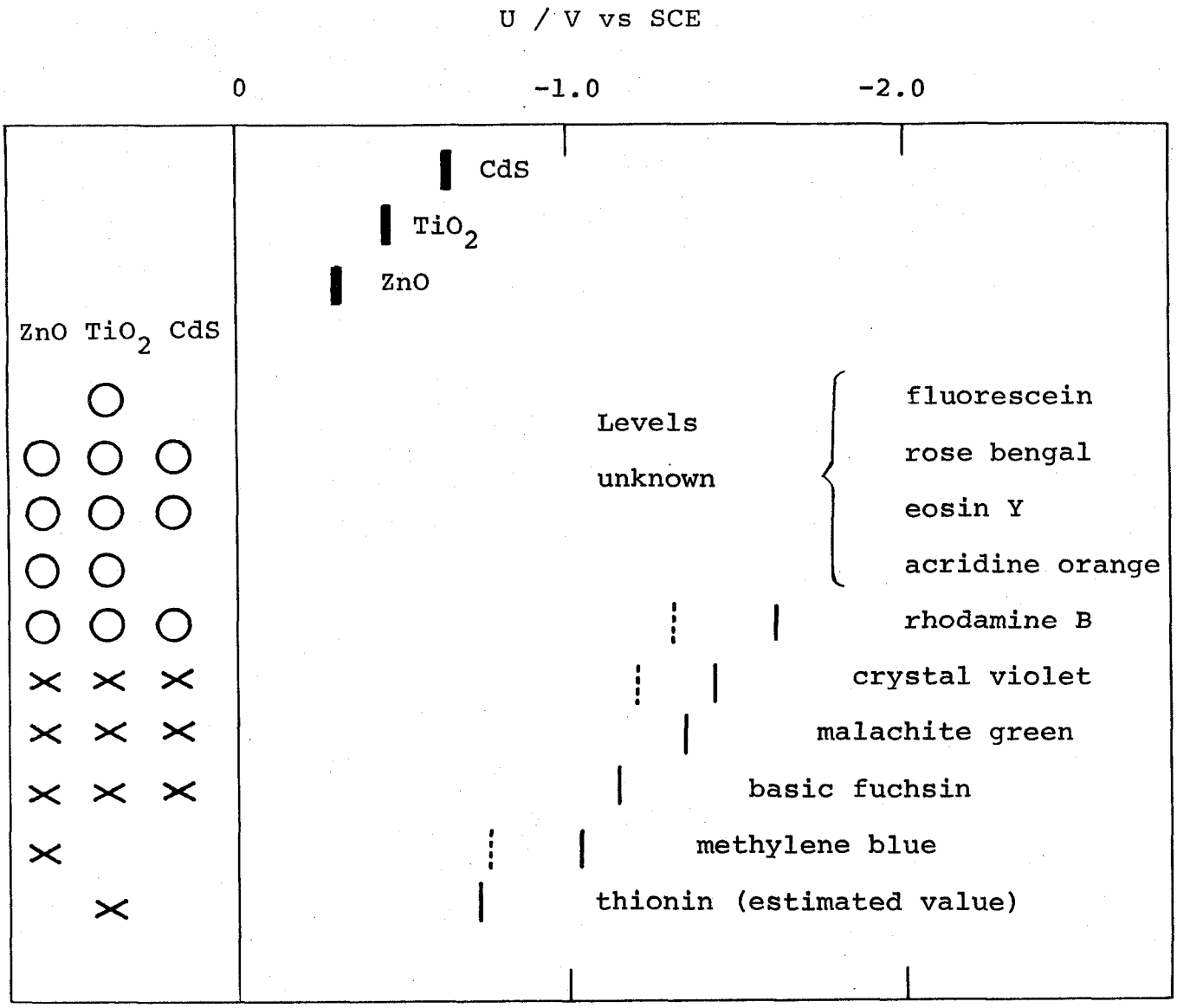

Fig. 4 The currelation between the energy levels of the semiconductors and dyes, and the presence (○) and absence (x) of the dye-sensitized photocurrent. ▬ Conduction band of the semiconductor. —— Singlet excited state of the dye. ---- Triplet excited state of the dye.

of fluorescein, rose bengal, and eosin Y are not known, but they could be fairly high, because all of them are anions, and the onset potentials for their anodic reactions with applied voltage in the dark are more negative than that of rhodamine B. This result supports the electron transfer mechanism rather than the energy transfer mechanism. A similar opinion was expressed by Fujishima et al.[11)]

It has been tacitly assumed by many authors so far that the dye-sensitized photocurrent is caused by the dye adsorbed on the electrode and not by that dissolved in solution. However, there has been no strong evidence for this. We can pick up the following three facts as such evidence from our experimental results.

1. The shift of the action spectrum for the photocurrent from the absorption spectrum of the solution, as shown in Fig. 2, indicates that the photocurrent is caused mainly by the dye adsorbed on the electrode.

2. From the photocurrent observed by use of the ZnO electrode and an aqueous solution of 6.7×10^{-7} M rose bengal, the apparent quantum efficiency of the photocurrent, η_{app}, defined as the number of electrons transferred divided by the number of incident photons, can be calculated to be 1.8 %, which means that at leaset 1.8 % of the photons are absorbed by the dye. If the photocurrent is assumed to be caused only by the dye in the bulk of the solution, 3 mm of the light path length

in the solution is required to make the absorption factor of the light 1.8 % at λ = 562 nm. However, the same photocurrent was observed with a light path length of 0.2 mm or shorter. This result indecates that the contribution of the dye in the solution is small or negligible.

3. The photocurrent indicates the tendency of saturation at a relatively low concentration of the dye, i.e., 5×10^{-6} M. It would be difficult to explain this by attributing the photocurrent to the dissolved dye. From our preliminary experiments, the adsorption isotherm of the dye adsorbed on the electrode surface has been found to be saturated at about the same low dye concentration as above.

4. When ZnO electrodes were dipped into dye solutions for some length of time, taken out from the solution, washed with water and dipped into an electrolyte solution not containing the dye, photocurrents of nearly the same intensity were observed as those in the dye solutions for the first few seconds.

On the basis of the conclusion that the photocurrent is caused by the dye adsorbed on the electrode, a high efficiency of the photocurrent is expected to be obtained by use of an electrode with large specific surface area. This will be discussed later.

Dependence of the Photocurrent on Time and the Effect of "Supersensitizers".

It has been reported by many authors[4,5,12] that the dye-

sensitized photocurrent in a ⟨semiconductor|aq. solution|Pt⟩ photo-cell is enhanced if a reducing agent such as hydroquinone or allylthiourea is added in the solution. This effect is often called super-sensitization by analogy to similar phenomena in photographic sensitization. Although these papers attribute the effect of the reducing agents or super-sensitizers to supplying electrons to the dye which has lost electrons by transfer to the electrode as illustrated in Fig. 3, explanation of the details of the action of these super-sensitizers remains controversial.

Figure 5 shows some of our results of the effect of N, N, N', N'-tetramethyl-p-phenylenediamine (TMPD) and hydroquinone (HQ) on the photocurrent in ZnO photo-cells sensitized by rose bengal. The dye-sensitized photocurrent generally decays with time as shown by curves 1 and 1' until they become nearly time independent. The decay is faster, the more intense the light. We explain this phenomenon by assuming that the exchange of photo-oxidized dye (D^+) on the surface with the neutral dye (D) in the solution is fairly slow and, therefore, during the first few seconds a considerable amount of the dye ions adsorbed on the surface are photo-oxidized. Consequently, the rate of D^+-D exchange or electron supply from outside is in equilibrium with photo-oxidation. Curves 2 and 2' show that the photocurrent decay is suppressed by addition of TMPD to the solution. This indicates that the TMPD molecules near the surface supply elec-

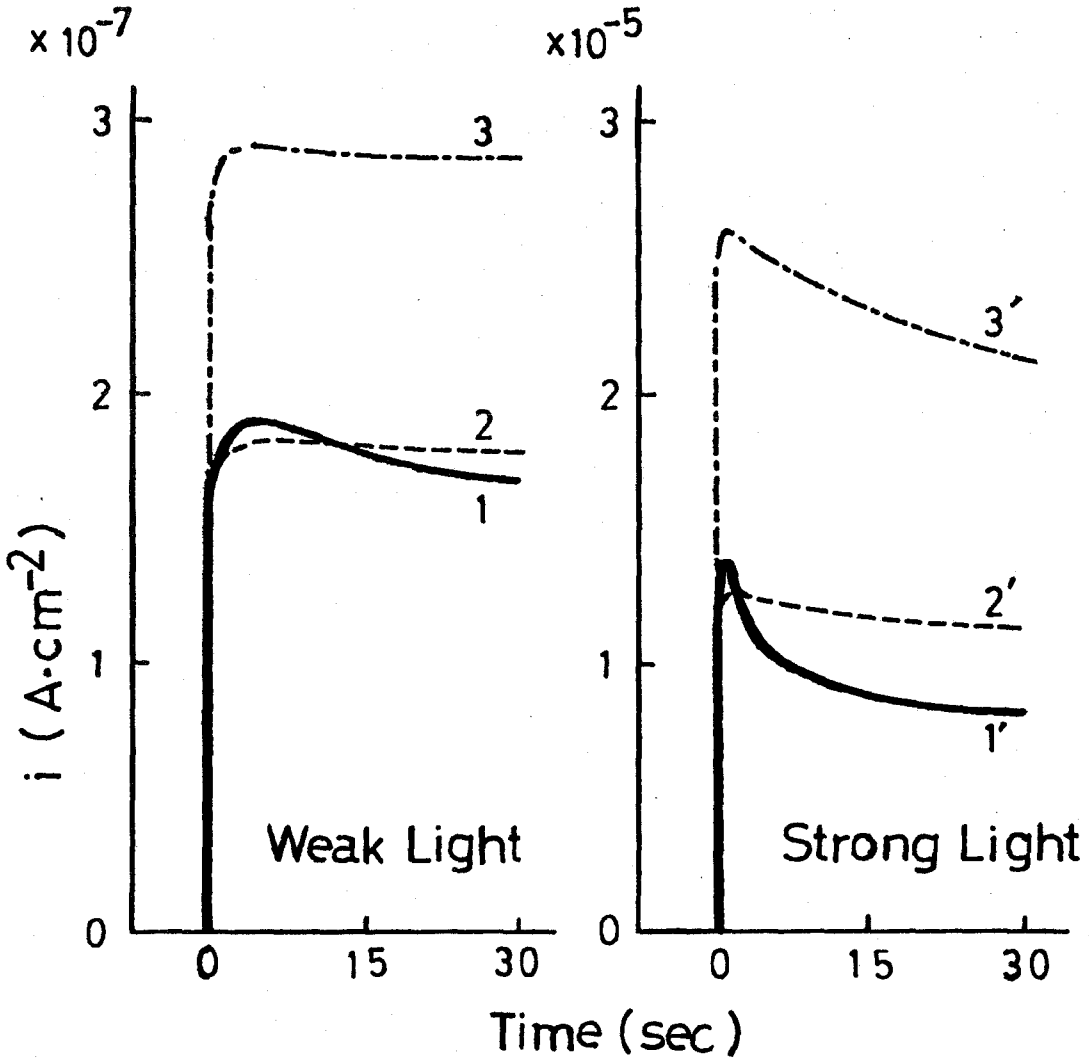

Fig. 5 The change of photocurrents with time for ⟨ZnO | rose bengal - reducing agent | Pt⟩. 1, Without any reducing agent; 2, with TMPD (6×10^{-4} mol/l); 3, with hydroquinone (6×10^{-4} mol/l). Rose bengal, 2.7×10^{-5} mol/l; Na_2SO_4, 0.2 mol/l; electrode potential, 0.2 V (vs SCE).

trons to the oxidized dye ions. In the time independent state, the current is controlled either by the rate of exchange of D^+ and D in the absence of TMPD, or by the rate of diffusion of TMPD in the presence of it. (The concentration of TMPD is much higher than that of the dye.)

When the platinum counter electrode was separated from the semiconductor electrode by a salt bridge, the electrical equivalent of the $TMPD^+$ cation (as indicated by its absorption spectrum) appeared in the solution as shown in Table 1. This result also shows that TMPD plays the role of electron supplier. Actually, this ion is formed to a small degree by irradiating the solution at the same wavelength with the circuit open. The amount of $TMPD^+$ formed under short-circuit conditions reduced by the amount formed with the circuit open agreed with the electrical charge flowing in the cell. The $TMPD^+$ cation is known as a very stable ion.

In the case where hydroquinone is added into the solution, the decay of the photocurrent is also suppressed as shown by curves 3 and 3' in Fig. 5. This effect of hydroquinone can be explained by a similar electron supply mechanism as in TMPD. The magnitude of the effect of the "super-sensitizer" on the photocurrent changes with time and with the light intensity. Sufficient attention was not devoted to this situation by previous investigators.

When the $\langle$ ZnO|aq. electrolyte-rose bengal|Pt $\rangle$ cell was

Table 1. The relation between the quantity of electricity flowing into the electrode and the quantity of $TMPD^+$ produced.

	Quantity of electricity (Faraday)	Quantity of $TMPD^+$ (Equivalent)
(a) Closed circuit	2.28×10^{-7}	3.50×10^{-7}
(b) Open circuit	0	1.29×10^{-7}
(a) - (b)	2.28×10^{-7}	2.21×10^{-7}

Illuminated by a 500 W Hg lamp with a glass filter(VO52) for 6 minutes. Rose bengal, 2.7×10^{-5} mol/l; TMPD, 7×10^{-4} mol/l; electrode potential, 0.25 V (vs. SCE).

under strong and prolonged illumination at short circuit, the photocurrent kept decreasing slowly with time, the surface of the ZnO electrode became colored, and the concentration of the dye in the solution diminished. The color was not removed by washing with water, showing that the dye photo-oxidized on the electrode surface caused an irreversible chemical change. No coloration occurred when the electrode was illuminated at open circuit, or when the electrode was illuminated under short circuit conditions in the presence of hydroquinone or other reducing agents. These results confirm the proposed explanation.

The enhancement of the photocurrent from t = 0 observed for the case of hydroquinone (Fig. 5) will be discussed in chapter 4, and the decay characteristics of the photocurrent will be discussed in next chapter in detail.

The stability of the ZnO electrode of the 〈 ZnO | rose bengal + hydroquinone (pH 6.8) | Pt 〉 photocell was examined by analyzing the concentration of zinc ion in solutions after prolonged illumination by atomic absorption analysis. From the results, it was found that in the case of the dye-sensitized photocurrent the photo-anodic dissolution of the electrode was trivial, whereas the electrode was dissolved considerably by the band-gap excitation of the ZnO electrode.

Photocurrent Efficiencies of Various Cells.

In Table 2, the data obtained for various types of photocells are given. In all cases, monochromatic light whose wavelength was near the peak of the dye absorption spectrum in solution was used. The photocurrents were measured at sufficiently high anodic biases. The above defined apparent quantum efficiency, η_{app}, can be expressed as

$$\eta_{app} = n_e/n_{ph}$$

where n_e and n_{ph} are the flow rates of the electrons and photons across the electrode, respectively. Further, η_o is defined as the electron flow rate n_e divided by the number of photons absorbed by the dye per second, n°_{ph}.

$$\eta_o = n_e/n^\circ_{ph}$$

Therefore,

$$\eta_{app} = \eta_o \cdot a$$

where a is the optical absorptivity of the dye adsorbed on the surface.

The data for column 3 were obtained for a ZnO electrode coated with a thin layer of eosin Y. In this case, an ethanol solution of eosin Y was sprayed on the surface of the electrode and the ethanol was allowed to evaporate. Then the electrode was immersed into 1,2-dichloroethane solution which did not dissolve the dye. The absorbance of the dye layer could be obtained by measuring the absorbance of the glass plate coated by the same dye using the same spraying procedure. The η_o

calculated in this way amounts to ca. 30 % which should represent roughly the probability of electron transfer from the excited dye to the semiconductor.

The η_{app} in column 1 which is for the dye solution and that in column 3 which is for the dye applied on the surface are both of the order of a few percent. These results suggest strongly that these low values are caused mostly by the weak absorptivity of the dye layer on the surface of the semiconductor. This suggested that the cell performance could be improved by applying thicker dye films. Therefore, we investigated the effect of dye film thickness on the photocurrent efficiency in systems similar to those described in column 3 of Table 1.

The results obtained showed that the efficiency η_{app} reaches a maximum of 0.05 at a very weak absorbance of the dye film (ca. 0.10). On the other hand, the η_o value decreased monotonically with the film thickness. These results can be explained by taking account of either an increase of the quenching processes for the dye excited state or the increase of the insulating effect of the dye film with the film thickness.

In the course of our work, we found that the ZnO disks sintered in our laboratory using ZnO powder from our stock showed a strong adsorptivity toward rose bengal and other xanthene dyes. When such sintered disks of ZnO were used as electrodes, a strikingly high photocurrent efficiency (η_{app}) was obtained.[13] A typical set of results is given in column 2 of Table 1. All

Table 2. Efficiencies of dye-sensitized ⟨semiconductor|solution|Pt⟩ Photo-cells.

semiconductor	ZnO	ZnO	ZnO	TiO_2
solvent	H_2O	H_2O	$C_2H_4Cl_2$	H_2O
supporting electrolyte	0.2 M Na_2SO_4	0.2 M Na_2SO_4	0.1 M Bu_4NClO_4	0.2 M Na_2SO_4
dye	rose bengal 3×10^{-5} M	rose bengal adsorbed	eosin Y applied on surface	eosin Y 7.8×10^{-5} M
reducing agent	none	hydroquinone	none	none
light intensity, mW/cm^2	0.74	0.47	0.13	0.40
wavelength, nm	568	563	530	538
obsd. photocurrent, $\mu A/cm^2$	3.3	41	1.9	0.0084
applied potential, vs. SCE	0.5 V	0.5 V	0.5 V	0.5 V
current efficiency η_{app}	0.010	0.19	0.035	0.000048
η_o			0.32	

other results described in this chapter have been obtained by use of well sintered ZnO prepared by Matsushita Electric Industries Co., Ltd. The difference between these two sintered ZnO specimens seems to be associated with differences in porosity. The reason for this difference in porosity and the improvement of the electrode will be discussed in chapter 6.

In the case of TiO_2 crystal, the dye-sensitized photocurrent was much smaller than in the case of sintered ZnO. One of the reasons for this difference is the low adsorptivity of dyes on the surface of the TiO_2 crystal. When its surface was abraded, the photocurrent was increased, but it was never as high as in the ZnO cells.

References

1) R. Williams, J. Chem. Phys., 32, 1505 (1960).

2) H. Gerischer, J. Electrochem. Soc., 113, 1174 (1966). Ber. Bunsenges. phys. Chem., 77, 771 (1973). Electroanal. Chem. Interfac. Electrochem., 58, 263 (1975).

3) S. R. Morrison and T. Freund, J. Chem. Phys., 47, 1543 (1967).

4) H. Tributsch and H. Gerischer, Ber. Bunsenges. phys. Chem., 73, 251, 850 (1969). H. Gerischer, Photochem. Photobiol., 16, 243 (1972).

5) R. Memming, Photochem. Photobiol., 16, 325 (1972). R. Memming and H. Tributsch, J. Phys. Chem., 75, 562 (1971).

6) H. Tributsch, Photochem. Photobiol., 16, 261 (1972).

7) K. Hauffe et al., J. Electrochem. Soc., 117, 993 (1970). Discussions Faraday Soc., 58, 281 (1974).

8) T. Watanabe et al., Bull. Chem. Soc. Japan, 49, 8 (1976). A. Fujishima et al., Chem. Lett., 1975, 13

9) A. Fujishima and K. Honda, Nature, 238, 37 (1972). A. Fujishima et al., Bull. Chem. Soc. Japan, 48, 1041 (1975); J. Electrochem. Soc., 122, 1487 (1975).

10) T. Ohnishi et al., Ber. Bunsenges. phys. Chem., 79, 524 (1975).

11) A. Fujishima, E. Hayashitani, and K. Honda, Seisan Kenkyu, 23, 31, 363 (1971).

12) H. Gerischer and H. Tributsch, Ber. Bunsenges. phys. Chem., 72, 437 (1968). H. Tributsch and M. Calvin, Photochem. Photobiol., 14, 95 (1971).

13) Part of the results has been reported in H. Tsubomura et al. Nature, 261, 402 (1976).

CHAPTER 2

Decay Characteristics and Quantum Efficiency of Dye-sensitized Photocurrents in Zinc Oxide Electrodes

Introduction

In chapter 1, it has been concluded that the electron injection is the most likely process for the origin of the dye-sensitization effect on the n-type semiconductor electrode. The photocurrent decays during the illumination, as the consequence of photo-oxidation of the dye on the electrode. The prevention of the photo-oxidized dye from the deterioration is indispensable for the application of the dye-sensitized photocurrent to the solar cell system.

In this chapter, the effect of reducing agents on the photocurrent will be discussed. The reducing agent supplies electrons to the photo-oxidized dye, the oxidized form of the reducing agent in turn accepts electrons from the counter electrode. The quantum efficiency of the photocurrent is also determined from the analysis of the decay curves of the photocurrent. In order to construct an efficient photocell, it is essential to deepen our knowledge on such problems.

Experimental

Zinc oxide sinter disks were used as the electrodes. They were prepared by moulding zinc oxide powder by compression and heating at 1300 °C in the air for 1 h. It was found that the adsorptive activity of the zinc oxide sinter for the dye depends on the source of the zinc oxide powder. In the following experiments, we made the sinter out of zinc oxide powder obtained from Kanto Chemical Co. without any purification or pre-treatment. The sinter had low adsorptive activity but gave a reproducible photocurrent. The density of the sinter is almost equal to that of a single crystal. The scanning electron micrograph shows a very compact array of crystalline grains and no visible pore (Fig. 6a in chapter 6). The sinter has low electric resistivity $\approx$ 10 Ωcm. One of the surfaces of the zinc oxide disk was coated with indium by employing the vacuum evaporation method so as to make an ohmic contact, and a copper wire was attached with silver paste. The structure of the electrode was mostly the same as that described in chapter 1. Before each measurement, the electrode was polished with silicon carbide abrasive, etched in hydrochloric acid or nitric acid, washed with water, and dried.

The potential of the semiconductor electrode versus the reference electrode (SCE) was controlled by use of a Hokutodenko HA-101 potentiostat and the current was measured with a Yokogawa-Hewlett-Packard4304B electrometer. A 500 W xenon lamp of Ushio

Electric Inc. was used as the light source. The light was monochromatized by use of a Japan Jarrell-Ash, 0.25 m Ebert type monochromator. The light intensity was measured with an Eppley, bismuth-silver type thermopile. A Shimadzu MPS-50L spectrometer was used for the measurements of absorption spectra.

All the solutions used contained 0.2 M ($mol \cdot dm^{-3}$) Na_2SO_4, KNO_3, etc. as the supporting electrolytes. Oxygen was removed by bubbling high purity nitrogen gas through the solutions before measurements. All chemicals were of reagent grade and used without further purification. The structural formulas of the dyes used are given below:

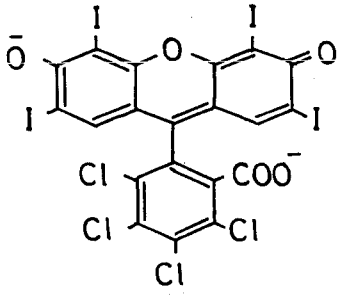

rose bengal

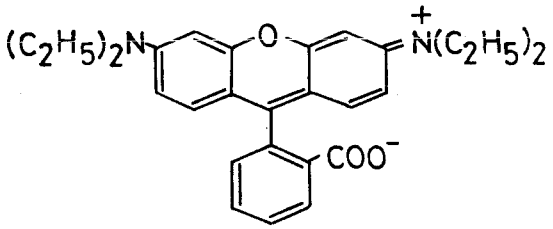

rhodamine B

Results

Figure 1 shows the dye-sensitized photocurrent-potential curves for the case of rose bengal. The anodic current was negligible in the dark, while it rose up under illumination in the wavelength range of the absorption band of rose bengal. When the solution contained no dye, the photocurrent was less

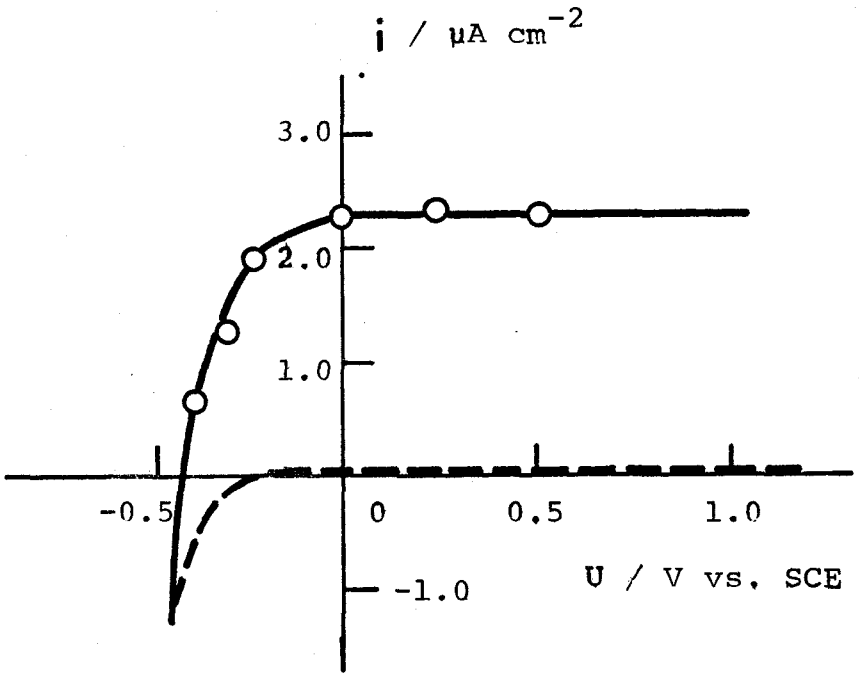

Fig. 1 Current-potential curves of the ZnO electrode in the presence of 6.5×10^{-7} M rose bengal and 0.2 M Na_2SO_4, ---- dark current, —— under illumination (λ 562 nm).

than 0.03 $\mu A \cdot cm^{-2}$ under illumination at the same wavelength and at the electrode potential of 0.35 V. Since the photocurrent decayed during the course of illumination, the photocurrent curve was plotted by using the value obtained immediately after the light had been turned on. The photocurrent appeared at the electrode potnetial more positive than -0.5 V vs. SCE, which nearly agreed with the flat band potential of the zinc oxide electrode reported by Lohmann,[1] and became constant at the potential more positive than 0.0 V. Therefore, most of the experiments were made at 0.35 V.

The photocurrent decayed rather quickly with time as shown in Fig. 2. The photocurrent was not restored to the initial value, even if the electrode was kept in the dye solution for a few minutes. The photocurrent fell down to zero when the light was turned off, and no overshoot to the cathodic side was observed. The decay of the photocurrent was suppressed or stopped by adding a reducing agent, e.g., potassium iodide, as shown by curve 3. The logarithm of the photocurrent gave a straight line for the first several seconds as shown by curve 2, from which we can obtain the initial value of the photocurrent, i°_{dye}, and the decay time constant, τ, namely the period of illumination for which the current decays to 1/e.

The surface of the zinc oxide electrode faintly colored pink, if it was dipped into the rose bengal solution. After

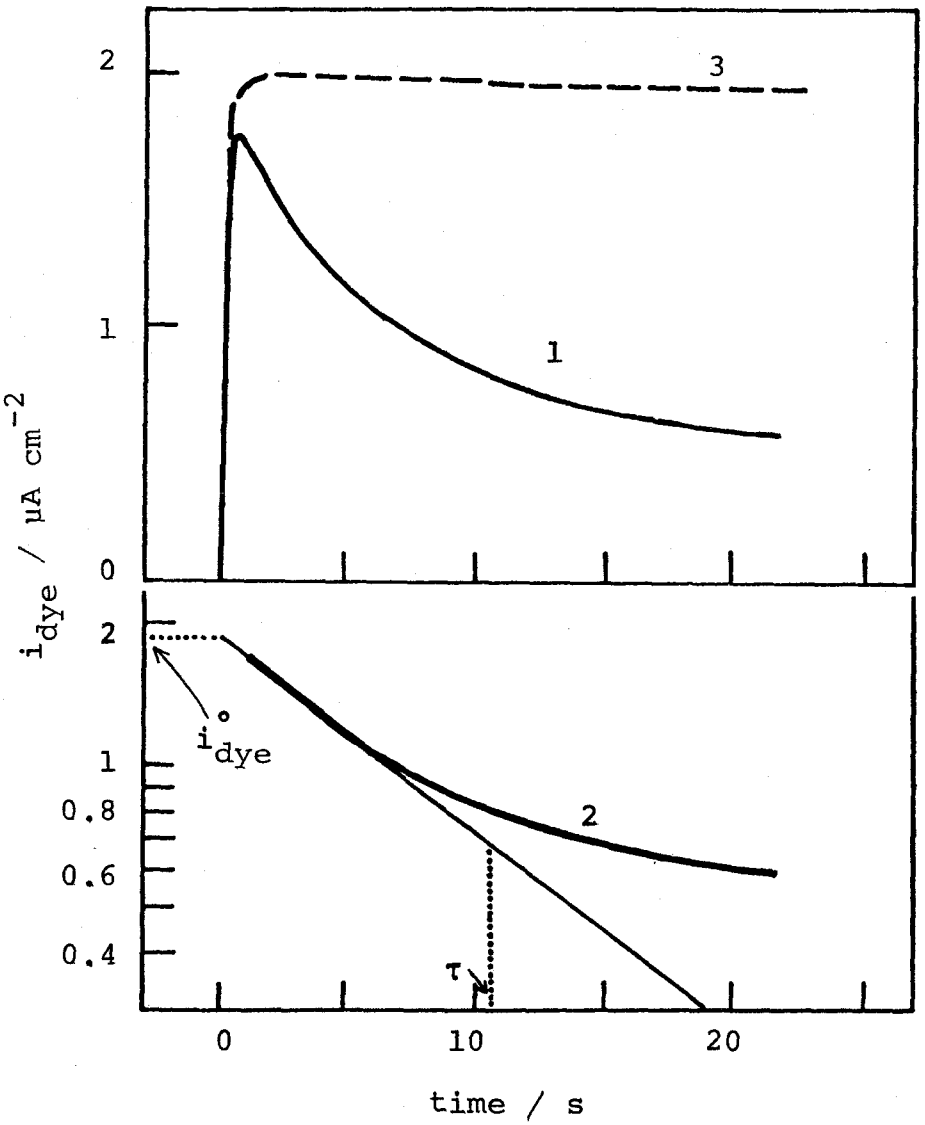

Fig. 2. The change of the photocurrent vs. time. Curve 1, for the solution of 6.7×10^{-7} M rose bengal and 0.2 M KNO_3. Curve 2, the logarithmic plot of the same result. Curve 3, for the case where 0.1 M KI is added.

prolonged illumination in the same solution at closed circuit, the color changed to brown-red. The color was not removed by washing with water. On the other hand, no color change occurred when the electrode was illuminated at open circuit or at closed circuit in the presence of a reducing agent.

The photocurrent action spectrum obtained for a solution containing a sufficient amount of potassium iodide is shown in Fig. 3. Almost the same action spectrum was obtained for a solution without any reducing agent by scanning rapidly under weak illumination. The peak of the action spectrum for the photocurrent shifted by 13 nm toward the longer wavelength from that of the absorption spectrum of the dye solution, and nearly coincided with that of the reflectance spectrum of the dye adsorbed on zinc oxide powder.

The initial value of the photocurrent increased proportionally with the illumination intensity, while the decay time constant was inversely proportional to it (Fig. 4). The value of i°_{dye} and τ scarcely changed over the electrode potential range 0.0 — 1.0 V. Figure 5 shows the change of i°_{dye} and that of τ with the concentration of rose bengal in the solution. The i°_{dye} value increased with the concentration of the dye and approached a constant. The τ was constant for the concentration of rose bengal up to 10^{-6} M, and increased by the concentration above 10^{-6} M.

The τ for rose bengal was not affected by the pH $<$ 8.0 of

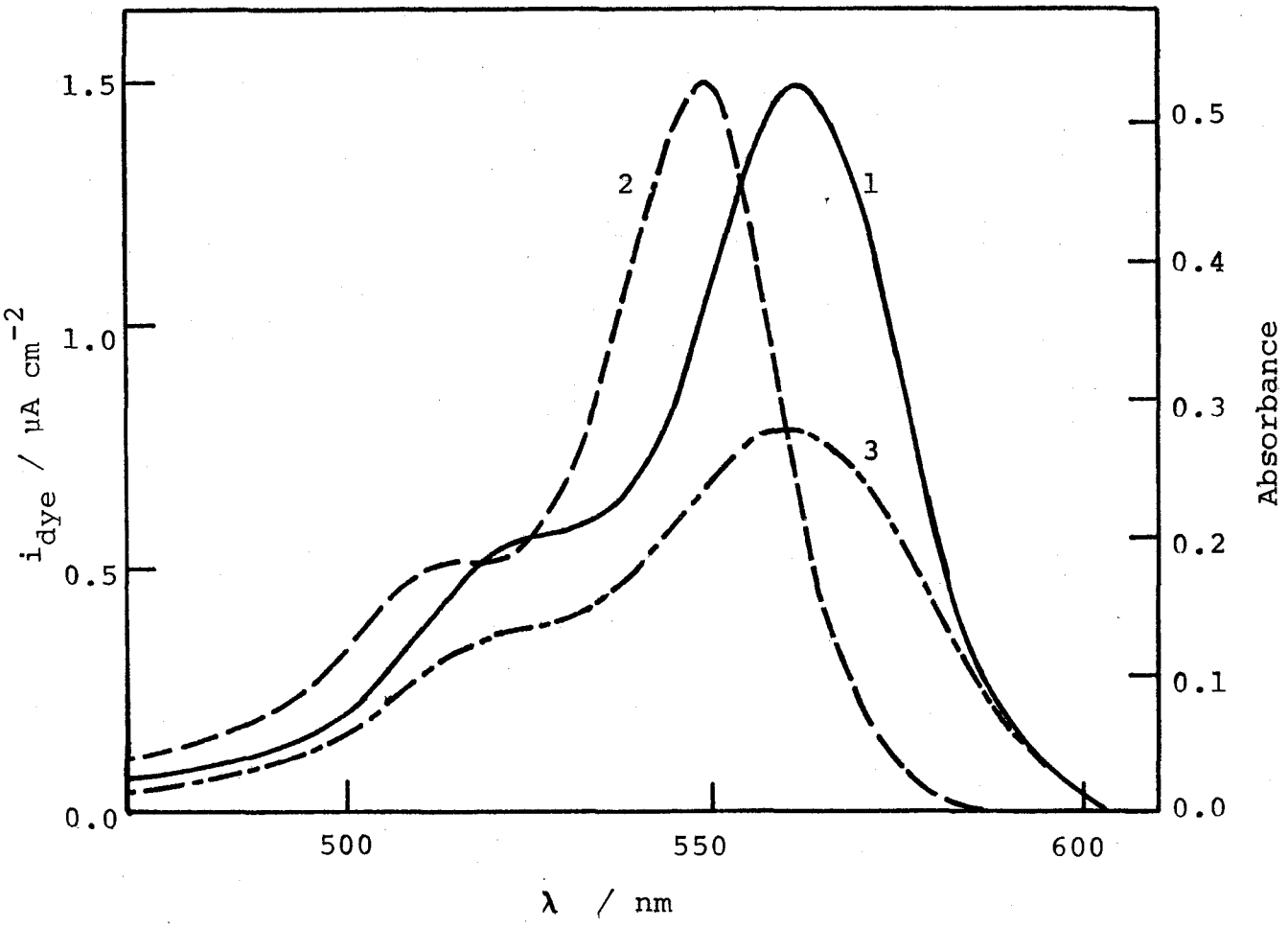

Fig. 3. (1) The action spectrum for the photocurrent for the solution of 5.3×10^{-7} M rose bengal and 0.1 M KI at the electrode potential 0.35 V vs SCE. (2) Absorption spectrum of the same solution, measured with a 10 cm cell. (3) Diffuse reflectance spectrum of the dye adsorbed on ZnO powder. The dye was adsorbed in the aqueous solution of 1.4×10^{-5} M rose bengal.

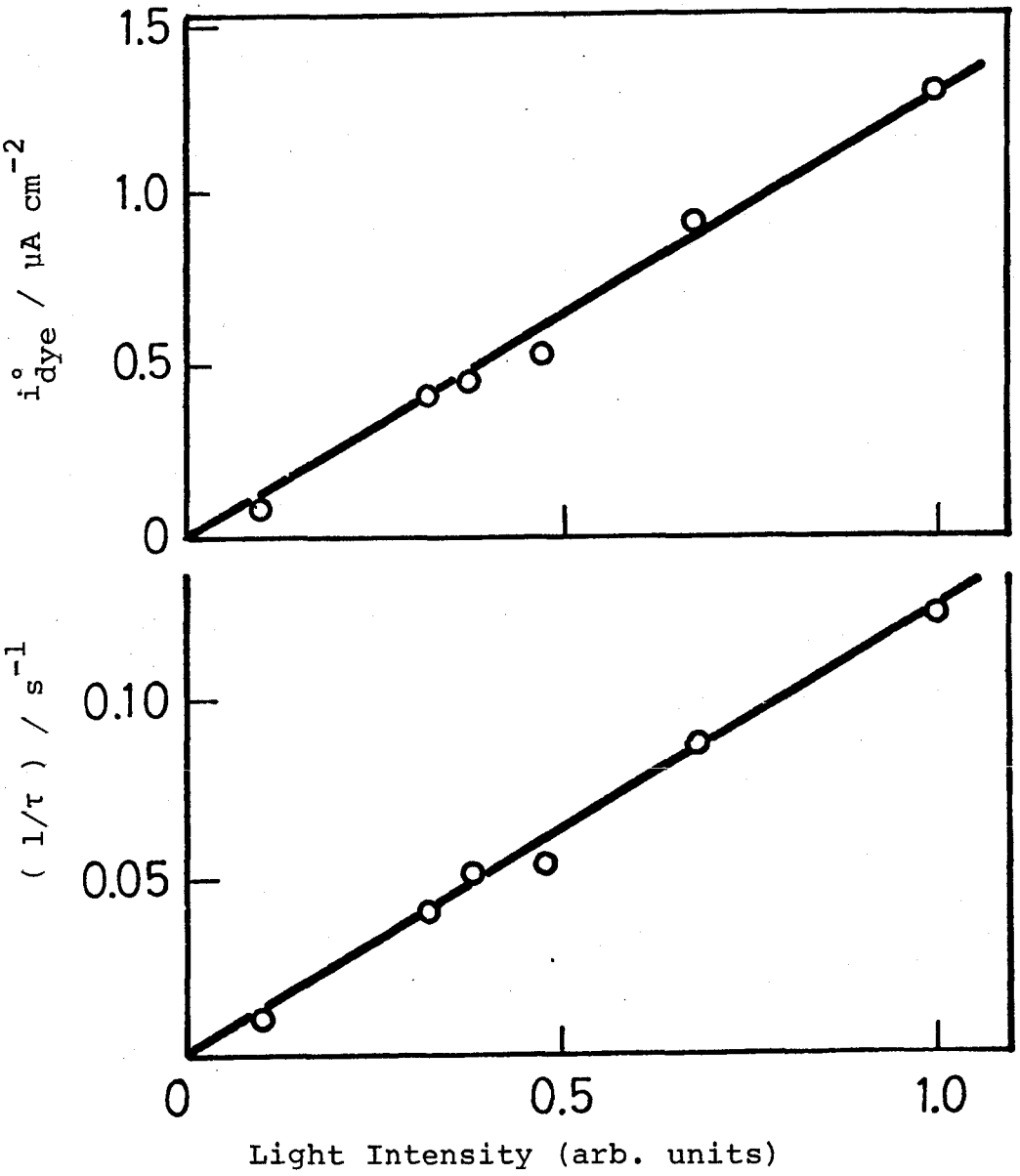

Fig. 4. The change of the initial value of the photocurrent (a), and the decay time constant of the photocurrent (b) with the light intensity: rose bengal, 6.5 x 10^{-7} M; Na_2SO_4, 0.2 M; electrode potential, 0.2 V vs. SCE.

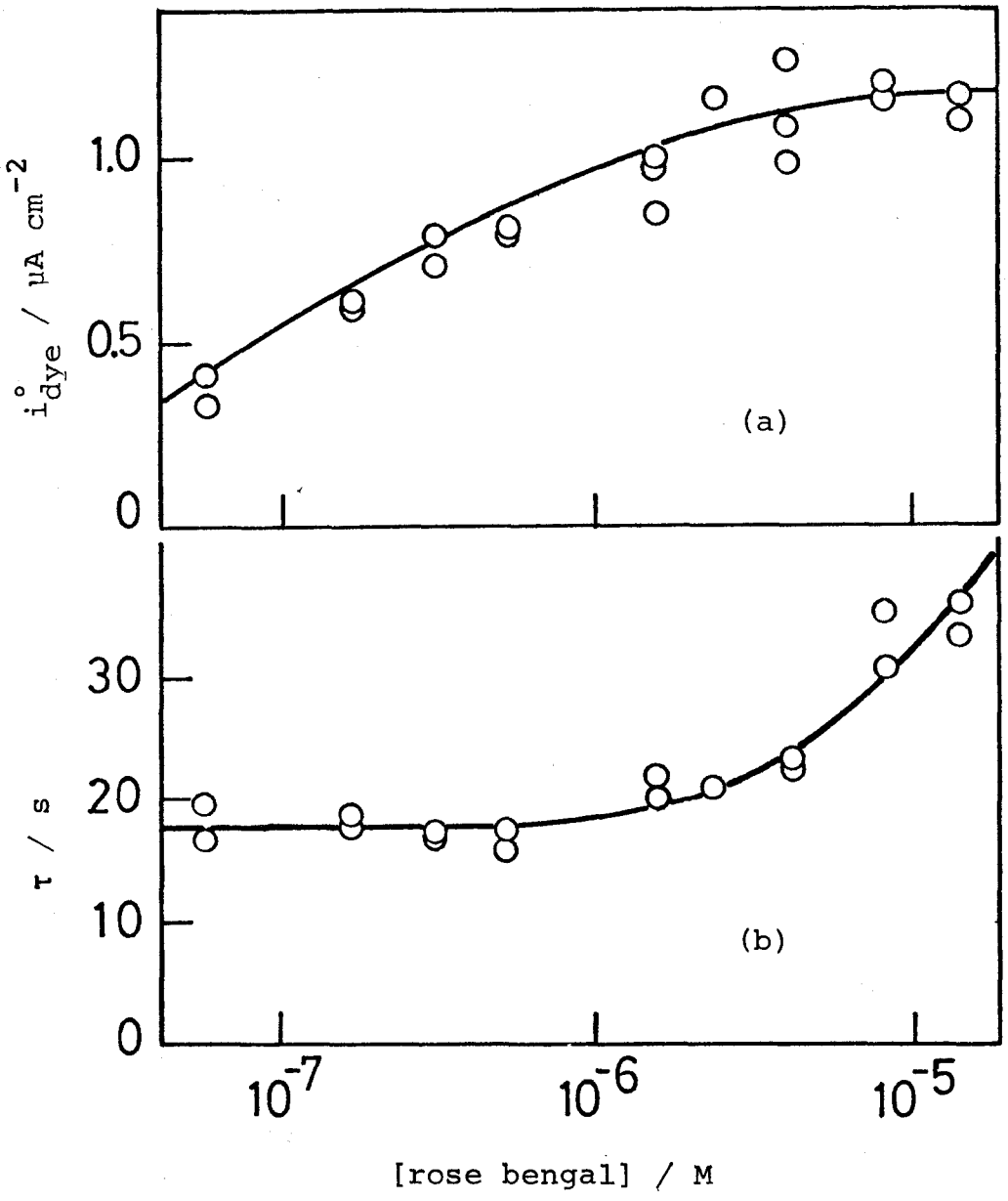

Fig. 5. The initial value of the photocurrent (a) and the decay time constant of the photocurrent (b) versus the concentration of rose bengal: Na_2SO_4, 0.2 M; electrode potential, 0.35 V vs. SCE.

the solution (Fig. 6). The τ value was practically independent of the supporting electrolytes, e.g., KNO_3, K_2SO_4, KCl, $KClO_4$, etc., while the i°_{dye} was affected a little by them. This is assumed to be caused by the adsorption of the electrolytes on the ZnO electrode in competition with the dye.

The photocurrent decay became slow by addition of a small amount of reducing agent, e.g., potassium iodide. The logarithmic plots of the photocurrents gave straight lines for the first several seconds. The τ obtained from the gradient of the straight lines increased with the concentration of the reducing agent as shown in Fig. 7 for the cases of potassium iodide and hydroquinone. The similar results were obtained by the addition of N, N, N', N'-tetramethyl-p-phenylenediamine (TMPD), allylthiourea, and manganase(II) nitrate. In these cases also, no recovery of the decayed photocurrent was observed, even after the electrode was kept in the solution in dark for ca. 30 s.

The photocurrent for rodamine B increased by addition of halide ions to the dye solution, while the dependence of the decay time constant of the photocurrent on the cencentration of the halide ions was more complicated (Fig. 8 a and b).

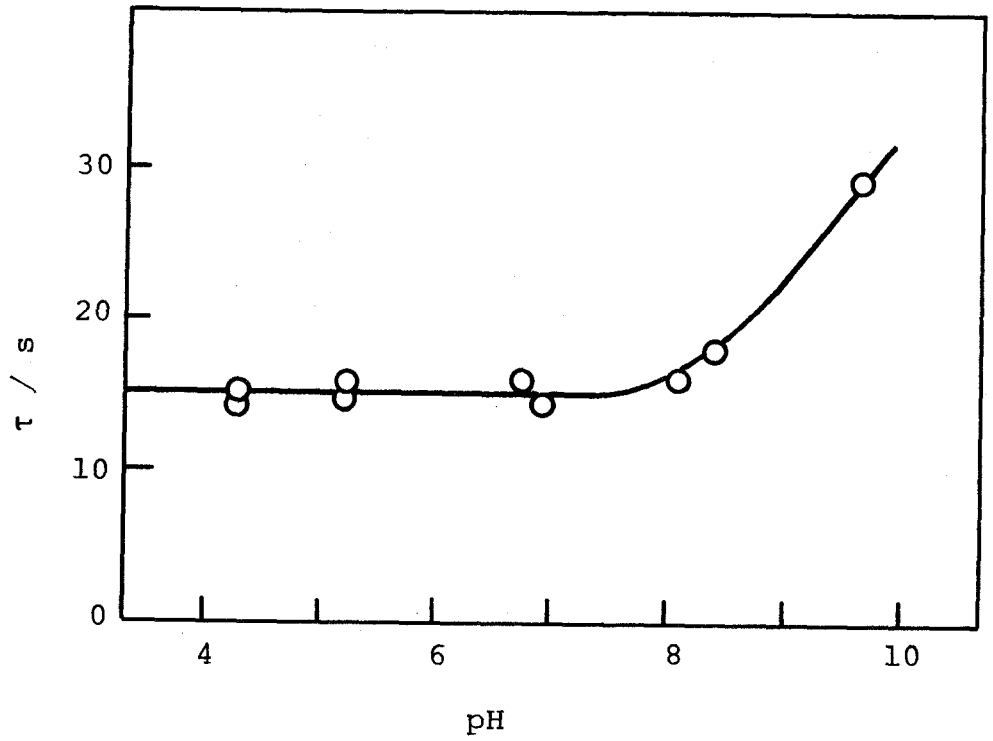

Fig. 6. The effect of pH on the decay time constant of the photocurrent sensitized by rose bengal: rose bengal, 1×10^{-6} M; KNO_3, 0.2 M; electrode potential, 0.35 V vs. SCE.

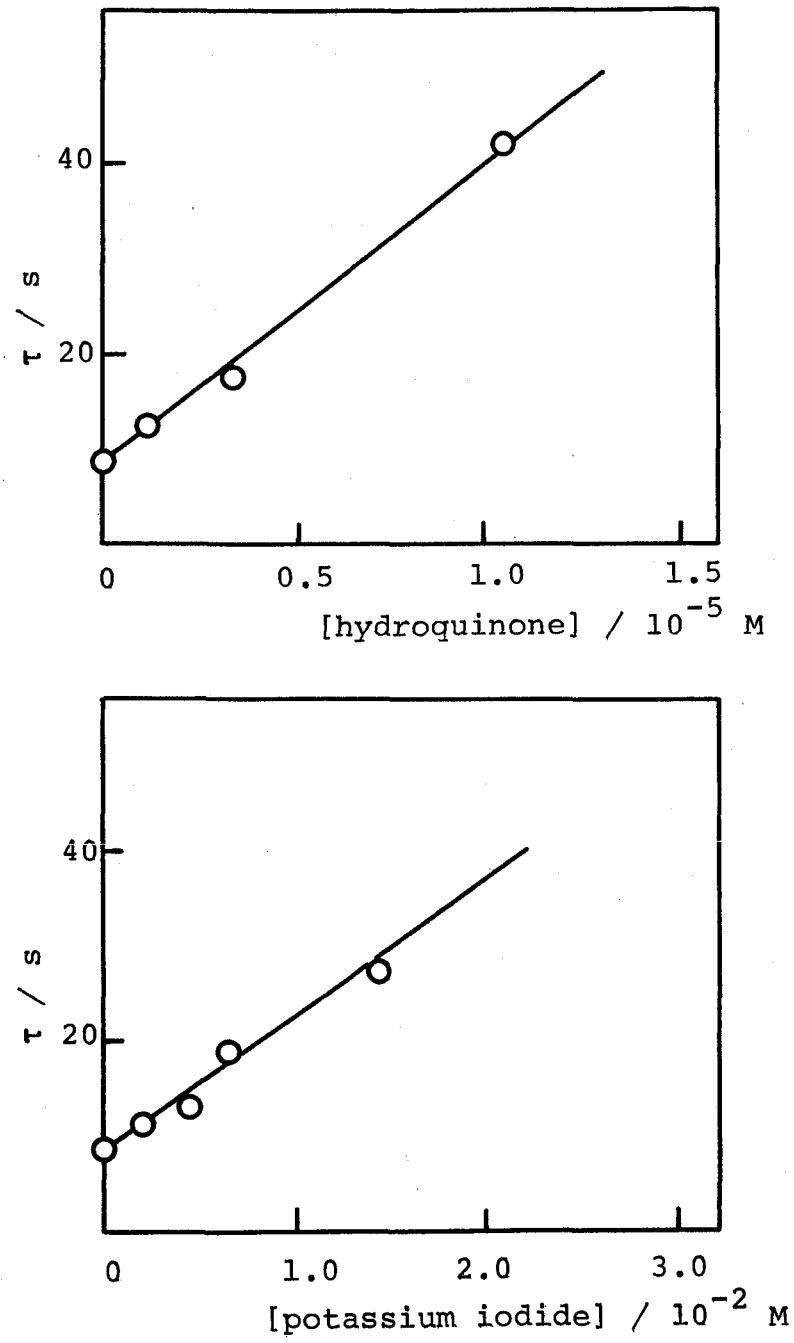

Fig. 7. The effect of hydroquinone (a) and potassium iodide (b) on the decay time constant of the photocurrent sensitized by rose bengal: rose bengal, 6×10^{-7} M; Na_2SO_4, 0.2 M; electrode potential, 0.35 V vs. SCE.

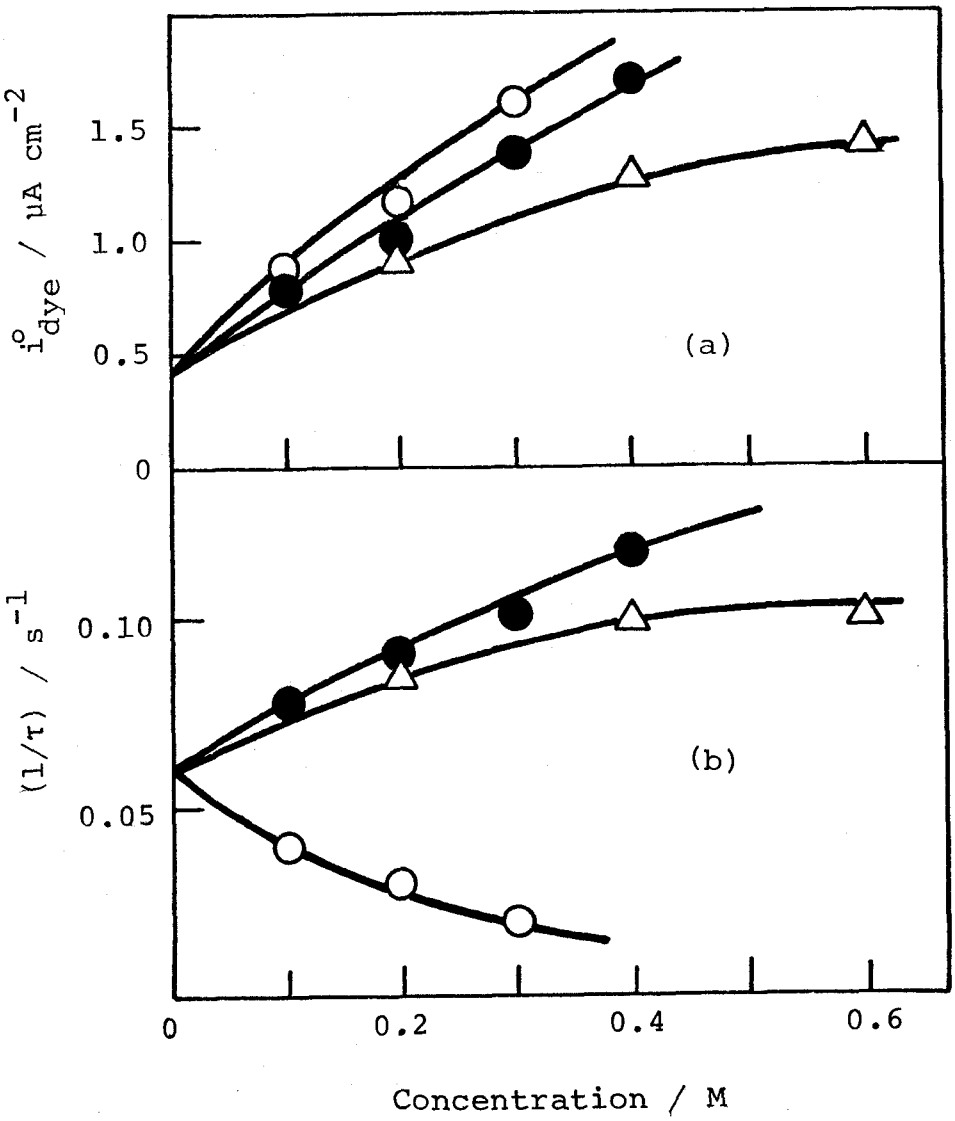

Fig. 8. The initial value of the photocurrent (a) and the decay time constant of the photocurrent (b) versus the concentraiton of the halide ions: rhodamine B, 1.0×10^{-6} M, Na_2SO_4, 0.2 M; electrode potential, 0.2 V vs. SCE; △, chloride ion; ●, bromide ion; ○, iodide ion.

Discussion

The mechanism of the dye-sensitized photocurrent can be explained by the energy diagram such as shown in Fig. 9, for the case of an n-type semiconductor. The electron injection from an excited dye (D*) into a conduction band is suggested by the fact that only those dyes whose excited energy levels are considerably higher than the conduction band of the semiconductor at the interface can act as effective sensitizers (chapter 1). The electron deficient dye (D^+) may undergo irreversible reaction, causing the color change of the electrode. The total reaction scheme can be represented as follows:

$$D + h\nu \longrightarrow D^*, \quad (1)$$

$$D^* \longrightarrow D^+ + e(\text{electrode}), \quad (2)$$

$$D^+ \longrightarrow \text{reaction product}. \quad (3)$$

The Decay Curve of the Photocurrent and the Quantum Efficiency of Electron Injection from the Excited Dye.

The photocurrent of some semiconductor-aqueous solution photocell decays with time owing to the deposition of opaque substance on the surface of the electrode, produced by the reaction with the holes generated. The photocurrent in the case of zinc oxide electrode does not decay, because in this case the products, zinc ion and oxygen, do not accumulate on the surface.[2)]

In the case of the dye-sensitized photocurrent for zinc

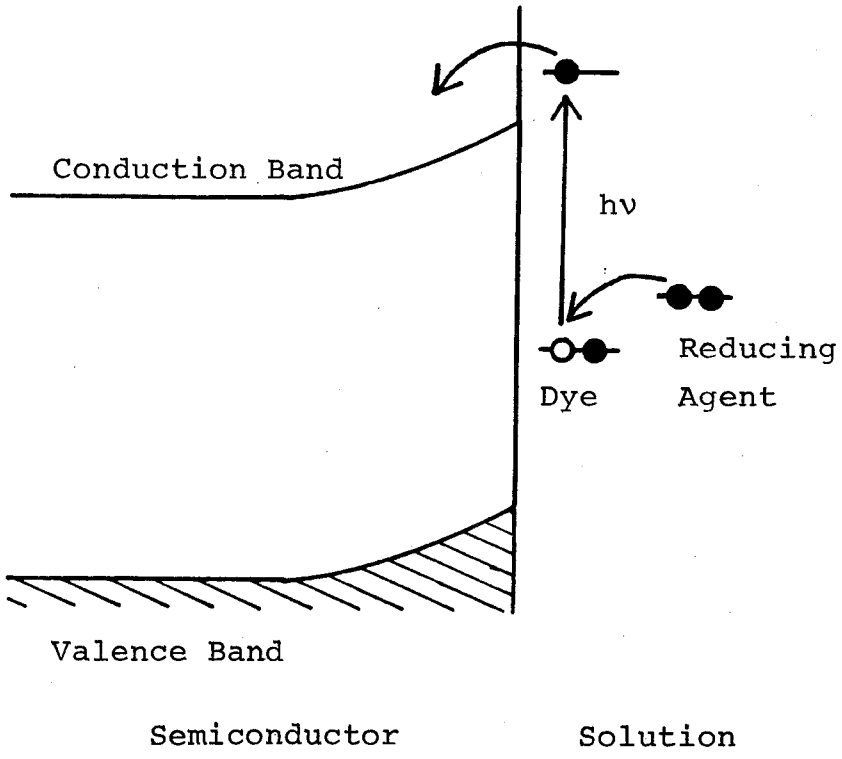

Fig. 9. A model for the electron injection.

oxide, the photon energy is less than the band gap, and so it is clear that the decay is not caused by the reaction of the electrode itself, since no free hole exists in the electrode. The decay of the photocurrent should then be attributable either to the decrease of the number of the unoxidized dye molecules (or ions) adsorbed on the electrode or to an accumulation of the deteriorated dye (Reactions 1-3).

The influence of the dye (D_{soln}) in solution on the decay of the photocurrent, as shown in Fig. 5, is explained by the following dye regeneration process :

$$D^+ + D_{soln} \longrightarrow D + D^+_{soln} \qquad (4)$$

Process 4 can be achieved either by the electron transfer or by the exchange of D^+ and D_{soln}. The decay of the photocurrent is suppressed if the reaction velocity for process 4 is greater than those for processes 2 and 3.

When the solution contains no reducing agent, the number of dye molecules (or ions), N, per unit area of the electrode surface will change according to

$$dN/dt = -\eta_o SN + kC(N_o - N) \qquad (5)$$

where η_o is the quantum efficiency of the electron injection from the excited dye, S the frequency of excitation of a dye molecule (or ion), N_o the number of the dye molecules (or ions) per unit area of the electrode before illumination, C[M] the concentration of the dye in the solution, and k the rate constant. The second term of the right hand side of Eq. 5

corresponds to the restoring rate of the oxidized dye on the electrode surface by Reaction 4.

When the concentration of the dye in the solution is very low, the second term of Eq. 5 can be neglected, and N can be written as

$$N = N_o \exp(-\eta_o St). \quad (6)$$

The photocurrent, assumed to be proportional to N, can be written as

$$i_{dye} = i^{\circ}_{dye} \exp(-\eta_o St), \quad (7)$$

and, hence

$$\eta_o = 1/\tau S. \quad (8)$$

The exponential decay of the photocurrent, as observed experimentally at the initial stage, coincides with Eq. 7.

The dependence of τ on the concentration of the dye shown in Fig. 5b can be explained as follows. When the concentration of the dye is high, the second term of Eq. 5 cannot be neglected. Therefore, Eqs. 6-8 are valid only in the range of the concentration where τ does not depend on C. Figure 5 shows that such a condition is satisfied when C is lower than 10^{-6} M.

The absorbance of the dye on the electrode can be written as

$$\log I_o/I = 1000\varepsilon N/N_A, \quad (9)$$

where ε [M^{-1} cm^{-1}] is the molar extinction coefficient of the dye, N_A the Avogadro constant, I_o the number of the photons idcident on the unit area of the dye layer on the electrode

per second, and I the number of the photons transmitted through the same layer. Since the absorption of light by the dye layer is small, the equation can be approximated as

$$(I_o - I)/I_o = 1000(\ln 10)\varepsilon N/N_A, \quad (10)$$

and

$$I_o - I = SN. \quad (11)$$

From these equations S can be written as

$$S = 1000(\ln 10)\varepsilon I_o/N_A. \quad (12)$$

The relation that τ is inversely proportional to I_o, as shown in Fig. 4b, can be derived from Eqs. 8 and 12.

The quantum yield η_o for rose bengal was determined to be 22 % by applying Eqs. 8 and 12 to the experimentally obtained photocurrent decay curves. The quantum yield was obtained for the illumination at the peak wavelength, and the molar extinction coefficient was assumed to be the same as that at the peak of the absorption spectrum of the solution. The reflection factor of light at the surface of the electrode was estimated to be 0.7 from the comparison of the reflected light intensity with that from magnesium oxide powder. This means that seven tenths of the incident light, which passes through the dye layer toward the inside of zinc oxide sinter, is reflected and passes again through the dye layer on the surface of the electrode. Therefore, we employed the value of measured number of photons incident upon the sample multiplied by 1.7 for I_o in Eqs. 9-12.

The derived quantum yield agreed well with that obtained from the measurement of the amount of the dye adsorbed on the electrode (chapter 3). This agreement substantiates the validity of the method of calculation of the quantum yield from the analysis of the decay of i_{dye}. The result, that τ is independent of the electrolytes and pH, indicates that the quantum efficiency of electron injection from the excited dye is not affected by the electrolytes and pH, suggesting that the structure of the dye on the electrode is not changed by pH and the electrolytes. The further details will be discussed in chapter 3.

When the surface coverage of the electrode by the dye was small, the supply of the fresh dyes from the solution phase to the surface of the electrode is easy, causing the approximation of Eq. 6 to be invalid. Therefore, the determination of the quantum yield of the photocurrent for the dyes with weak adsorptivity was unsuccessful. Similarly, the increase of τ at higher pH is thought to be caused by the decrease in adsorptivity of the electrode for the dye.

The Effect of Reducing Agents on the Decay of the Photocurrent.

The life time of D^+ in aqueous solution is estimated to be no longer than 1 s, from the result that the photocurrent did not recover from the decayed value even when the electrode

was kept in the solution containing a redusing agent. Therefore, the retardation of the decay velocity of the photocurrent by the reducing agent is concluded to be caused by the electron supply from the reducing agent, R, to D^+:

$$D^+ + R \longrightarrow D + R^+ \qquad (13)$$

Since this is a process competing with the comsumption of the dye (Eq. 3), the time constant of the decay velocity of the photocurrent in the presence of reducing agents can be written as

$$\tau = (k_3 + k_{13}[R])/k_3\eta_o S \qquad (14)$$

where k_3 and k_{13} represent the rate constants of Eqs. 3 and 13, respectively. This relation between τ and [R] agrees with the experimental results shown in Fig. 7. From the figure, the k_{13} value of hydroquinone is found to be larger than that of potassium iodide by ca. 3 orders. By analyzing the decay of the photocurrent in this manner, the electron supplying velocity from the reducing agents to the photo-oxidized dye was determined to decrease in the following order; hydroquinone $\approx$ allylthiourea $>$ TMPD $>$ potassium iodide $>$ manganase (II) nitrate.

Effect of Halide Ions on the Dye-sensitized Photocurrent.

Hauffe et al.[3] found that the dye-sensitized photocurrent at a zinc oxide electrode was increased by addition of halide ions to the dye solution. The results shown in Fig. 8a

indicate similar effects of the halide ions on the photocurrent. The increase in the photocurrent becomes greater in the sequence $Cl^- < Br^- < I^-$. This order is the same as that of the electron donating ability of the ions, i.e., the oxidation potential increases in the reverse order.

Essentially, the visible spectra of the dye solution were not changed by the addition of halide ions. Therefore, the effect of the halide ions on the photocurrent is attributable to one of the following two reasons: (1) the formation of exciplex between the excited dye and halide ions, which injects an electron into the electrode more efficiently, (2) the change of the amount of the dye adsorbed on the electrode caused by the halides. From the careful measurements of the amount of the dye adsorbed on the electrode, the latter reason was concluded to be more likely. The details will be described in chapter 3.

Hauffe et al. proposed the reduced dye formation by the electron transfer from halide ions to the excited dye, the reduced dye injecting an electron into the electrode. According to their mechanism, the dye should not deteriorate, in contradiction with the experimental result that the decay is faster in the presence of chloride and bromide ions (Fig. 8).

References

1) F. Lohmann, Ber. Bunsenges. phys. Chem.,70, 428 (1966).

2) H. Gerischer, J. Electrochem. Soc., 113, 1174 (1966).

3) U. Bode, K. Hauffe, Y. Ishikawa, and H. Pusch, Z. Phys. Chem. (N. F.), 85, 144 (1973).

CHAPTER 3

The Relation between the Dye-sensitized Photocurrents and the Adsorption of the Dyes on Semiconductor Electrodes.

Introduction

It has been concluded in the previous chapters that the dye-sensitized photocurrent is caused by the electron injection from the excited dye adsorbed on an n-type semiconductor into the conduction band of the semiconductor. For further understanding of the mechanism, the elucidation of the structure and the amount of the adsorbed dye is indispensable.

It was reported by some authors that the dye-sensitized photocurrents were affected by the pH of the solution,[1,2] and the solutes in it.[3] They discussed these phenomena on the assumption that the adsorption of the dye was not affected by the pH and the additives. This assumption, however, is found to be invalid as will be described later. Other authors discussed the phenomena on the basis of the results obtained for the adsorption of the dyes on the powder of semiconductors. However, their conclusions should be reexamined, since the adsorptivity is expected to depend on the structure of the adsorbents, e.g., powder, sinter, single crystal, etc.

In this chapter, the adsorpiton of dyes on semiconductor

electrodes is presented. Based on the results, the mechanism of the dye-sensitized photocurrents will be discussed.

Experimental

Materials. Rose bengal, erythrosin, phloxine B, eosin Y, uranin, ethyl eosin, rhodamine B, rhodamine 6G, and 1,1'-diethyl-2,2'-cyanine chloride were used as the sensitizing dyes. Their structural formulas in neutral aqueous solutions are shown below:

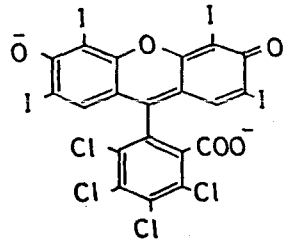

rose bengal

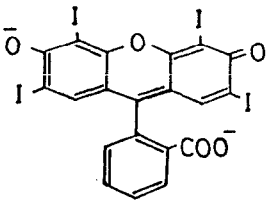

erythrosin

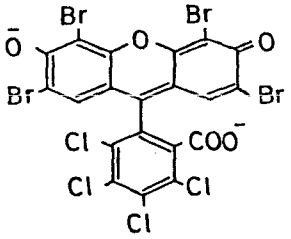

phloxine B

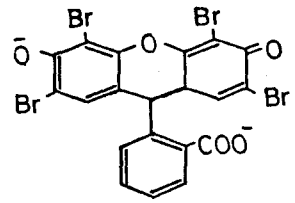

eosin Y

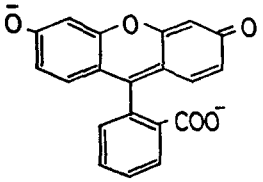

uranin

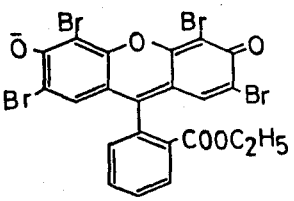

ethyl eosin

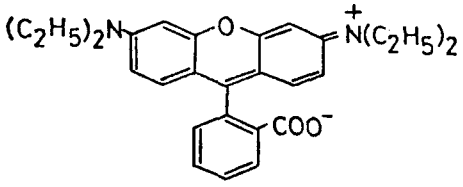

rhodamine B

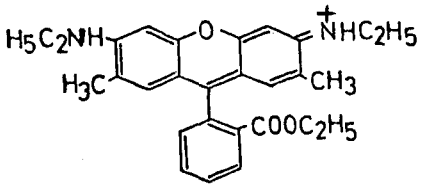

rhodamine 6G

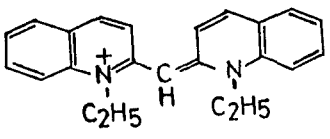

1,1'-diethyl-2,2'-cyanine

All the dyes, except uranin, showed no structural change over the pH range 5 - 12. The chemicals employed were of reagent grade and used without further purification.

Semiconductor Electrodes. As the n-type semiconductor electrodes, the single crystals of CdS and TiO_2 were used, which were obtained from Teikoku Tsushin Co., Ltd. and Nakazumi Crystals Co., Ltd., respectively. The TiO_2 electrode was constructed with its (001) face in contact with the dye solution. For the case of CdS, three types of the electrodes were prepared, which had their $(11\bar{2}0)$, (0001), and $(000\bar{1})$ faces, respectively in contact with the solution. The CdS electrodes were polished with alumina of 0.3 μm in size and etched in concentrated hydrochloric acid for 15 s, before the measurements. In some cases, the CdS electrodes were etched in 2 N hydrochloric acid. The TiO_2 electrode was not etched, but washed with ethanol and water before the measurements. The ZnO sintered disks were also used as the electrodes, the method of the preparation being described in chapter 2.

The Photocurrent and the Flat Band Potential. The experimental set-up was the same as that described in chapter 2. Unless otherwise noted, aqueous solutions with 0.1 M KNO_3 as the supporting electrolyte were used. The flat band potential was determined from the differential capacitance at the ZnO electrode-electrolyte interface. The capacitance was

measured by use of a Yokogawa Hewlett-Packard 4265B universal bridge at a frequency of 1 KHz.

The Adsorption of the Dyes. The amount of the dye adsorbed on the ZnO sinter was determined from the diffuse reflectance spectra of the sinter which was immersed in and taken out of the dye solution, the residual solution on the sinter being soaked with filter paper. The absorbance of the dye at the wavelength of the maximum absorption was measured, from which the amount of the adsorbed dye was determined. Although the adsorption of the dye practically reached saturation by immersing the sinter in the dye solution for ca. 1 min., the measurements were made for samples immersed in the solution for longer than 3 min.

Similarly, the amount of the dye adsorbed on the single crystals of CdS and TiO_2 was determined from the absorption spectra of the single crystals, which were immersed in and taken out of the dye solution.

Results and Discussion

1. The Photocurrents in the ZnO Electrodes Sensitized by Anionic Xanthene Dyes, and the Adsorption of the Dyes.

The Adsorption Isotherm of Xanthene Dyes.

The amounts of dyes adsorbed from aqueous neutral solu-

tions (pH 5.8 - 6.2) on the ZnO sinter, Γ, are plotted against the concentration of the dye, C, in Fig. 1 for the case of rose bengal and phloxine B. The Γ values represent the absorbance of the dyes adsorbed on the ZnO sinter obtained from the diffuse reflectance spectra. As shown in Fig. 2, the adsorption isotherms fit in with Langmuir adsorption isotherm represented as

$$\frac{C}{\Gamma} = \frac{C}{\Gamma_o} + \frac{b}{\Gamma_o} \qquad (1)$$

where Γ_o is the saturation value of the amount of adsorbed dye, and b a constant. The adsorption equilibrium can be expressed by the following equation

adsorbed solvent (or electrolyte) + dye in solution

$\rightleftharpoons$ adsorbed dye + solvent (or electrolyte) in solution

(2)

The equilibrium constant is given by

$$K = (a_2^s \; a_1^b)/(a_1^s \; a_2^b) \qquad (3)$$

where a_1 and a_2 are the activities of the solvent and dye, respectively, and the superscripts s and b indicate that the values are for the surface and the bulk, respectively. Since a_1^b can be approximated to be constant, Eq. 2 is written as

$$K = K' \; a_1^b \qquad (4)$$

where K' is an apparent equilbrium constant which is the reciprocal of b in Eq. 1.

The adsorption isotherm for other xanthene dyes were

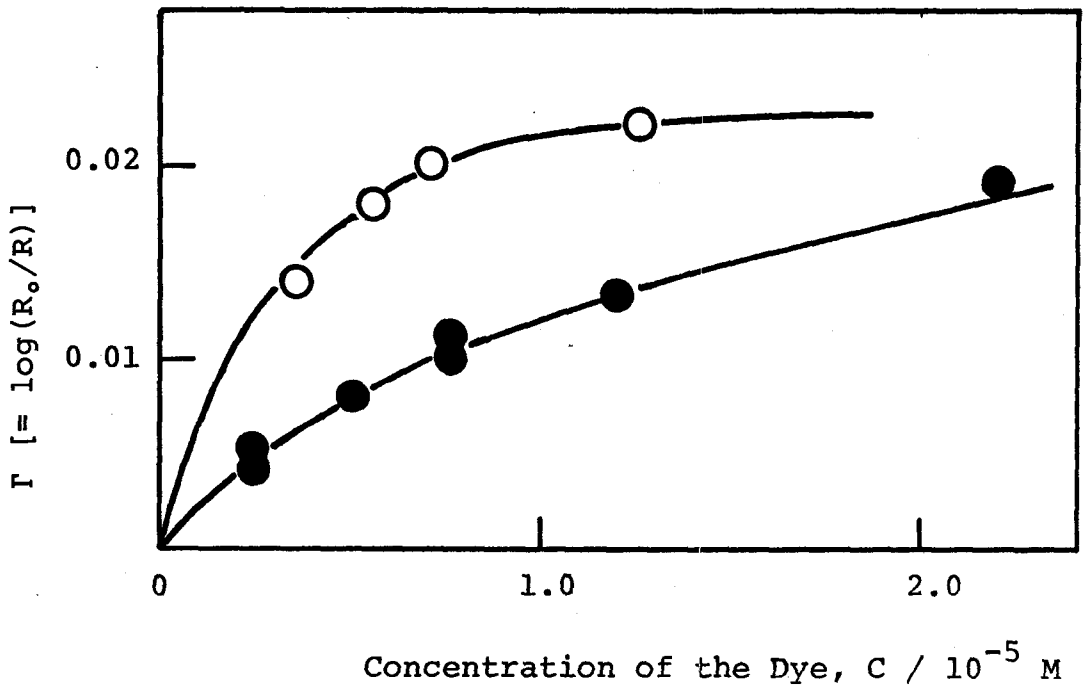

Fig. 1. Adsorption of dyes from the aqueous neutral solutions containing 0.1 M KNO_3 on the ZnO sinter at 22 °C: ○, rose bengal; ●, phloxine B. The ordinate indicates the absorbance of the adsorbed dyes obtained from the diffuse reflectance spectra of the ZnO sinter at the wavelengths of 562 nm(rose bengal) and 551 nm (phloxine B).

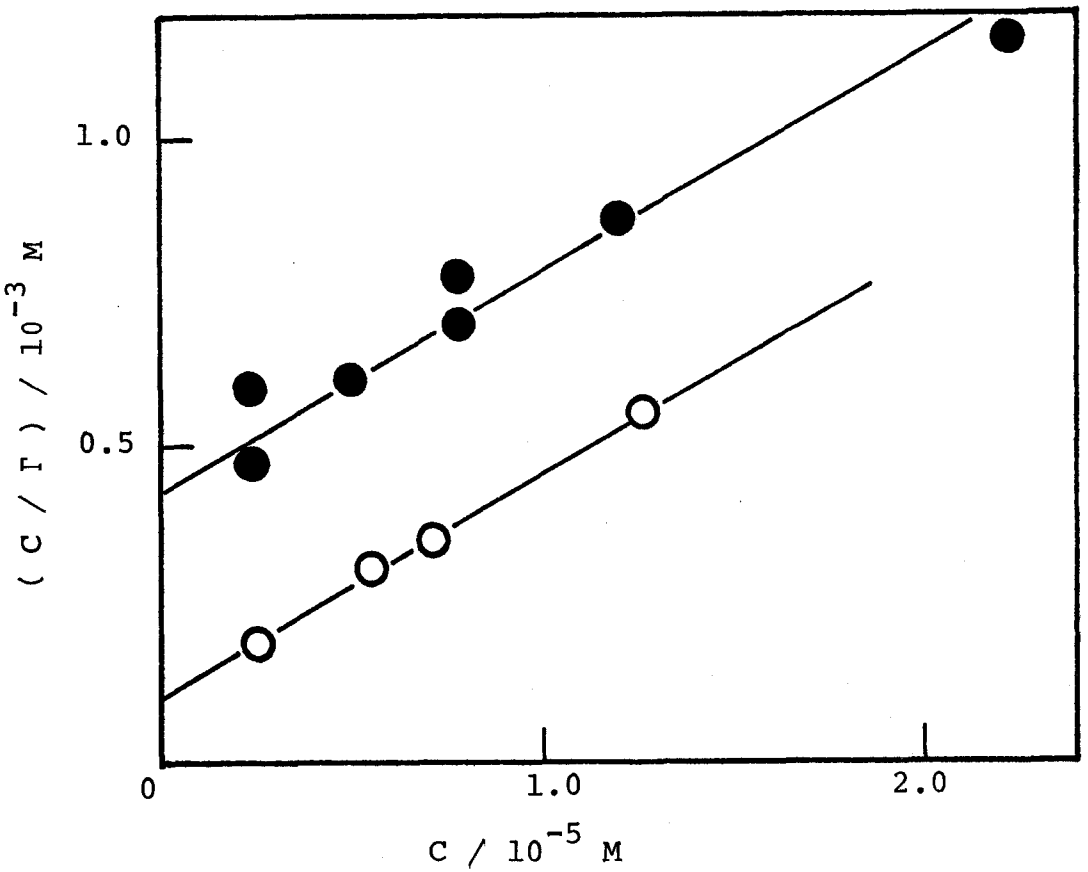

Fig. 2. A Langmuir-plot for the same result shown in Fig. 1: ○, rose bengal; ●, phloxine B.

also measured and the Γ_o and b values obtained are shown in Table 1. The halogen substitution and the esterification of the dye cause no significant effect on the Γ_o values. As the peak molar extinction coefficients of the dyes are almost unaffected by such a change, this result indicates that the saturation values for the adsorption on ZnO are also unchanged. However, the b values are decreased considerably by the halogen substitution in the order of H < Br < I.

The heat of adsorption of the dye, Q_{ads}, is represented as

$$Q_{ads} = RT \ln K - T\Delta S^\circ \qquad (5)$$

or

$$Q_{ads} / RT = - \ln b + A \qquad (6)$$

where A is a constant. The Q_{ads} and A for rose bengal are found to be 21 kJ mol^{-1}, and -4.3, respectively, from the temperature dependence of b value (Fig. 3). The change in entropy by the adsorption for the other divalent xanthene dye anions is expected to be nearly the same as that of rose bengal. Therefore, the A value for them may be assumed to be equal to that of rose bengal. The Q_{ads}'s calculated from Eq. 6 by taking A to be -4.3 and employing the values shown in Table 1 for b are also listed in the table.

The Q_{ads} becomes larger by substituting the dye with I, Br, and Cl, respectively as can be seen in Table 1. This result suggests that van der Waals force participates in the adsorptivity of the dye, as pointed out for the adsorption

Table 1. Adsorption of xanthene dyes from aqueous solutions containing 0.1 M KNO_3 on the ZnO sinter at 22 °C.

Dye	Γ_o	b / 10^{-6} M	Q_{ads} / KJ mol^{-1}
rose bengal	0.027 ± 0.03 (562 nm)	2.6 ± 0.3	21
erythrosin	0.027 ± 0.03 (538 nm)	3.0 ± 0.3	20
phloxine B	0.027 ± 0.03 (551 nm)	11 ± 1	18
eosin Y	0.027 ± 0.03 (530 nm)	20 ± 2	16
ethyl eosin	0.026 ± 0.03 (534 nm)	10 ± 1	—

* Γ_o indicates the absorbance of the dyes adsorbed on the ZnO sinter at the wavelengths shown in the parentheses.

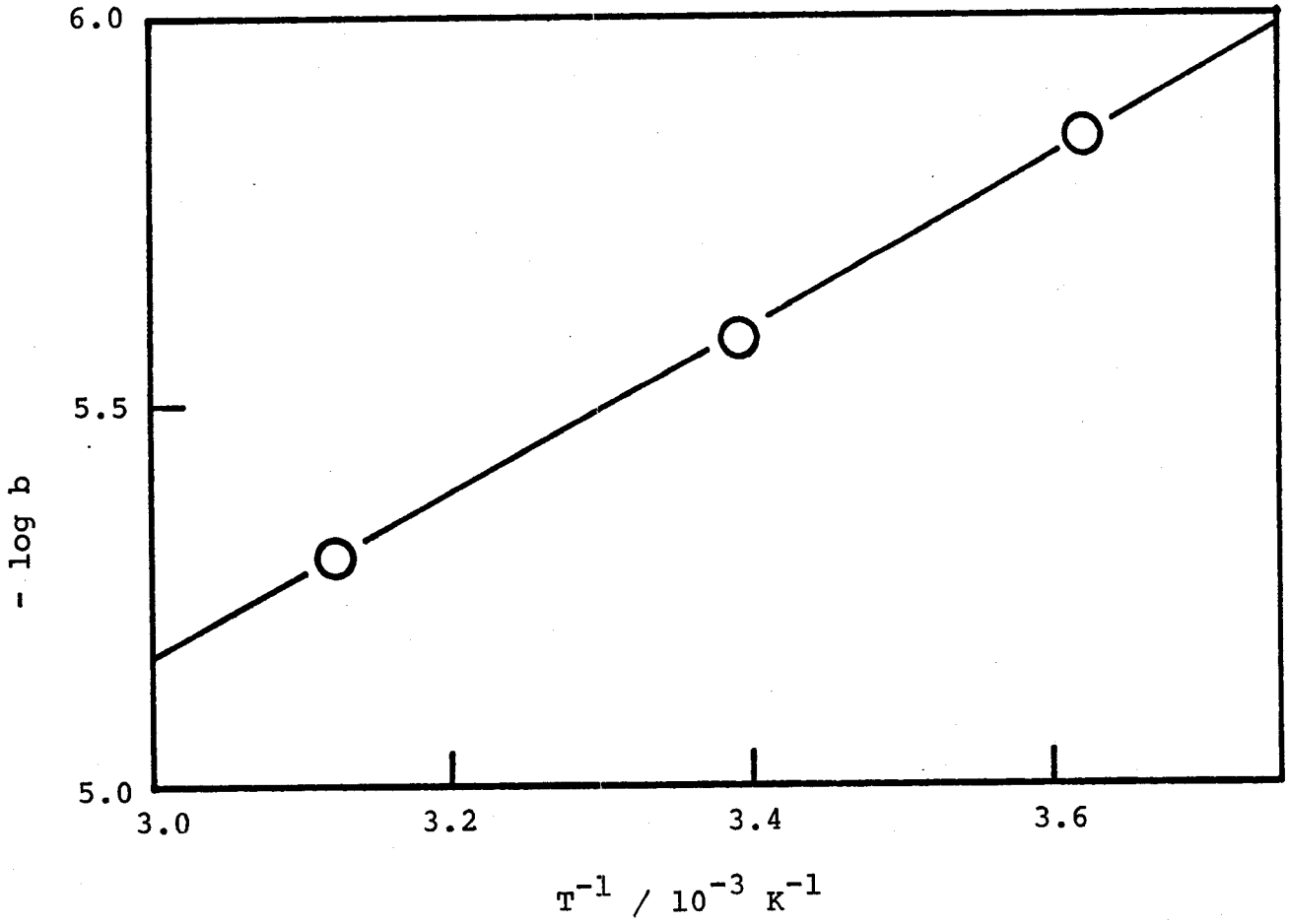

Fig. 3. Temperature dependence of the b value of Eq. 6 for rose bengal.

on the ZnO powder.[4] However, the b values for the ZnO sinter are found to be ca. 10 times smaller than those for the powder.

As rose bengal had the largest Q_{ads}, it was expected that the most reliable results could be obtained for this dye. Therefore, experiments were mostly performed by use of rose bengal as a sensitizing dye.

The pH Dependence of the Adsorptivity of the Dye and the Surface Structure of ZnO.

The saturation value of the dye adsorption on ZnO sinter is found to increase as the pH becomes lower (Fig. 4), indicating that the number of the adsorption sites for the dye is increased by lowering the pH.

The pH dependence of the amounts of the adsorbed dye in a solution of 1.5×10^{-5} M rose bengal containing 0.1 M KNO_3, at which the adsorption practically reaches saturation, is plotted in Fig. 5a. In the experiment, the solutions were not buffered, and the pH was adjusted by adding a small amount of aqueous KOH and HNO_3 solutions. The change of the ionic strength by the pH controll can be neglected, because the solution contains large amount of KNO_3. The absorption and fluorescence spectra of the dye in aqueous solutions are scarcely changed over the pH range 5.0 - 12.0. Therefore, the change in the adsorptivity must be caused by the effect of pH on the structure of the ZnO surface.

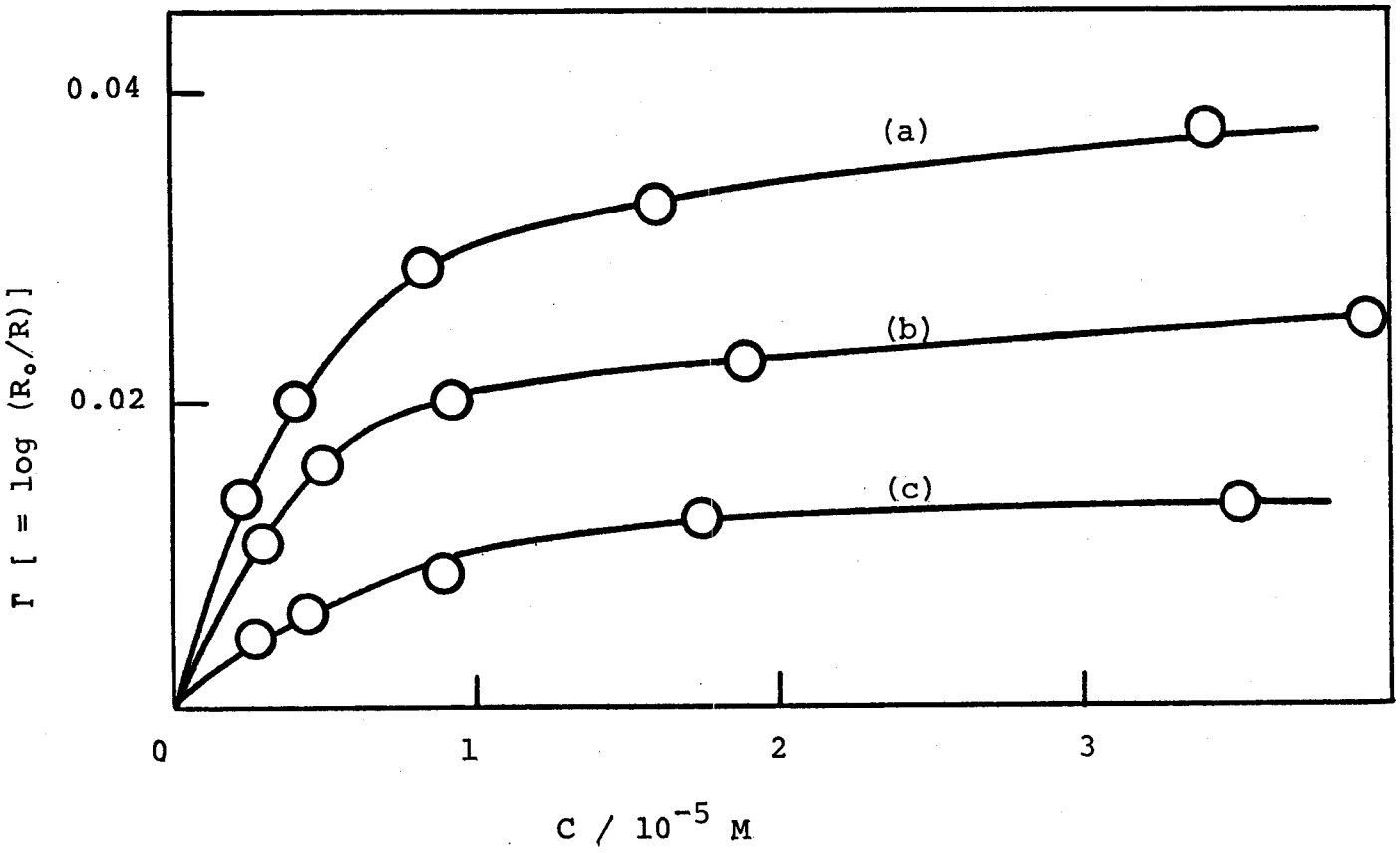

Fig. 4. Adsorption of rose bengal from buffered solutions on ZnO sinter at 22 °C: a, pH 5.4 (acetate buffer); b, pH 7.9 (borate buffer); c, pH 9.4 (borate buffer).

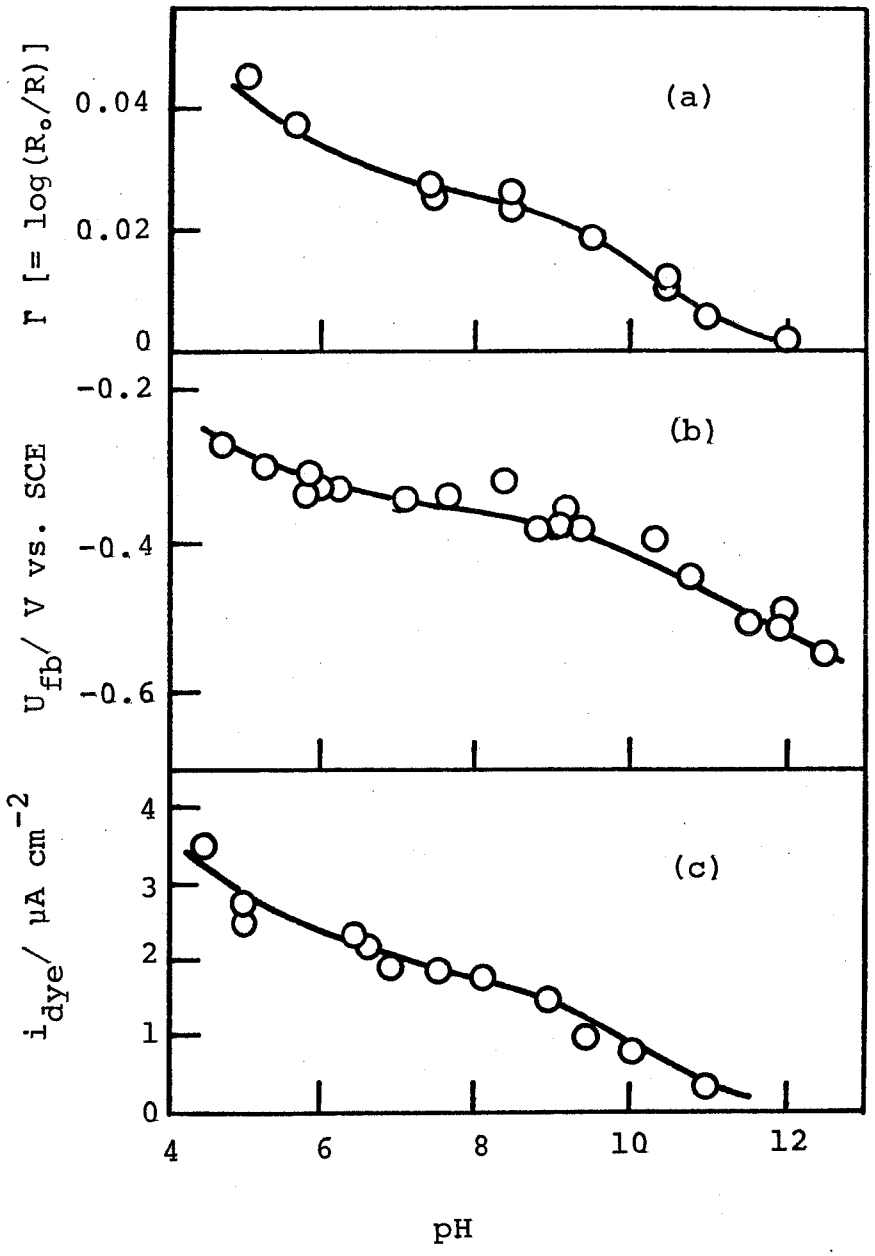

Fig. 5. The pH-dependence of the adsorption of rose bengal on ZnO sinter (a), flat band potential of the ZnO electrode (b), and the sensitized photocurrent at the electrode potential, U, of 0.3 V vs. SCE (c); rose bengal, 1.5×10^{-5} M; KNO_3, 0.1 M.

The information on the electrical double layer at the ZnO/electrolyte interface can be obtained from the measurement of the flat band potential, U_{fb}, of the ZnO electrode, the electrode potential at which the space charge layer in the semiconductor vanishes. The flat band potential of the ZnO sinter electrode in 0.1 M KNO_3 solution increases as the pH decreases, as shown in Fig. 5b. In this case, the solutions are not buffered like the case for the adsorption measurement, and the plot does not lie on a straight line. On the other hand, the plot fits on a straight line when the measurements are performed in buffered solutions, as reported by Lohmann.[5)]

The pH dependence of the U_{fb} for the oxide electrodes has been explained by the dissociation of the surface OH groups as[5)]

$$\gtrless ZnO^- + H^+ \rightleftharpoons \gtrless ZnOH \qquad (7)$$

$$\gtrless ZnOH \rightleftharpoons \gtrless Zn^+ + OH^- \qquad (8)$$

As the pH decreases, the equilibria are shifted to the right sides of the equations and hence the potential of the ZnO electrode becomes positive.

The surface zinc ion, $\gtrless Zn^+$, is concluded to work as the adsorption site for the anionic xanthene dyes by reasons given below:

1. The resonance Raman spectrum of rose bengal adsorbed on ZnO is similar to that of a zinc salt of the dye as shown in

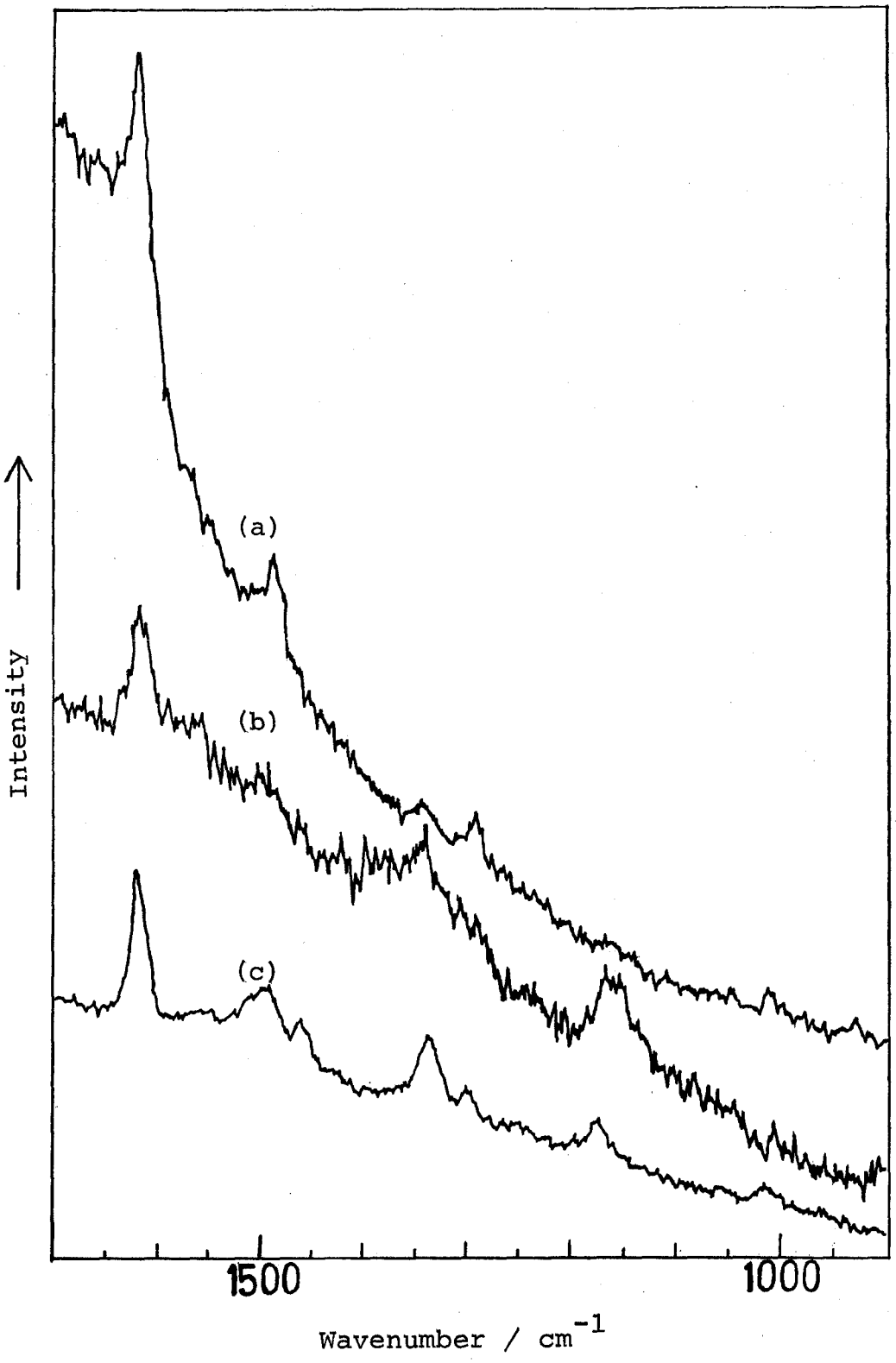

Fig. 6. Resonance Raman spectra of rose bengal: (a) aqueous solution of the dye, (b) the dye adsorbed on the ZnO sinter, (c) zinc salt of the dye.

Fig. 6. This suggests that the dye is bonded to the surface zinc ion. The Coulombic force between the zinc ion and the anionic dye is thought to act as the driving force for the bond formation. The result that ethyl eosin, which has no anionic carboxyl group, shows the same Γ_o value with those of the other xanthene dyes (Table 1) indicates that the Coulombic force due to the carboxyl group is not important for the adsorption of the dye. Therefore, the dyes are concluded to be adsorbed on the surface zinc ion at the negatively charged xanthene ring. The van der Waals force may also participate in the bonding as discussed above.

2. Since the iso-electric point of ZnO has a relatively high value, i.e., 9.2[6], the surface potential of ZnO in neutral and acidic solutions are mostly determined by the number of surface zinc ions, and the change of U_{fb} is expected to be proportional to the change of the number of surface zinc ions. Therefore, the similarity between the Γ-pH and U_{fb}-pH curves leads us to conclude that the surface zinc ion works as the adsorption site for the dye.

3. On the assumption that the change of U_{fb} with the pH in neutral and acidic solutions is determined by the change of the number of the surface zinc ion, and that a dye is adsorbed on a surface zinc ion, the capacity at the ZnO/electrolyte interface can be written as

$$e\,\Delta\Gamma_n = C\,\Delta U_{fb} \qquad (9)$$

where e is the elementary electric charge, Γ_n the number of the adsorbed dyes on the electrode per unit area, and C the capacity at the electrode/dye solution interface. The capacity at ZnO/ rose bengal solution interface is calculated to be ca. 0.6 F m^{-2} from Eq. 9, by using the values shown in Figs. 5 and 6 and by assuming the roughness factor of 2 for the surface. The number of the dyes adsorbed on the ZnO sinter is obtained from the absorbance of the dye with the molar extinction coefficient of 1.0×10^5 M^{-1} cm^{-1}. Here, the light absorption is assumed to be twice that of the single transmission of the dye layer in the measurement of the diffuse reflectance spectra, because the light is reflected at the grain boundaries in the bulk of the sinter. Blok and de Bruyn[7] determined the capacity at the ZnO/0.1 M $NaNO_3$ interface to be ca. 0.5 F m^{-2} from the potentiometric titration method. The approximate agreement of this value with that derived from Eq. 9 also substantiates the adsorption model for the dye.

The pH Dependence of the Photocurrent Sensitized by Rose Bengal.

The photocurrent sensitized by rose bengal was found to increase by lowering the pH of the solution as shown in Fig. 5c. The i_{dye} observed over the pH range from 4 to 10 is approximately proportional to the amounts of the dye adsorbed

on the ZnO electrode (see Figs. 5a and 5c). Since the absorbance due to the adsorbed dye is quite low, the number of photons absorbed by the dye can be approximated to be proportional to the amount of the adsorbed dyes. Therefore, the proportionality between the i_{dye} and Γ indicates that the quantum efficiency of the photocurrent is independent of the pH of the solution. Spitler and Calvin[8] also reported that the quantum efficiency for the TiO_2-rose bengal system was unchanged by the pH. These results are in contradiction to those reported by the previous authors for other dyes.[1,2,9] We have reexamined some of the systems similar to those reported by them, and found that the quantum efficiencies are independent of the pH, in contrast with their reports. This will be described in section 3.

The quantum efficiency of the photocurrent for the ZnO-rose bengal system is calculated to be ca. 28 % from the results shown in Fig. 5 and the number of photons passed through the dye layer. This value nearly agrees with that determined from the decay curve of the photocurrent (chapter 2). The photocurrent is most probably caused by the electron transfer from the lowest vacant orbital of the dye to the 4s orbital of the surface zinc ion. Conceivably, the relatively high quantum efficiency observed in this system arises from the fact that the dye is directly coordinated with the surface zinc ion. Since the 4s orbital of the zinc ion con-

stitutes the conduction band of zinc oxide,[10] it is expected that the electron is injected toward the bulk of the semiconductor efficiently.

The Effect of Salts in the Solution on the Photocurrent and on the Adsorption of the Dye.

The addition of potassium nitrate and potassium perchlorate into the solution caused no significant effect on the dye adsorption and the photocurrent when the concentration of the salts is lower than 0.1 M. However, with the addition of cyanide, ferrocyanide, and phosphate salts, both the amount of adsorbed dye and the photocurrent decreased drastically as shown in Fig. 7. These are attributable to the adsorption of the anions (CN^-, $Fe(CN)_6^{4-}$, and PO_4^{3-}) on the surface zinc ion competing with the dye adsorption, because the anions are known to cause stable complexes with zinc ion. Spitler et al.[11] reported that the quantum efficiency of i_{dye} for ZnO-rose bengal was decrease by the addition of $Fe(CN)_6^{4-}$. They attributed this effect of $Fe(CN)_6^{4-}$ to its quenching of the triplet state of the dye. However, our results show that the quantum yield is hardly affected by the addition of the ion at the concentrations lower than 1×10^{-4} M. Consequently, the $Fe(CN)_6^{4-}$ ion is concluded to inhibit the adsorption of the dye in the same manner as the CN^- and PO_4^{3-} ions.

On the other hand, the dye adsorption is enhanced by the addition of multivalent metal cations such as Al^{3+}, Gd^{3+}

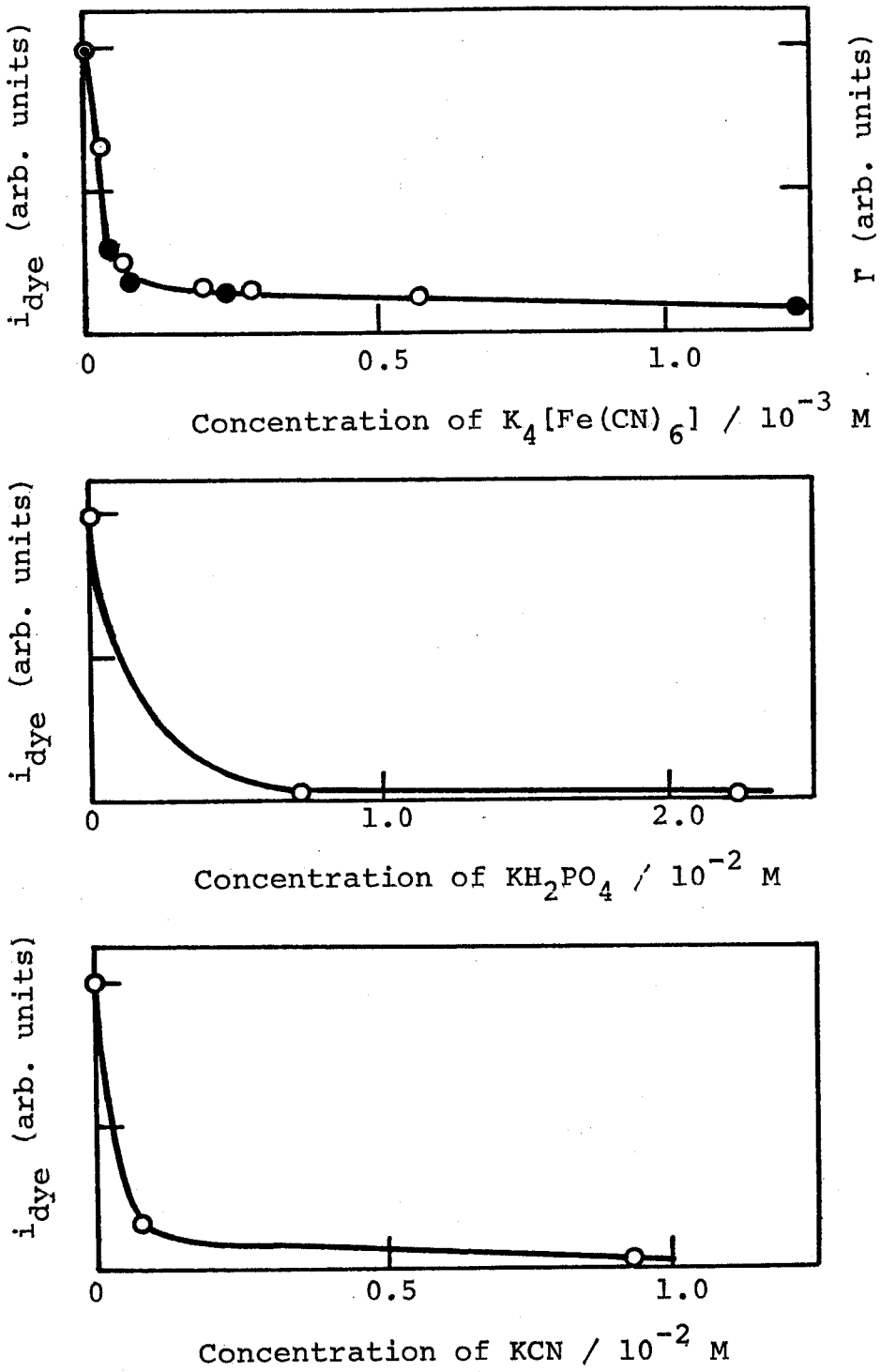

Fig. 7. The adsorption of rose bengal on the ZnO sinter (●), and the sensitized photocurrent (○) vs. the concentration of $K_4[Fe(CN)_6]$ (a), KCN (b), KH_2PO_4 (c): rose bengal, 1×10^{-5} M; U, 0.3 V vs. SCE.

Ni^{2+}, Cu^{2+} as shown in Fig. 8a for the case of Al^{3+} ion for example. The metal cations are expected to be adsorbed on ZnO surface, causing the accumulation of positive charge density at the surface. Therefore, the anionic dyes will be attracted by the Coulombic force of the cationic charge toward the surface (Fig. 9). However, the photocurrent does not increase in porportion to Γ as shown in Fig. 8b, the small increase of i_{dye} by the addition of $Al(NO_3)_3$ being attributable to the change of the pH of the solution. The number of surface zinc ions, $\geq Zn^+$, is not expected to be affected by the addition of the metal cations, unless the capacity at the ZnO-electrolyte interface is drastically changed, because the potential determining ions for ZnO are the hydrogen and hydroxyl ions. From these results, we may conclude that the excessive dyes adsorbed on ZnO are mostly attached on the multivalent metal cations and are ineffective for the photocurrent.

When the concentration of the dye was low, however, the photocurrent was enhanced by the addition of the multivalent metal cations to within the saturation value at high dye concentration. The effect is especially strong for the photocurrent caused by the dyes with small heats of adsorption, such as uranin and eosin Y. These results are attributable to the enhanced adsorption brought about by the Coulombic force between the dye and metal cations adsorbed on ZnO.

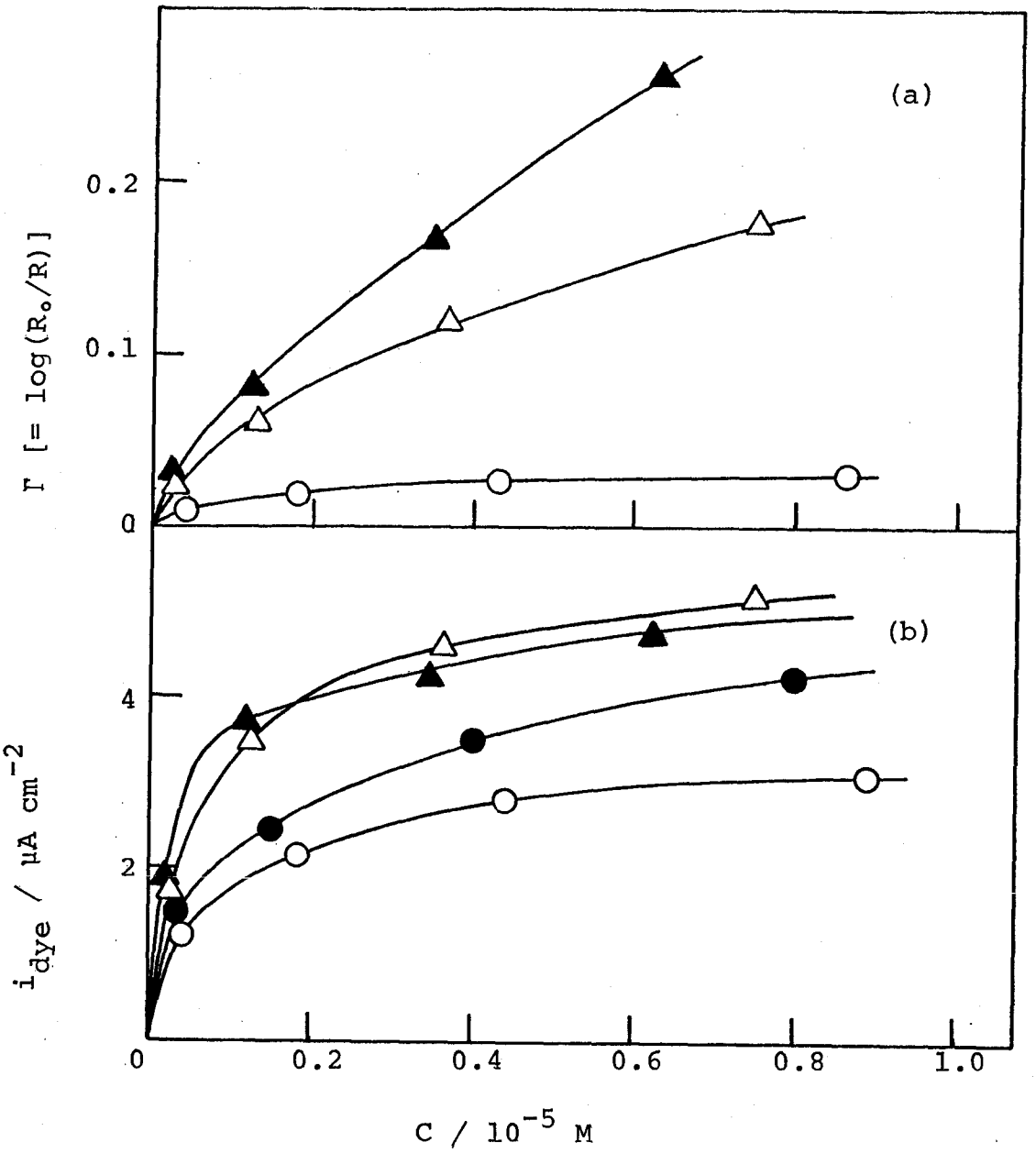

Fig. 8. The effect of $Al(NO_3)_3$ on the adsorption of rose bengal (a), and the sensitized photocurrent (b): rose bengal, 1×10^{-5} M; KNO_3, 0.1 M; U, 0.2 V vs SCE; ○, 0 M $Al(NO_3)_3$ (pH 6.0); ●, 2×10^{-5} M $Al(NO_3)_3$ (pH 4.9); △, 1×10^{-4} M $Al(NO_3)_3$ (pH 4.7); ▲, 1×10^{-3} M $Al(NO_3)_3$ (pH 4.4).

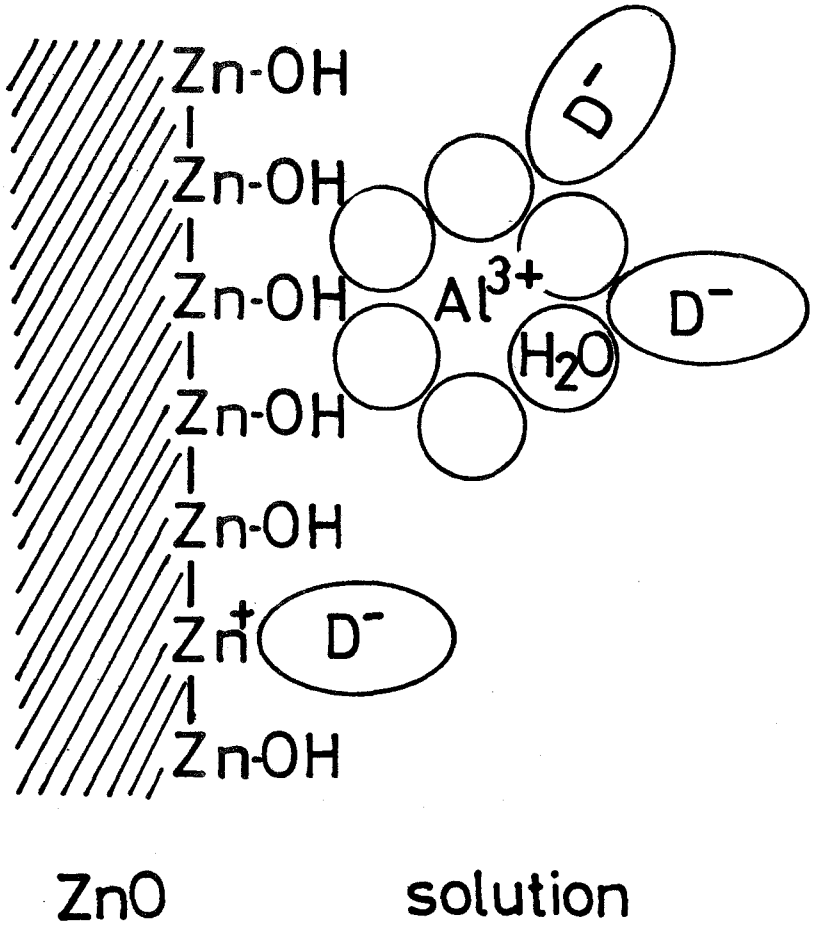

Fig. 9. A model for the adsorption of rose bengal (D^-) on ZnO from an aqueous solution containing the aluminum ion.

2. The Dye-sensitization Effect on the CdS and TiO_2 Electrodes.

The flat band potential of the CdS electrode with the $(11\bar{2}0)$ face exposed was constant at the pH increasing to 10, beyond which it decreased as shown in Fig. 10 a. The constancy of the U_{fb} on pH over such a wide pH range indicates that the potential determining ions for CdS are not hydrogen and hydroxyl ions but cadmium and sulfide ions.[12] The similar result has been reported for the (0001) face of CdS by Watanabe et al.[13] At a higher pH range, the hydroxyl ion will diminish the surface cadmium ion, $\gtrless Cd^+$, and decrease the U_{fb} according to the following equilibrium.

$$\gtrless Cd^+ + OH^- \rightleftarrows \gtrless CdOH \qquad (11)$$

The photocurrent sensitized by rose bengal and the amount of the dye adsorbed on the surface of CdS also depend on the pH, in a manner similar to that of the flat band potential as shown in Fig. 10 b and c. By comparison of the i_{dye} -pH to Γ-pH curves, the quantum yield is found to be ca. 18 %, being hardly affected by the pH. These results suggest that the dye is adsorbed on the positive site of the surface, i.e., $\gtrless Cd^+$, as in the case of ZnO.

The density of the photocurrent sensitized by rose bengal on the $(000\bar{1})$ face was found to be only one-tenth that observed at (0001) and $(11\bar{2}0)$ faces. This result is explained by taking account of the difference in the surface structures of CdS

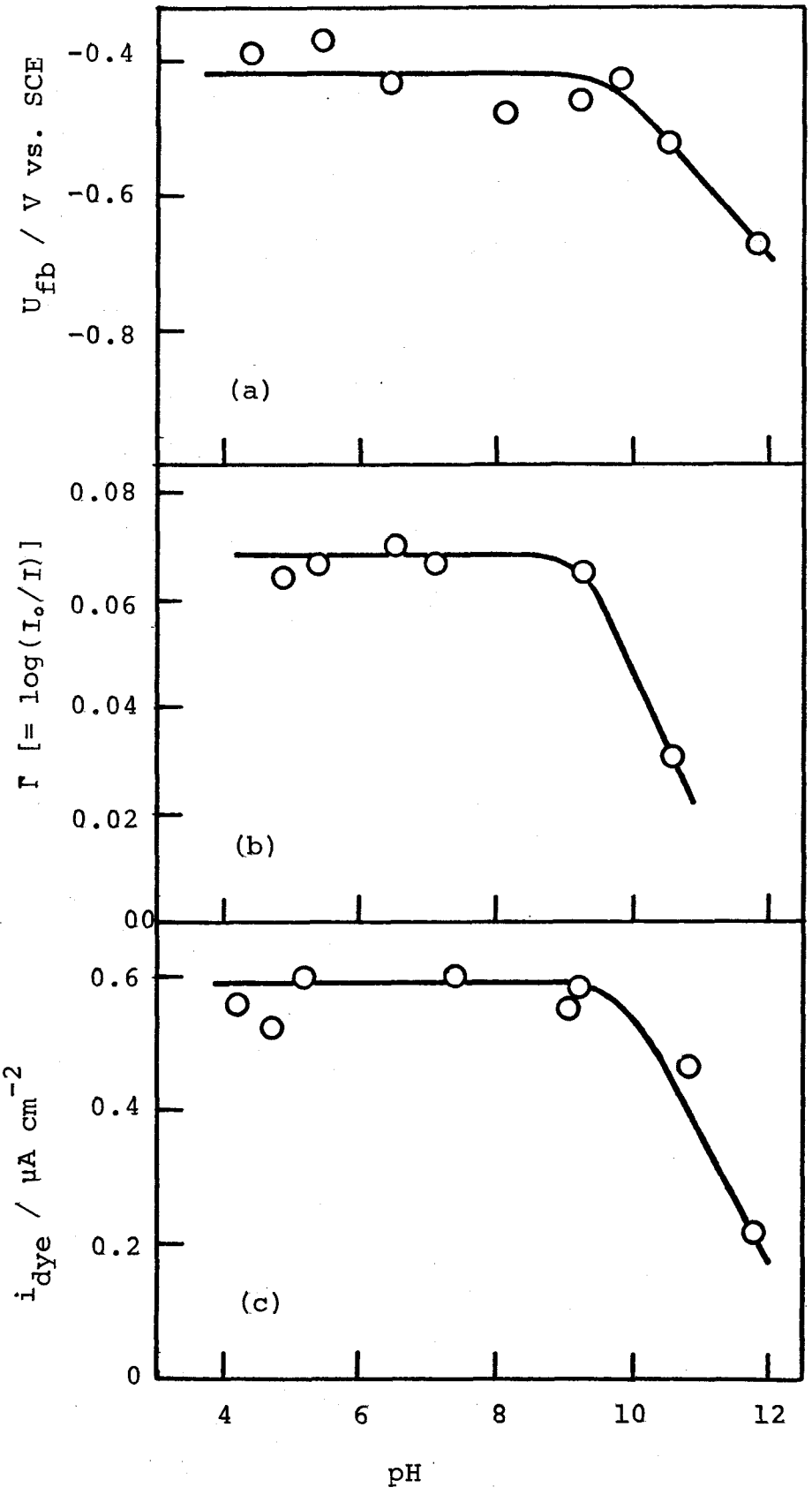

Fig. 10. The pH-dependence of the flat band potential of the CdS electrode (a), the adsorption of rose bengal on a CdS crystal (b), and the sensitized photocurrent at the electrode potential of 0.6 V vs SCE (c): rose bengal, 1 x 10^{-5} M; KNO_3, 0.1 M; crystal face ($11\bar{2}0$).

crystal at the three crystal faces. Since the cadmium atoms are buried under the sulfur atoms at the $(000\bar{1})$ face, the low current density at this face is attributable to the lack of the adsorpiton site, i.e., $\gtrless Cd^{+}$, on the crystal face. The difference in the density of the photocurrents at the crystal faces was observed only when the electrodes were etched in 2 N HCl for less than 15 minutes. By etching the electrodes in a more concentrated acid, the surface became rough and the difference in the photocurrents disappeared. The difference in the behavior of the CdS electrodes at (0001) and $(000\bar{1})$ faces was reported also by Tsuiki et al.[13] in the study of the flat band potential.

For the case of the TiO_2 electrode, the i_{dye} and Γ increased as the pH decreased (Fig. 11). The quantum yield was not affected by the pH of the solution as reported by Spitler and Calvin.[8] These results are similar to those obtained for the ZnO electrode. However, the increase of i_{dye} and Γ occurred at a lower pH than that observed for the ZnO electrode. This difference between the TiO_2 and ZnO electrodes probably arises from the difference in the acid-base dissociation equilibria at the surfaces of the electrodes. Since the iso-electric point of TiO_2 is ca. 4.5 lower than that of ZnO, the formation of the positive site, adsorption site, on TiO_2 takes place at a lower pH region than for ZnO.

The quantum efficiency of the photocurrent sensitized by

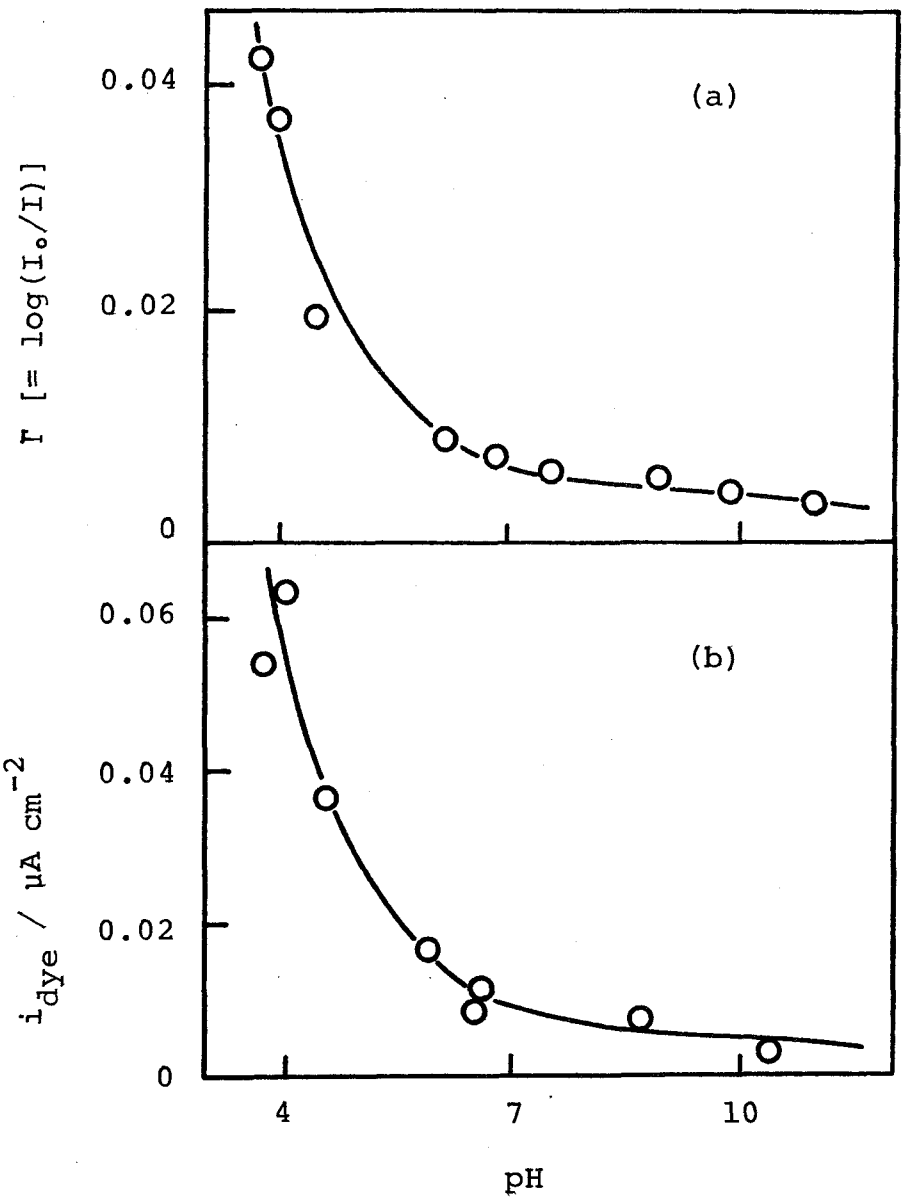

Fig. 11. The pH-dependence of the adsorption of rose bengal on a TiO_2 crystal (a), and the sensitized photocurrent at the electrode potential of 0.5 V vs SCE (b): rose bengal, 1 x 10^{-5} M; KNO_3, 0.1 M.

rose bengal is ca. 1.5 %, about one-fifteenth that for ZnO. Such a difference in quantum efficiency between the TiO_2 and ZnO electrodes might be due to the difference in the structure of the adsorbed dye on the two electrodes, and possibly the difference in the position of the electron accepting levels on the electrodes.

3. The Photocurrent in the ZnO Electrode Sensitized by Zwitter-ionic and Cationic Dyes.

The aqueous solutions of zwitter-ionic and cationic dyes caused the precipitates on standing, when halide salts were added into the solution. Therefore, unless otherwise stated, the photocurrent and the adsorption were measured with freshly prepared solutions. The solutions were prepared by adding halide salts or supporting electrolytes into the dye solution, whose pH had been adjusted by addition of KOH and HNO_3 solutions.

As Fig. 12 shows, the photocurrents sensitized by rhodamine B and rhodamine 6G have maxima at the pH of 7 and 10, respectively, in contrast to the case of the anionic xanthene dyes (section 1). The amounts of the adsorbed dyes on ZnO sinter were approximately proportional to i_{dye}. The pH dependences of Γ and i_{dye} suggest that the adsorption sites for the zwitter-ionic and cationic dyes are different

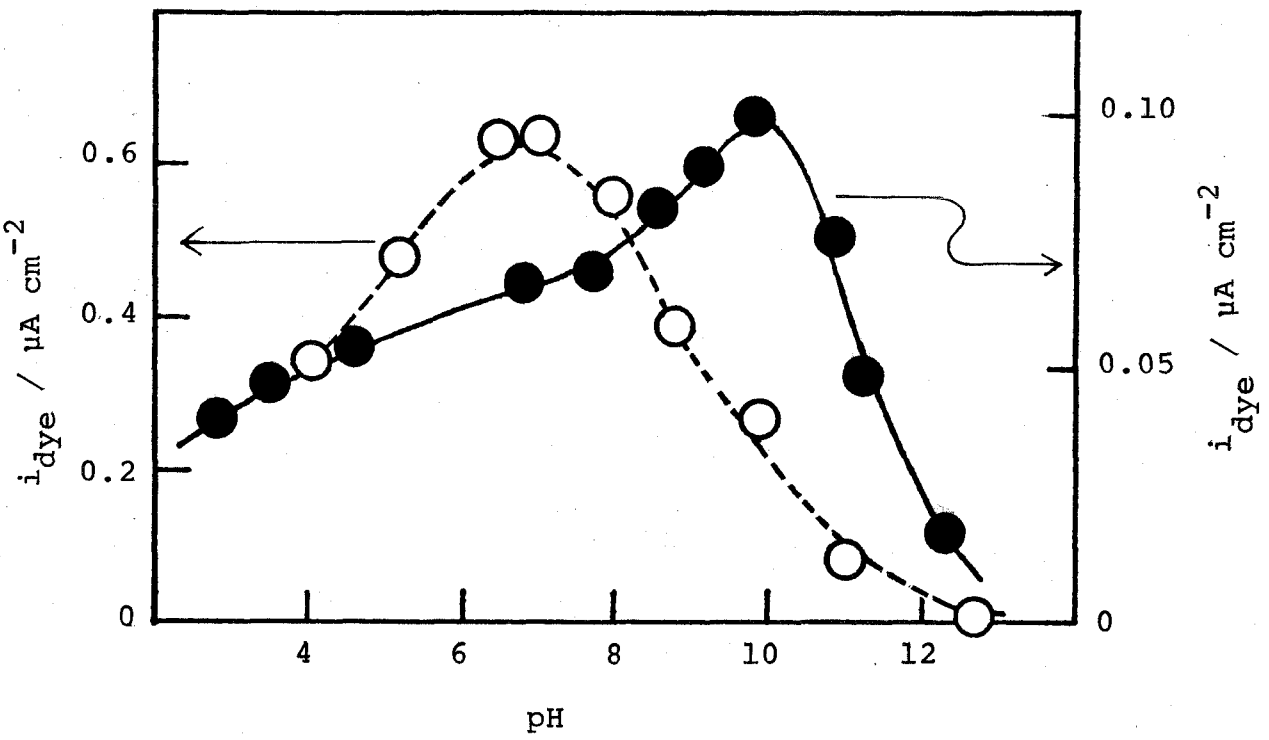

Fig. 12. The pH-dependence of the dye-sensitized photocurrent at the ZnO electrode: ○, rhodamine B (1.6×10^{-5} M, λ 556 nm); ●, rhodamine 6G (1.5×10^{-5} M, λ 540 nm); KNO_3, 0.1 M; U, 0.5 V vs SCE.

from those for anionic xanthene dyes.

The i_{dye} sensitized by rhodamine B in the acidic solution is enhanced by the addition of halide salts as shown in Fig. 13 a. The apparent quantum yield of the photocurrent observed in the presence of 1.0 M KI reaches ca. 2.5 % at pH 2.0. Certainly, this effect of the halide salts comes from the enhanced dye adsorption on ZnO, as Γ also increases approximately proportionally to i_{dye} as shown in Fig. 13.

The acidic solutions of rhodamine B containing halide salts caused precipitates gradually. The photocurrents became as low as those without the halides, when they were measured by use of the solutions which had been left standing for several hours. Therefore, it is probable that the photocurrent enhancement is due to the deposition of the dye on the electrode from the supersaturated dye solution (salting out). The solubility of rhodamine B in the solution containing halide salts decreases as the pH decreases, as shown by the solid line in Fig. 14. This result explains the enhanced photocurrent in the acidic solution. On the other hand, the solubility of rhodamine 6G, whose structure has no singificant difference from that of rhodamine B except for the esterification of the carboxyl group, is lower than that of rhodamine B by a factor of 10 - 100, over the pH range 3 to 11.

As has been mentioned before, in the case of the anionic xanthene dyes, the photocurrent scarcely increased, even if

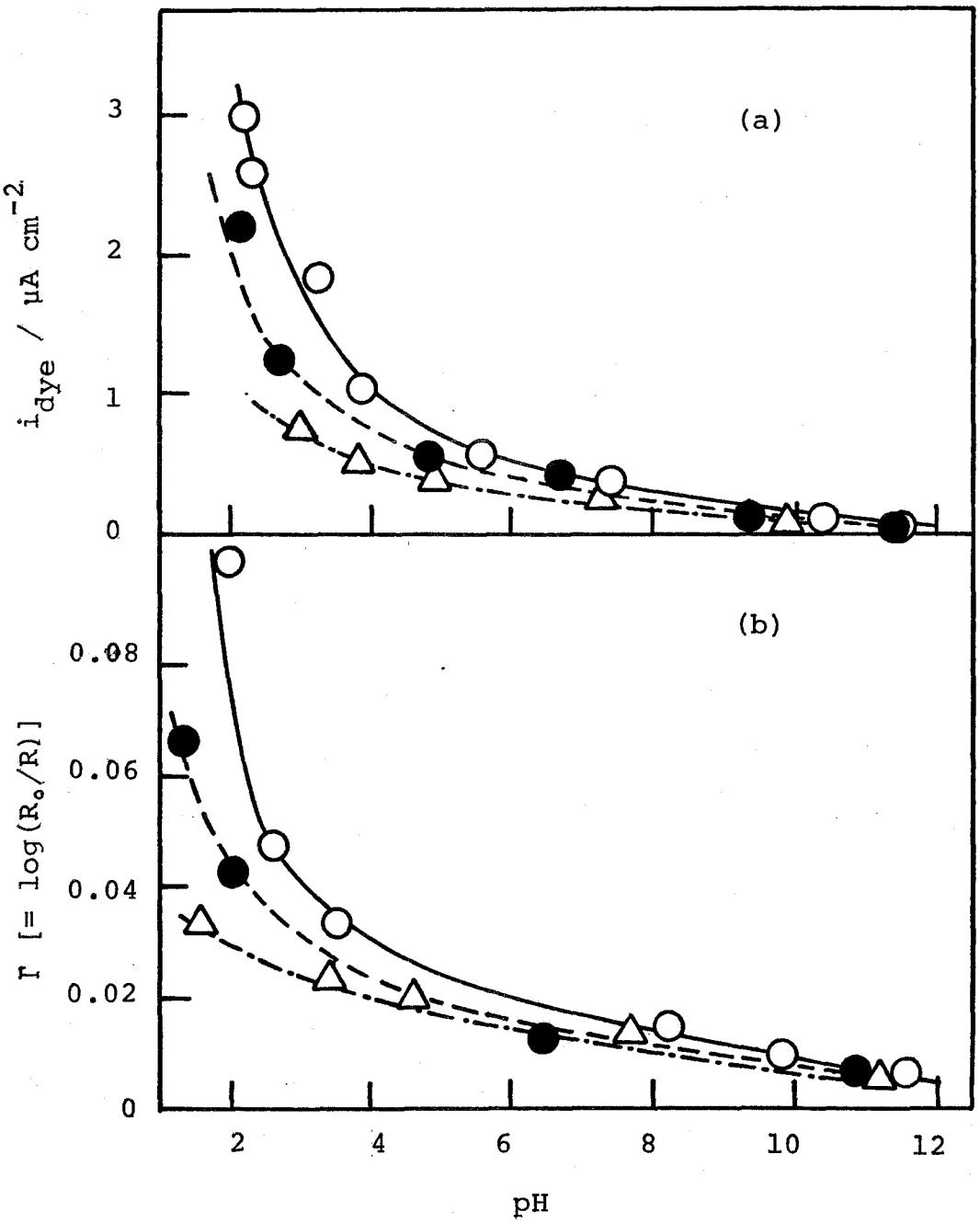

Fig. 13. The effect of alkali halides on the photocurrent sensitized by rhodamine B (a), and the adsorption of the dye on the ZnO sinter (b): rhodamine B, 2 x 10^{-5} M; ○, 1M KI; ●, 1 M KBr; △, 1 M KCl.

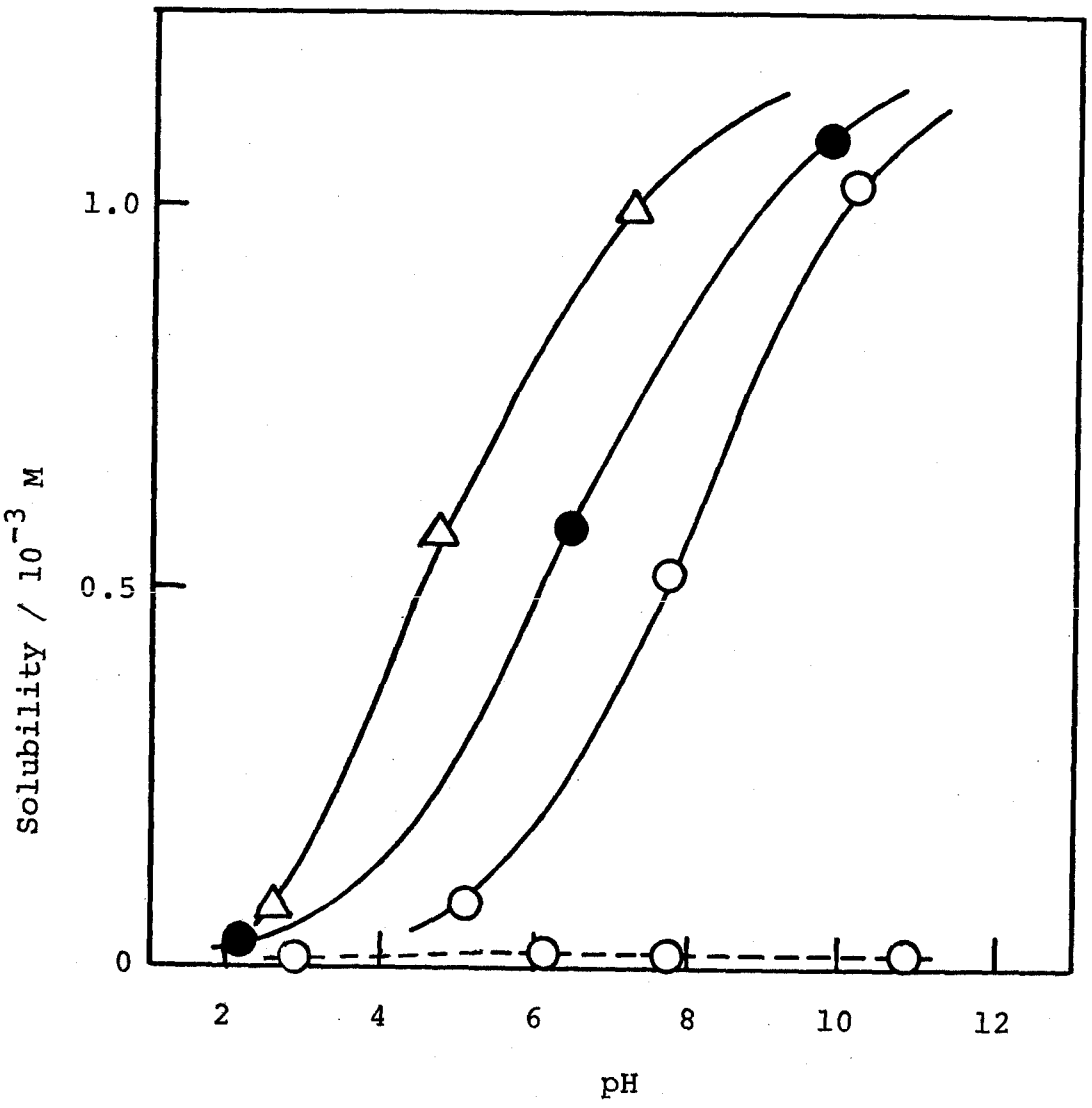

Fig. 14. The pH-dependence of the solubility of rhodamine B (———) and rhodamine 6G (-----) in the aqueous solution containing alkali halides: ○, 1 M KI; ●, 1 M KBr; △, 1 M KCl

the dye adsorption on the electrode was increased beyond the saturation value for the adsorption equilibrium by addition of metal cations (Figs. 8 and 9), or by using an electrode thickly covered with the dye by the spraying method. The enhancement of the photocurrent, in the case of the deposited rhodamine B, might be due to the crystallization of the dye, the regular array of the dye being favorable to the energy transfer.

The action spectrum of the photocurrent enhanced by the halide salts shifts by ca. 25 nm toward longer wavelength from that observed in a neutral 0.1 M KNO_3 solution, accompanied a minor change in the intensity ratio of the shoulder with respect to the maximum as shown in Fig. 15. The change of the action spectra is probably caused by the formation of the dye aggregates on the ZnO surface.

That a high i_{dye} is produced by the aggregate is favorable for a solar cell. However, in this case the suppression of the decay of i_{dye} by the reducing agent is found to be more difficult than in the case of the monomer dyes, probably because of a low electron mobility in the dye aggregate.

Bode et al.[3,14] also reported an increase of i_{dye} by the addition of halide salts into a buffered solution of pH 4.6. Daltrozzo and Tributsch[2] observed that the i_{dye} in 1.0 M KCl solution increased at lower pH. These authors attributed the increase of i_{dye} to an increased quantum efficiency of

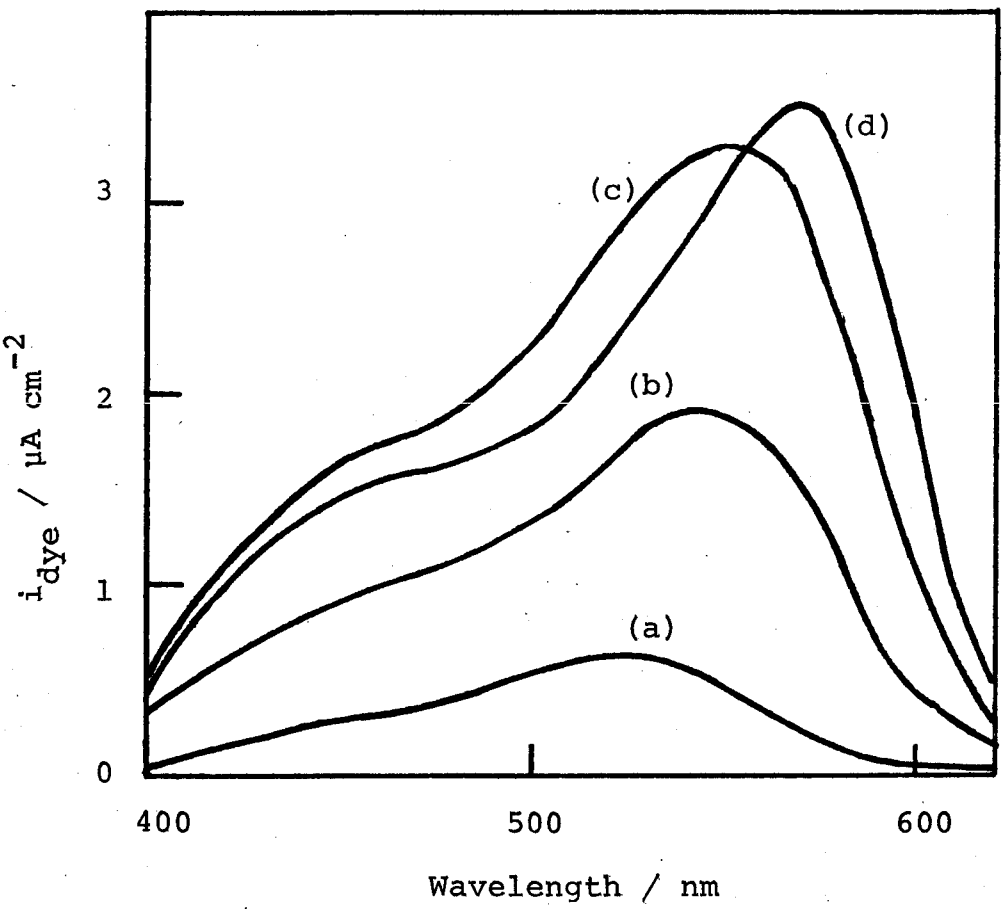

Fig. 15. Action spectra of the photocurrent sensitized by rhodamine B observed at the ZnO electrode in the aqueous solution of 1 M KI: (a) pH 7.4; (b) pH 3.2; (c) pH 2.1; (d) pH 0.9; U, 0.5 V vs SCE.

electron injection from the exited dye, caused by the decrease of the energy barrier (Tributsch) or a formation of reduced dye or triplet state of the dye by the interaction between the dye in the excited singlet state and halide ions (Bode). However, their conclusions should be reexamined, since they were drawn by assuming that Γ was not affected by the addition of the salts or the change of pH

The photocurrent sensitized by 1, 1'-diethyl-2, 2'-cyanine, which is a cationic dye, shows a pH dependence similar to that for rhodamine 6G, as shown by a broken line in Fig. 16 b. The photocurrent is about a hundred times as low as that for rose bengal, and was enhanced by the addition of alkali halides, with the formation of the J-aggregate as was reported by Tributsch[15], and Honda et al.[16] The action spectra of the photocurrents caused by the monomeric dye and the J-aggregate are shown in Fig. 17. Much less photocurrent due to the J-aggregate was observed for an electrode immersed in a solution of the dye and alkali halide, which had been left standing for several hours, as shown in Fig. 16 b. In such a solution the precipitate of the dye was gradually formed, whose reflection spectrum was practically identical to the absorption spectrum of the J-aggregate. From these results, we can conclude that the J-aggregate is generated from a supersaturated dye solution as in the case of the deposition of rhodamine B.

The i_{dye} and Γ due to the J-aggregate increased as the

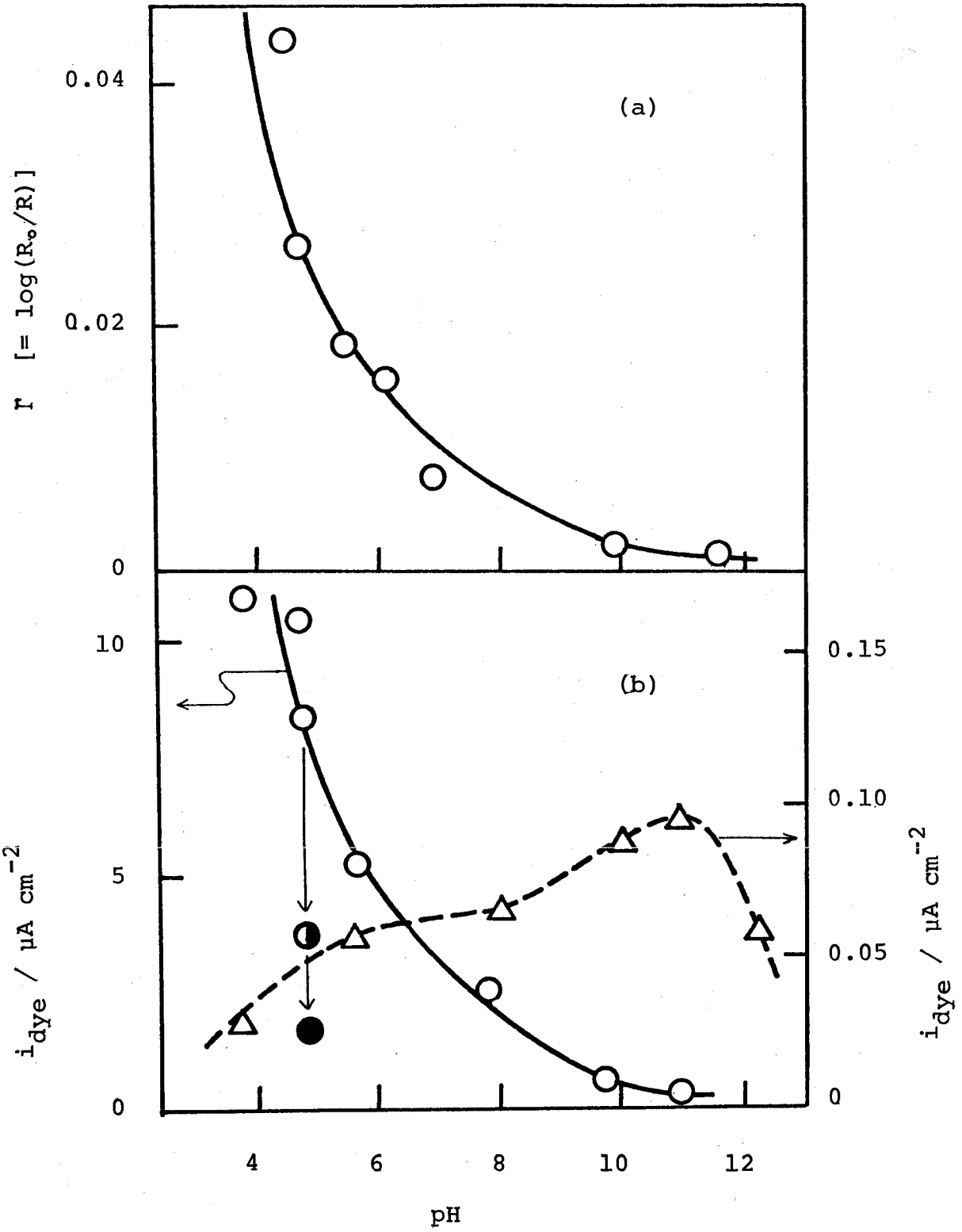

Fig. 16. The pH-dependence of the adsorption of 1,1'-diethyl-2,2'-cyanine (3×10^{-5} M) on the ZnO sinter (a), and the sensitized photocurrent at the electrode potential of 0.3 V vs. SCE (b): ○, 0.5 M KBr; △, 0.02 M KNO_3; ◑ and ● are plotted for the values observed in 0.5 M KBr after the solution is permitted to stand for 6 and 48 hours, respectively.

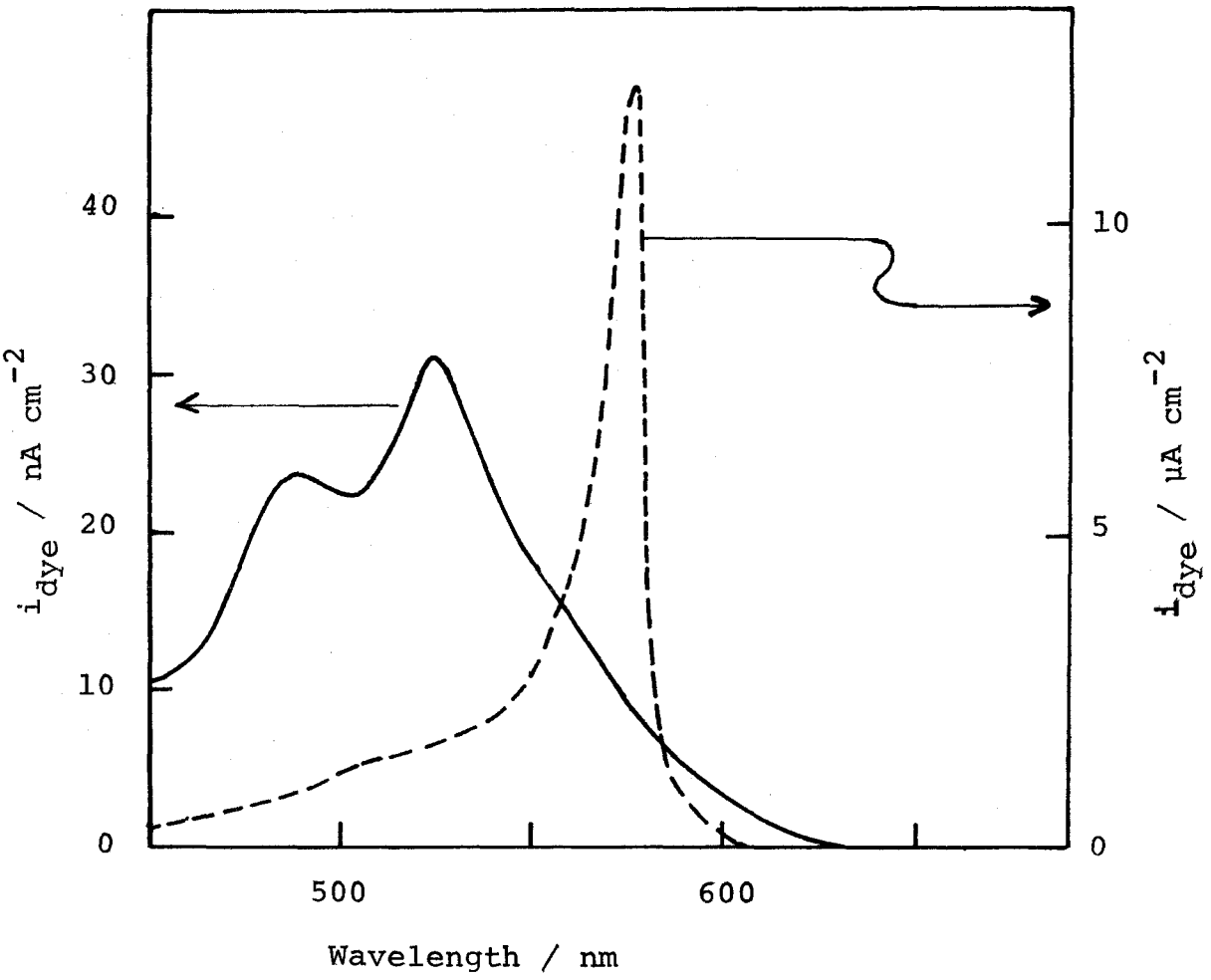

Fig. 17. Action spectra of the photocurrents at the ZnO electrode sensitized by 1,1'-diethyl-2.2'-cyanine (3×10^{-5} M): U, 0.5 V vs SCE; ———, 0.02 M KNO_3; -----, 0.5 M KBr.

pH became lower as shown by solid lines in Fig. 16, whereas the solubility was hardly affected by the pH. The result indicates that the quantum efficiency of the photocurrent is almost independent of the pH. The formation of the J-aggregate on the ZnO surface seems to be promoted in an acidic solution.

From the results shown in this chapter, the pH dependence of the photocurrents sensitized by the anionic, cationic, and zwitter-ionic dyes are concluded to be mostly due to the change in the amount of the dyes adsorbed on the semiconductor electrodes. On the other hand, some of the previous authors[1,2,9] usually attributed the pH dependence of the photocurrents to the change of the quantum efficiency for several semiconductor-dye systems similar to those handled in this chapter, e.g., ZnO-rhodamine B, TiO_2-1, 1'-diethl-2,2'-cyanine, etc. They explained the effect on the basis of the pH-dependent change of the flat band potential of the semiconductors, which affected the quantum efficiency of the electron injection by changing the potential difference across the electric double layer (Helmholz layer) between the semiconductor and the dye in the solution. Such a conclusion seems to be due to their incorrect assumptions that the adsorption is not affected by the pH or by the structure of the adsorbents. On the basis of our results derived from the measurements of the dye adsorption on the semiconductors, the electron injection is

concluded to be hardly affected by the change of the potential difference across the Helmholz layer.

References

1) T. Watanabe, A. Fujishima, O. Tatsuoki, and K. Honda, Bull. Chem. Soc. Jpn., 49, 8 (1976).

2) E. Daltrozzo and H. Tributsch, Photogr. Sci. Eng., 19, 308 (1975).

3) U. Bode, K. Hauffe, Y. Ishikawa, and H. Pusch, Z. Phys. Chem. N. F., 85, 144 (1973).

4) T. Tani, S. Kikuchi, and K. Hosoya, Kogyo Kagaku Zasshi, (J. Chem. Soc. Jpn. Ind. Chem. Sec.), 70, 2216 (1967).

5) F. Lohmann, Ber. Bunsenges. Phys. Chem., 70, 428 (1966).

6) G. A. Parks, Chem. Rev., 65, 177 (1965).

7) L. Blok and P. L. de Bruyn, J. Colloid Interface Sci., 32, 533 (1970).

8) M. T. Spitler and M. Calvin, J. Chem. Phys., 66, 4294 (1977).

9) W. D. K. Clark and N. Sutin, J. Am. Chem. Soc., 99, 4676 (1977).

10) F. J. Morin, in "Semiconductros" ed. N. B. Hannay, Reinhold, New York (1959).

11) M. Spitler , M. Lübke, and H. Gerisher, Chem. Phys. Lett., 56, 577 (1978).

12) H. Minoura, T. Watanabe, T. Oki, and M. Tsuiki, Japan J. Appl. Phys., 16, 865 (1977).

13) T. Watanabe, A. Fujishima, and K. Honda, Chem. Lett., 1974, 897.

14) U. Bode and K. Hauffe, J. Electrochem. Soc., 125, 51 (1978).

15) H. Tributsch, Ber. Bunsenges. phys. Chem., 73, 582 (1969).

16) A. Fujishima, T. Watanabe, O. Tatsuoki, and K. Honda, Chem. Lett., 1975, 13.

CHAPTER 4

Effect of Etching on Intrinsic and Dye-sensitized Photocurrents in Zinc Oxide Electrodes

Introduction

The photocurrent arising from the band-gap excitation of the semiconductor electrode is referred to as the intrinsic photocurrent, i_{int}, of the semiconductor electrode. Both of the intrinsic and dye-sensitized photocurrents of the semiconductor electrode are expected to be sensitive to the surface treatment of the semiconductor, because the electron transfer at the electrode-solution interface is often the rate-determining step. In this chapter, the effect of grinding and etching of the ZnO electrode on the photocurrents will be discussed. The abrading of the semiconductor produces localized states near the surface,[1)] and the etching recovers the energy band structure of the semiconductor by dissolving the defective layers. To study the difference between the properties of the intrinsic and dye-sensitized photocurrents will help us to elucidate the characteristic nature of the dye-sensitized photocurrent, which is the main theme of the present work. The effect of reducing agents will also be discussed by the aid of models of the semiconductor electronic bands.

Experimental

The dye-sensitized photocurrents were studied in aqueous solutions of rose bengal and 0.2 M (mol dm^{-3}) potassium nitrate, the pH of the solution being 6.1. For the measurements of intrinsic photocurrents, the pH of the solution was adjusted to 7.8 with a borate buffer. Dissolved oxygen was removed by bubbling the solution with high purity nitrogen. In many cases, the zinc oxide sinter was ground with a silicon carbide abrasive (No. 2000), etched in 2 M hydrochloric acid, washed with water and dried. The method of preparation of the ZnO sinter used as the electrode and the experimental set-up for the electrochemical measurements have been described in chapter 2.

The luminescence intensity of zinc oxide sinter excited by the same light source used for the photocurrent measurements was measured by use of an RCA 1P28 photomultiplier equipped with Toshiba B46 and O52 glass filters. The luminescence spectra were measured with an Aminco-Bowman spectrofluorimeter. The absorption spectra and the diffuse reflectance spectra were measured with a Shimadzu MPS-50L spectrophotometer. The ZnO sinter was colored slightly after dipping in the dye solution. The amount of the dye adsorbed on the electrode was estimated from the diffuse reflectance spectra of the ZnO sinter taken out of the dye solution, the residual solution on the sinter being soaked with filter paper.

The differential capacitance at the semiconductor-elec-

trolyte interface was measured with a Yokogawa Hewlett-Packard 4265B universal bridge at a frequency of 1 kHz.

Results

The dye-sensitized photocurrent under steady illumination decayed exponentially during the first several seconds (curve 1, Fig. 1). The initial value of the dye-sensitized photocurrent, i°_{dye}, was determined by extrapolating the curve to zero time of the illumination. When the dye solution contained a reducing agent such as hydroquinone, allylthiourea, or potassium iodide, the decay was suppressed. In some cases the initial value of the photocurrent was enhanced as shown by curve 2 for the case of hydroquinone as a reducing agent. The decay of i_{dye} was suppressed by addition of hydroquinone or allylthiourea at a concentration as low as 5×10^{-5} M, while the increase of i°_{dye} was small at such a low concentration and reached saturation at ca. 1×10^{-3} M. In the case of iodide ion, the decay of i_{dye} was not prevented at concentrations below 5×10^{-2} M, and the increase of i°_{dye} could not be observed even at 1.0 M. The difference seems to arise from the weaker electron donor strength of the iodide ion than hydroquinone or allylthiourea. On the other hand, the intrinsic photocurrent did not decay even when the electrolyte solution contained no reducing agent, nor was it affected by the reducing

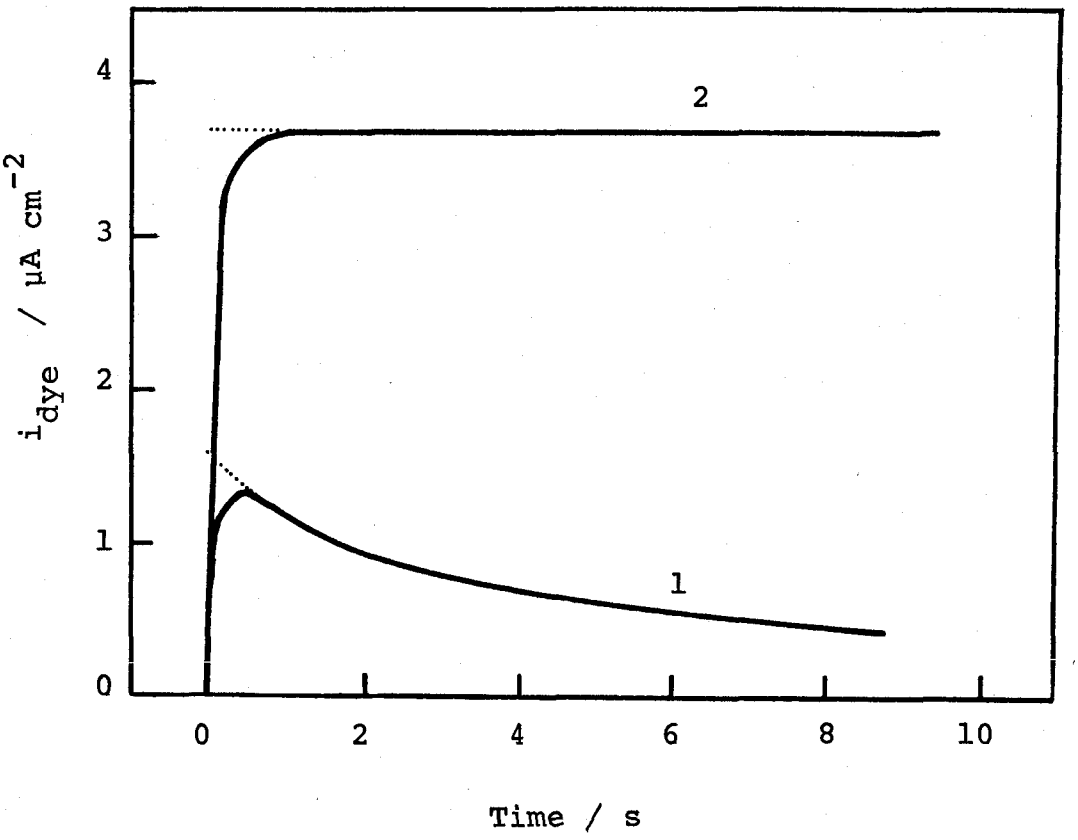

Fig. 1. Change of photocurrent vs. time for unetched electrodes in a solution of 2×10^{-5} M rose bengal at potential of 0.4 V vs. SCE. Curve 1, without hydroquinone. Curve 2, with 1.6×10^{-3} M hydroquinone.

agent.

The photocurrent-potential curves of both i_{int} and i°_{dye} for electrodes etched for various periods of time are shown in Fig. 2. The photocurrents are proportional to the illumination intensity, the shapes of the photocurrent-potential curves not being changed by decrease in the illumination intensity to 1/7. The apparent quantum efficiency of i_{int}, defined as the number of electrons flowing per the number of incident photons on the electrode, is ca. 80 % for the electrode etched for more than 120 s and polarized at a higher electrode potential than 0.3 V (vs. SCE). The onset potentials of the photocurrents did not change with etching. The flat band potentials of ZnO electrodes in the solutions used for the measurements of i_{int} and i_{dye} as determined by the Mott-Schottky plots of the differential capacitance are ca. -0.48 and -0.32 V (vs. SCE), respectively, agreeing nearly with the onset potentials of photocurrents. The donor densities were determined to be in the range 4.9×10^{22} - 7.1×10^{22} m^{-3} by assuming the roughness factor of 2 for the electrode surface.

The photocurrents observed at the electrode potential of 0.4 V (vs. SCE) are plotted against the etching time in Fig. 3. The i°_{dye} value becomes constant at an etching time much shorter than that for the i_{int}. The enhancement of i°_{dye} by hydroquinone occurs only at etching periods less than 15 s. The addition of hydroquinone up to the concentration of 10^{-2} M did not affect

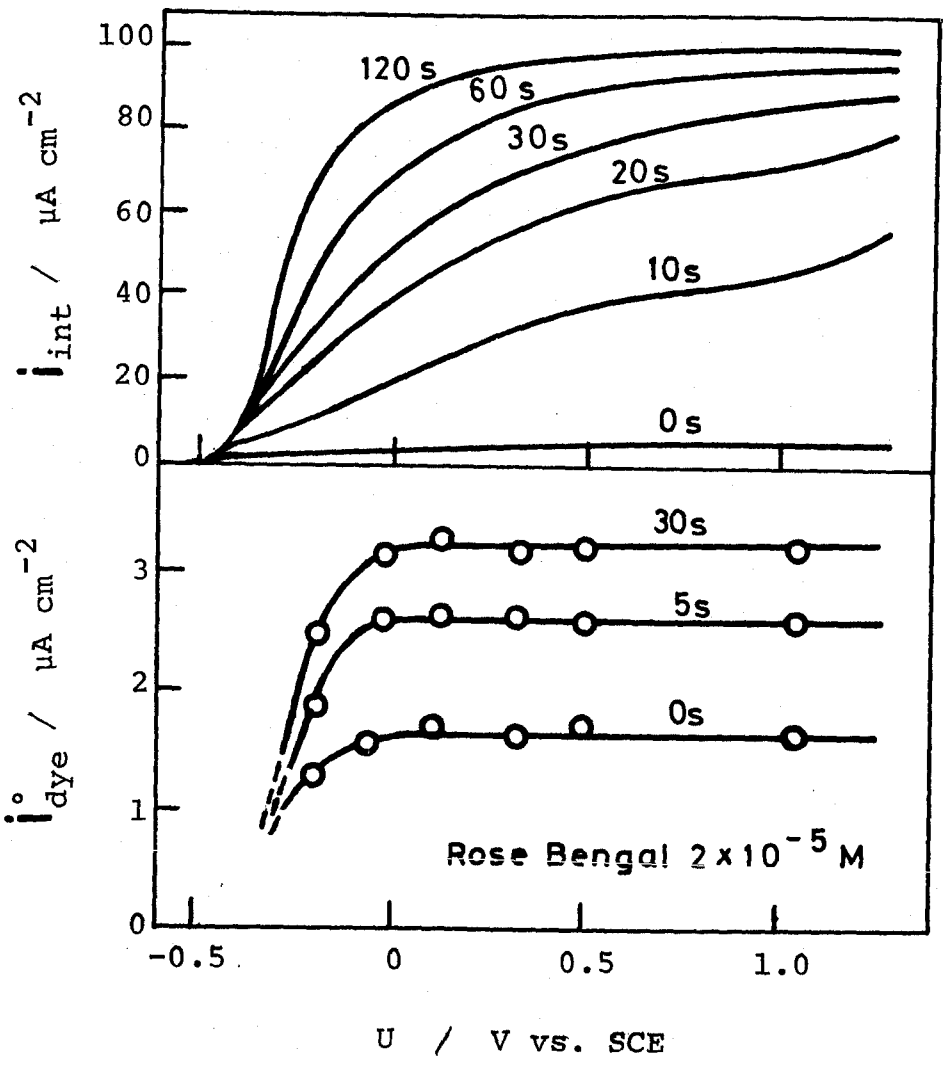

Fig. 2. Current-potential curves of (a) intrinsic photocurrents (excited at λ 360 nm) and (b) the initial values of dye-sensitized photocurrents (λ 562 nm) of ZnO electrode etched for various periods of time.

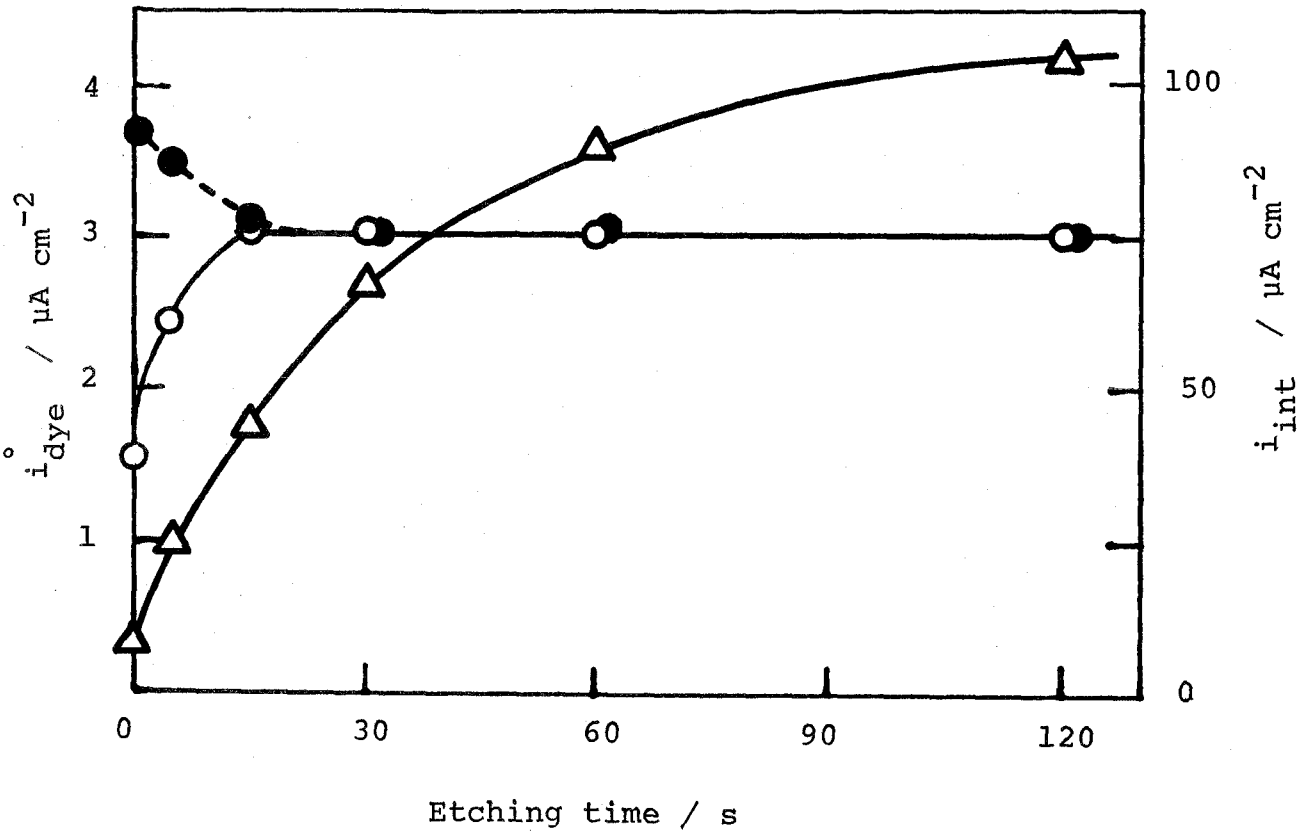

Fig. 3. The photocurrent (at 0.4 V vs. SCE) vs. etching time in the electrode ground with an abrasive.

○ : Initial values of dye-sensitized photocurrent (λ 562 nm) in the presence of 2×10^{-5} M rose bengal;

● : the dye-sensitized photocurrent obtained by addition of 1.6×10^{-3} M hydroquinone into the solution;

△ : the intrinsic photocurrent (λ 360 nm).

the adsorptivity of dye. The amount of the dye adsorbed on the electrode changed slightly by etching, being approximately proportional to the i_{dye} observed in the presence of hydroquinone. This might be due to the change of the surface area caused by etching.

The ZnO sinter emits luminescence when exposed to ultraviolet light. The emission band lies in the range 400-750 nm with a maximum near 530 nm (Fig. 4). The luminescence intensity was quenched drastically by grinding the sinter, but was gradually restored with etching. By etching for 150 s, the luminescence intensity returned to the value before grinding. Figure 5 shows the luminescence intensity at various electrode potentials. The luminescence intensity falls near the onset potential of the photocurrents, decreasing nearly to zero at potential where the i_{int} value is saturated.

By measuring the weight loss of the ZnO sinter etched in 2 M HCl, the average thickness of the ZnO sinter dissolved by the solution was determined to be 4.3 μm min^{-1}.

Discussion

Our results have revealed that there are fundamental differences between the behavior of the intrinsic photocurrent (i_{int}) and that of the dye-sensitized photocurrent (i_{dye}) :

1. The i_{int} is weakened to a greater extent than i_{dye} by

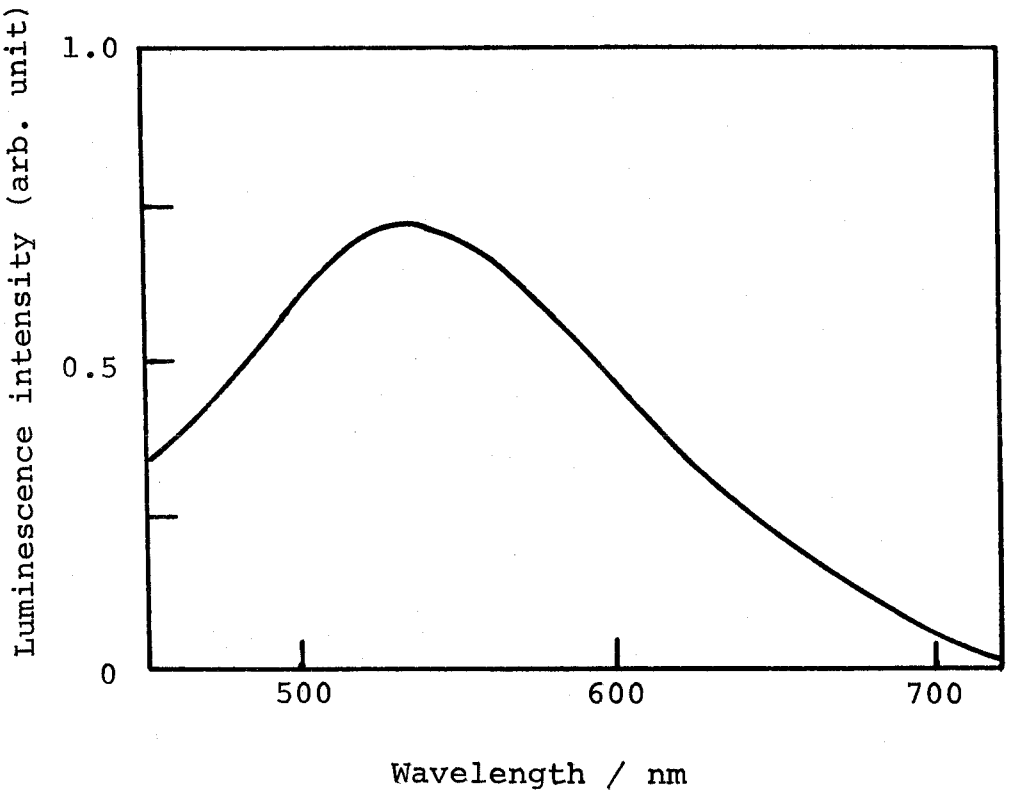

Fig. 4. The luminescence spectrum of the ZnO sinter excited at 360 nm.

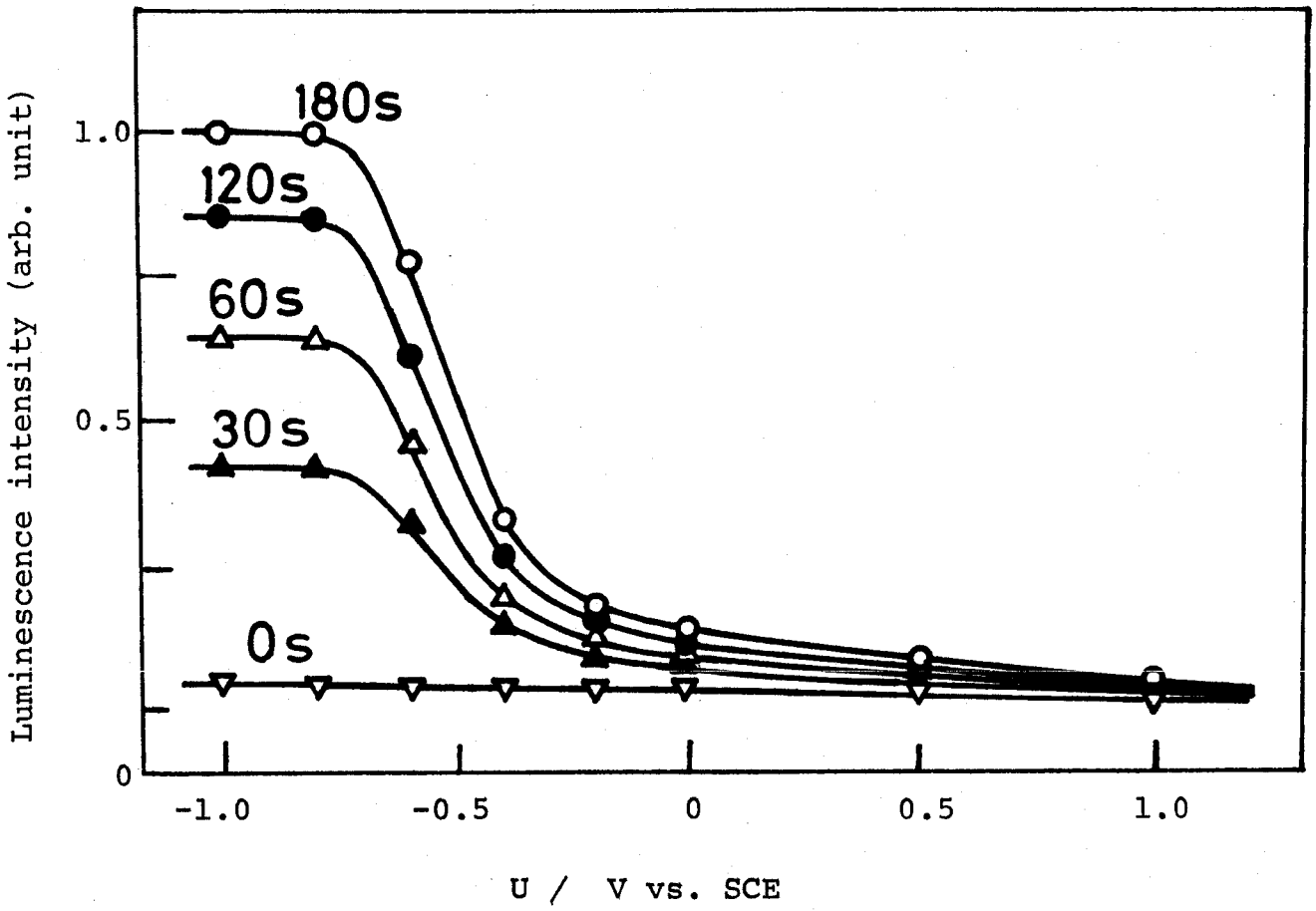

Fig. 5. The luminescence intensity of the zinc oxide electrode etched for various periods of time vs. electrode potential. The luminescence was excited at 360 nm.

grinding the electrode.

2. The increase in i_{dye} with etching reaches saturation when etching time is ca. 15 s. The i_{int} value increases much more slowly by etching, reaching saturation at ca. 120 s.

3. The i_{int} value for an insufficiently etched electrode rises gradually as the electrode becomes anodically polarized up to quite high voltages, whereas i_{dye} rises sharply and is saturated at 0.0 V (Fig. 2).

4. By addition of reducing agents to the solution, the decay of i_{dye} is suppressed. Sometimes i°_{dye} increases, whereas i_{int} is hardly affected.

Based on these results, we shall discuss the mechanism of these photocurrents.

Intrinsic Photocurrent.

The mechanism of the generation of i_{int} is shown in Fig. 6a. When an n-type semiconductor immersed in an electrolyte is polarized anodically, a potential gradient develops in the space charge layer. By the band-gap excitation, the electrons in the valence band are excited to the conduction band. The electron-hole pairs thus generated in the space charge layer are separated efficiently by the electric field.

The i_{int} value of a well-etched electrode reaches saturation at the electrode potential of ca. 0.3 V (Fig. 2). The quantum efficiency of the saturated i_{int} is regarded to be

almost 100 %,if the reflection of the incident light at the surface is taken into account.

The depth of the space charge layer, L, is approximately given by[2)]

$$L = \sqrt{2(U - U_{fb})\varepsilon\varepsilon_o/N_d e} \qquad (1)$$

where U is the electrode potential in the bulk, U_{fb} the flat band potential, ε the dielectric constant, ε_o the permittivity of vacuum, and e the elementary electric charge. The value of L is calculated to be 110 nm at the electrode potential of 0.3 V, at which i_{int} of a well-etched electrode reaches saturation, by substituting U_{fb} = -0.48 V, ε = 8.5, $N_d = 6 \times 10^{22}$ m^{-3} (the mean value of the observed donor density) into Eq. 1. On the other hand, the penetration depth of the incident light (λ 360 nm) in ZnO, defined as the distance at which the light intensity becomes 5 %, is calculated to be ca. 100 nm from the absorption constant of ca. 3×10^7 m^{-1},[3)] in good agreement with the above derived L value. The result suggests that the recombination is negligible in the space charge layer of a well-etched electrode.

On the other hand, the i_{int} value for an insufficiently etched electrode did not reach saturation even when the electrode potential was raised to 5 V (vs. SCE). This cannot be explained by the ralation between the penetration depth of the light and the depth of the space charge layer, but by taking into account the recombination center of electron-hole

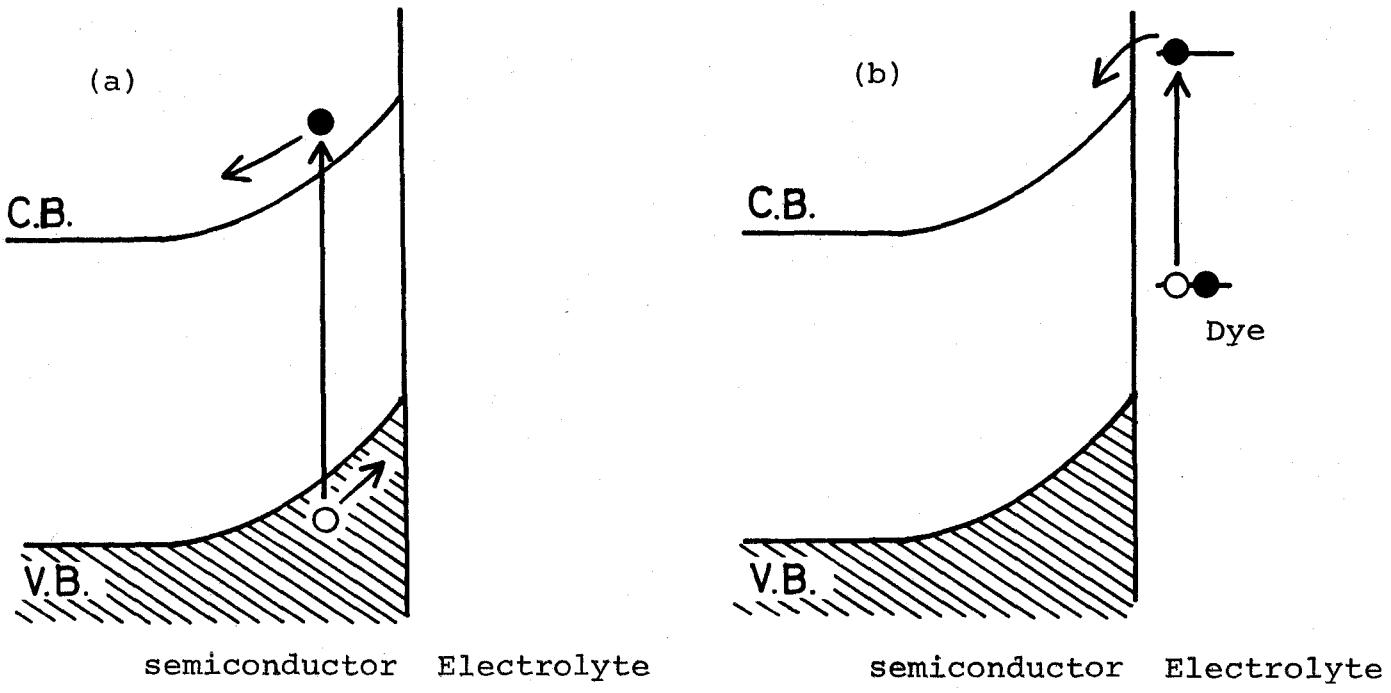

Fig. 6. The energy level diagrams of the semiconductor illustrating the mechanism of the intrinsic photocurrent (a) and the dye-sensitized photocurrent (b).

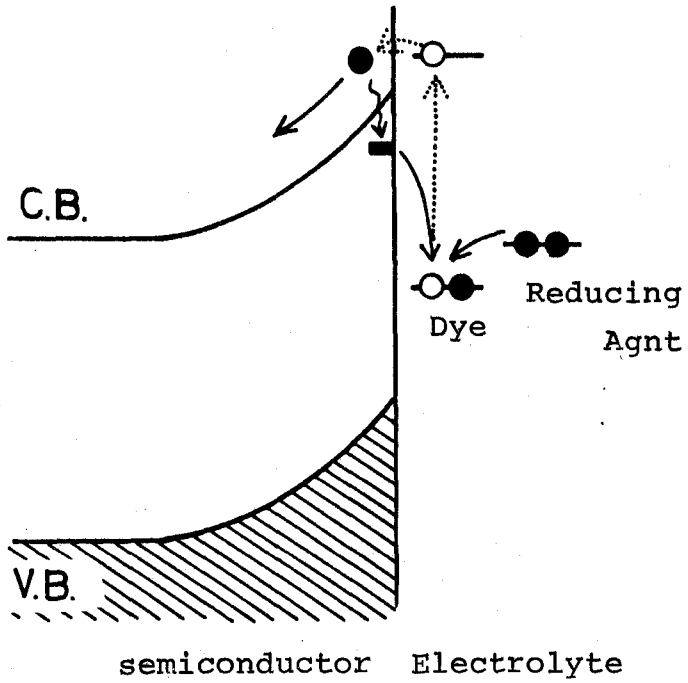

Fig. 7. The energy level diagram explaining the influence of the surface defect and the reducing agent on the dye-sensitized photocurrent.

pair in the space charge layer generated by the grinding. At a higher anodic polarization, the electric field strength near the surface of the electrode increases and the electrons and holes are separated more rapidly, leading to a higher photocurrent.

This mechanism is supported by the measurements of luminescence from ZnO. The luminescence drops sharply at around -0.5 V (vs. SCE) to the more positive region where i_{int} begins to rise (Figs. 2 and 5). This is reasonable since the luminescence is caused by a recombination of the electron-hole pairs. The figures also indicate that non-radiative recombination centers are generated by grinding the electrode, since both the luminescence and i_{int} are weak when the etching time is short, increasing in a similar way with longer etching.

Dye-sensitized Photocurrent.

It is generally admitted that the dye-sensitized photocurrent (i_{dye}) is caused by an electron injection from the excited dye into the conduction band, the electrons being driven inward by the electric field in the space charge layer (Fig. 6b). In the case of i_{dye}, free holes do not exist in the valence band, and, therefore, the recombination process does not take place even though defects are present in the space charge layer. This can explain i_{dye} being less affected than i_{int} by grinding of the electrode.

The effect of grinding on i°_{dye} can be explained by assuming the formation of electron traps near the surface which capture electrons injected from the dye and send them back to the dye. The fact that the photocurrent at sufficiently high anodic polarization became constant by etching for 15 s indicates that the density of the traps is high in the region very close to the surface (Fig. 3).

Sintered ZnO, normally slight yellow, turns deep yellow on grinding. The increase in absorbance of the sinter from 380 to 650 nm thus produced can be measured by diffuse reflectance spectroscopy. This can be removed by ethcing for ca. 15 s, which is comparable to that necessary to make i°_{dye} reach saturation. The increased absorbance seems to be due to the surface defects, which trap the injected electrons.

The Effect of Reducing Agents on i_{dye}.

There are two features of the effect of reducing agents on i_{dye},[4] the increase of i°_{dye} and the prevention of decay of i_{dye}.

Hydroquinone increases i°_{dye} for an electrode etched for less than 15 s, but not for a sufficiently etched electrode (Fig. 3). This can be explained by assuming the presence of surface traps (Fig. 7). Without a reducing agent, a part of the injected electrons are captured by the surface traps, returning to the dyes which have injected these electrons.

Such a backward movement of electrons is prevented by a rapid electron supply from the reducing agent, increasing i°_{dye}.

Some authors pointed out that the effect of reducing agents on i_{dye} is attributable to either an electron transfer from the reducing agent to the dye in excited state or an exciplex formation between the dye and the reducing agent. In the present case, however, the results are explained in terms of the electron transfer from the reducing agents to the photo-oxidized dye. There seems to be no general "super sensitization" effect of the reducing agents.

From the present study, the dye-sensitized photocurrent has been proved to be less sensitive to the defects in the electrode than the intrinsic photocurrent, especially when the solution contains reducing agents. This is one of the advantages of the dye-sensitized photocurrent as regards utilization of imperfect solid specimens for electrochemical photocells.

References

1) J. Higinbotham, and D. Haneman, Surface Sci., 32, 466 (1972).

2) H. Gerischer, J. Electroanal. Chem. Interfac. Electrochem. 58, 236 (1975).

3) G. Heiland, E. Mollwo, and F. Stöckmann, "Solid State

Physics," Academic Press, New York (1959), Vol. 8, p.191.

4) M. Matsumura, Y. Nomura, and H. Tsubomura, Bull. Chem. Soc. Jpn., 50, 2533 (1977).

CHAPTER 5

Chelation Effect of Alizarin Dyes on the Semiconductor-Aqueous Solution Systems

Introduction

As has been described in chapter 1, the dye-sensitized photocurrent is caused by the dye adsorbed on the semiconductor electrode. The dye dissolved in the solution sometimes loweres the photocurrent by absorbing the incident light before it reaches the surface of the electrode. Therefore, it is desirable for an efficient photocell to have the dye only on the surface of the semiconductor electrode. This chapter deals with the photocurrents arising from alizarin dyes chelated to the semiconductor electrodes. Recently, a similar work was reported by Danzmann and Hauffe, mainly on azo dyes and zinc oxide crystal.[1)]

Experimental

Titanium dioxide single crystal disks with the (001) face and zinc oxide sintered disks, both n-type semiconductors, were used. The structure of the electrodes was described in chapters 2 and 3. The surface of the TiO_2 disk

was ground with rough silicon carbide abrasive to make the surface area large. Alizarin, alizarinS, and quinalizarin were used as the photosensitizers. The structural formulas of the dyes are given below:

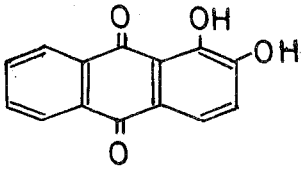

alizarin

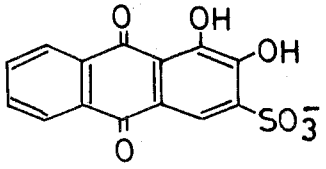

alizarin S

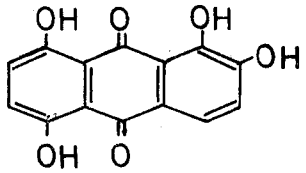

quinalizarin

Aqueous solutions of 0.2 M Na_2SO_4 as the suppporting electrolyte were used. The experimental set-up was the same as described in chapter 2.

Results and Discussion

When TiO_2 powder was added into an aqueous solution of alizarin at the pH of 4.3, the powder colored reddish purple. Figures 1 a) and b) show the absorption spectrum of an aqueous solution of alizarin and that of a potassium bromide disk containing the colored powder, respectively. The absorption spectrum of an ethanol solution of titanium tetrachloride and alizarin nearly coincided with that of the colored TiO_2 powder. It is therefore concluded that the coloration is caused by a chelate compound formed between alizarin and titanium ion at

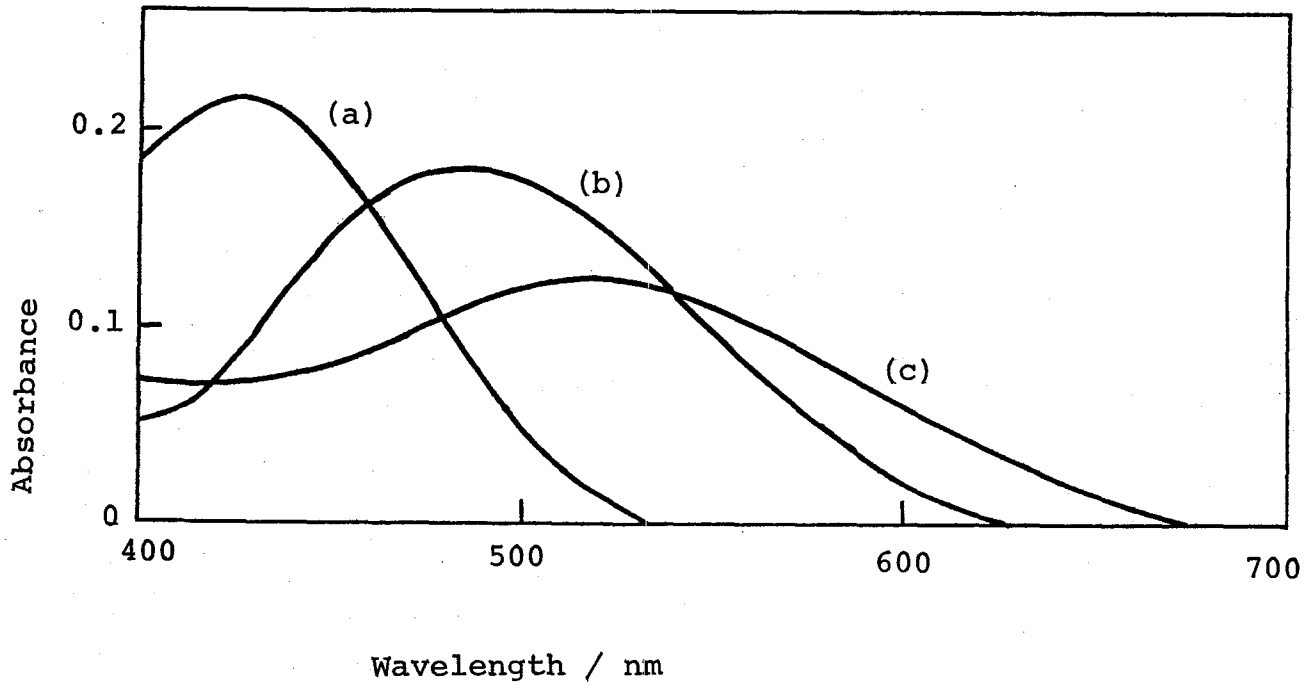

Fig. 1. Absorption spectra of alizarin and the colored powder; (a) a 5.2 x 10^{-6} mol/l aqueous solution of alizarin, pH = 4.3, measured with a 10 cm cell, (b) colored TiO_2 powder in a KBr disk, the absorbance of TiO_2 powder being subtracted, (c) colored ZnO powder in a KBr disk, the absorbance of ZnO powder being subtracted.

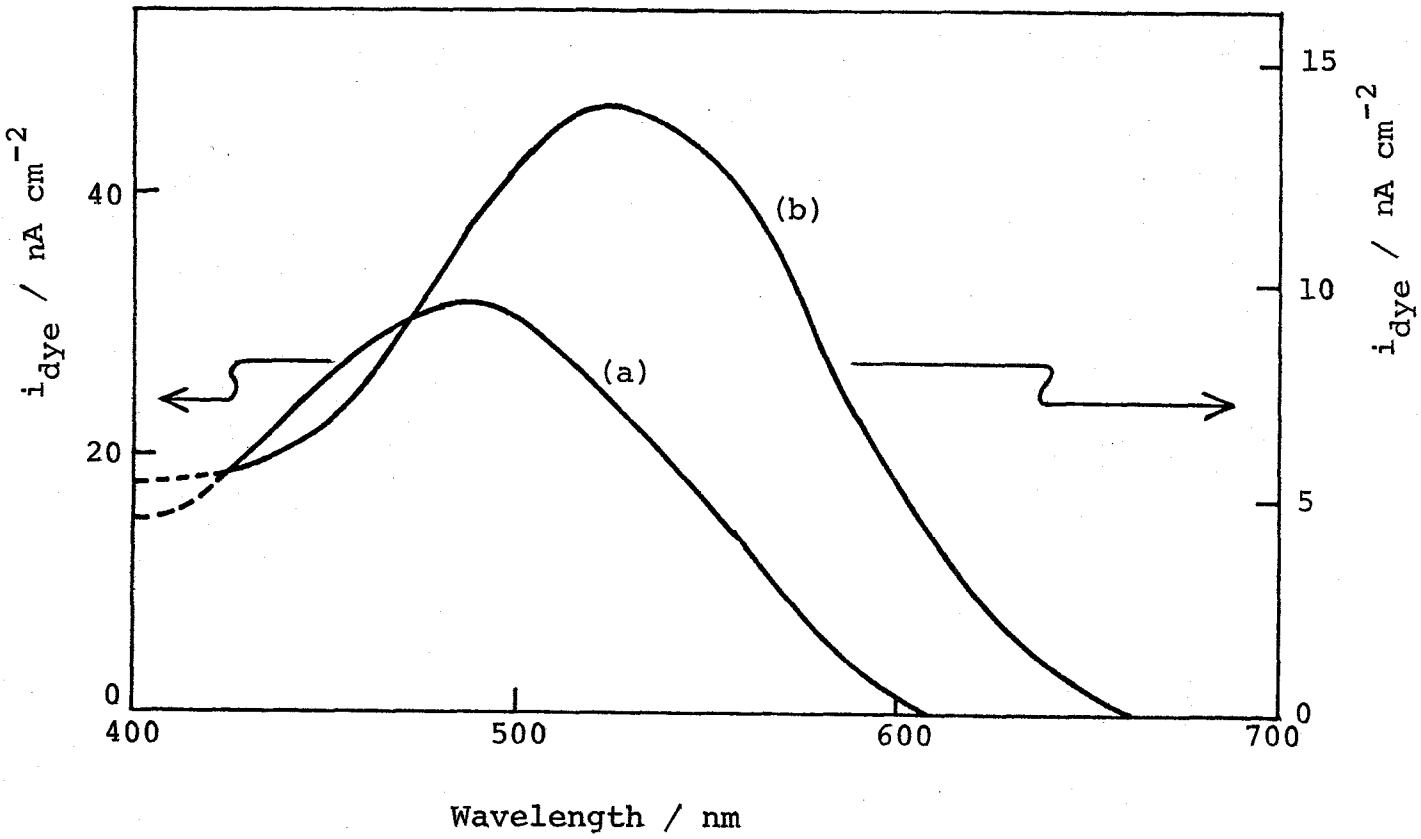

Fig. 2. Photocurrent action spectra in the solution of 5.2×10^{-6} mol/l alizarin at the anodic bias of 0.5 V. The photocurrents are corrected so that they correspond to the values for a uniform light intensity at all wavelengths. (a) For the TiO_2 electrode, with the illumination intensity $I = 1.4 \times 10^{14}$ photons / $cm^2 s$. In these conditions the dark current i_d was 10 nA / cm^2. (b) For the ZnO electrode, $I = 4.6 \times 10^{13}$ photons / $cm^2 s$. i_d = 4 nA / cm^2.

the surface of the TiO_2 powder. The absorption spectrum of the chelate compound on a TiO_2 single crystal was measured through the single crystal, which was similar to that formed on the powder.

When ZnO powder was added into an aqueous alizarin solution, the powder colored purple whose absorption spectrum is shown by Fig. 1 c). This coloration is also considered to be due to the chelate formation at the ZnO surface.

Figure 2 shows the action spectra of the photocurrents for the TiO_2 and ZnO electrodes in the alizarin-electrolyte solution. They were obtained with a weak illumination intensity, so that the photocurrents did not change during the measurements and the wavelengths were scanned at the high speed of 250 nm/min. The intensity of the photocurrent was also confirmed to be proportional to the illumination intensity at several wavelengths. The action spectra nearly agreed with the absorption spectra of the colored powder and not with those of the solutions. Consequently, the photocurrents are concluded to be caused by the sensitization due to the chelate compounds formed on the surface of the electrodes and not by the photochemical reactions of the dye in the solution. When the photocurrents were measured in an electrolyte solution free from the dye by using the electrodes which had been immersed in an alizarin solution for a while and washed with water, their action spectra agreed with those shown

in Fig. 2. In this case, the intensities of the photocurrents were nearly the same as those observed in the alizarin-electrolyte solution systems. This indicates that the chelate compounds formed on the electrode surfaces are insoluble. The intensities of the photocurrent decayed gradually with illumination, the decay being the faster, the higher the illumination intensity. In the case of the TiO_2 electrode the decayed photocurrents recovered to the initial values, when the electrode was kept in the dark solution for a day. This seems to show that electrons are supplied by some means from the solution to the chelate compound.

Photocurrent measurements were also made for alizarin S and quinalizarin which form chelates similar to that of alizarin. The action spectra for alizarin S were confirmed to agree with the absorption spectra of the chelate compounds on the TiO_2 and ZnO powders. For the case of quinalizarin, the photocurrents also seem to be due to the chelate compounds, for their action spectra do not agree with the absorption spectrum of the dye in solution.

Concerning the photo-active species, two structures are considered; one is the alizarin dye directly coordinated to the metal ion which is still in the lattice of the oxide, and the other is the complete chelate compound physically adsorbed on the oxide surface. At present, we cannot decide which of the two models is the correct one. Trial to obtain a stoichio-

metric chelate compound in a pure state failed.

In conclusion, the photocell sensitized by surface chelate has the merit that the illumination of the electrode is not hindered by the dye in the solution phase. Unfortunately, however, the chelating dyes so far studied have the quantum efficiencies less than those of the xanthene dyes. The present results have also shown that the photo-electrochemical measurements provide a highly sensitive means to obtain the electronic spectra of very small quantities of materials on solid-liquid interface.

Reference

1) H. J. Danzmann and K. Hauffe, Ber. Bunsenges. phys. Chem. 79, 438 (1975).

CHAPTER 6

Dye-sensitized ⟨ZnO | aqueous electrolyte | Pt⟩ Photocells.

Introduction

Some of the fundamental properties of the dye-sensitized photocurrents in the semiconductor electrodes have been described in the previous chapters. In this chapter, on the basis of the knowledge thus obtained, the dye-sensitized photocell which consists of a ZnO electrode, a platinum counter electrode, and a solution of a redox couple is investigated. Search for optimal conditions of both the solution and the electrode is necessary for attaining efficient photocells. In section 1, the effect of the contents of the solution, e.g., the redox couple, its concentration, etc., on the performance of the photocell will be described. In section 2, the trials to increase the adsorptive activity for the dye and the electric conductivity of the ZnO electrode by doping and the sintering methodes will be described.

Experimental

The ZnO sinter containing no dopant was prepared by

moulding ZnO or $ZnCO_3$ powder with compression followed by heating at 800 to 1300° C in air. For the preparation of ZnO sinter doped with Al_2O_3 or Li_2O, ZnO powder (99.99 % pure) was kneaded with an aqueous solution of $Al(NO_3)_3 \cdot 9H_2O$ or $LiNO_3$. The slurry thus made was dried with an infrared lamp, ground in agate mortar, calcinated in air at 650° C for 6 hours, ground again in an agate mortar, moulded and sintered.

The structure of the ZnO electrode has been described in chapter 2. The surface area of the electrode was 0.5 to 0.7 cm^2. A platinum plate with a surface area of 2 cm^2 was used as a counter electrode. The solutions were bubbled with high purity nitrogen gas during the measurements. Unless otherwise mentioned, the electrochemical measurements were performed without an external bias between the ZnO and platinum electrodes.

Results and Discussion

1. The Performance of the Dye-sensitized Photocell Having a Redox Couple and a Well-sintered ZnO Electrode.

The well-sintered ZnO electrode containing no dopant adsorbed very small amount of the dye, and gave reproducible photocurrents. Therefore, such electrodes were used to investigate the effect of the solutes on the performance

of the photocell.

The energy diagram for a dye-sensitized photocell with an n-type semiconductor electrode, such as ZnO, is shown in Fig. 1. The electrons injected from the excited dye into the conduction band of the semiconductor electrode move toward the counter (metal) electrode through an external circuit, and transferred into the solution phase. The redox couple in the solution acts as the charge carrier; the reduced form of the redox couple donating electrons to the photo-oxidized dye, and the oxidized form accepting electrons from the counter electrode, and the photocell works continuously.

When the electrodes are connected through an external resistance, R, photovoltage is generated between the electrodes by the illumination of the semiconductor electrode. Since the potential of the counter electrode is fixed at the redox potential of the solution, the photovoltage, U_{ph} (= i_{dye} x R), shifts the potential of the semiconductor electrode, as shown in Fig. 1. The maximum U_{ph} being able to be obtained is limited by the difference between the flat band potential of the semiconductor electrode and the redox potential, U_{redox} - U_{fb}, because the potential of the semiconductor electrode cannot be raised above the flat band potential.

The photocurrent observed for the anodically polarized ZnO electrode immersed in the solution of reducing agents did not decay during the illumination, nor showed overshoot

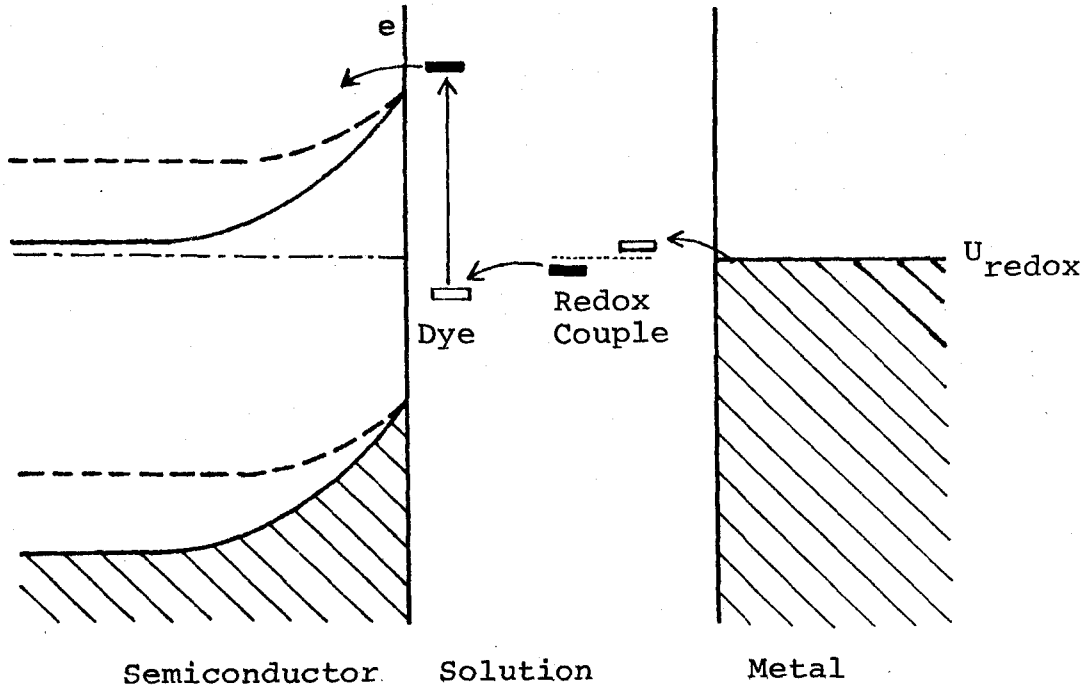

Fig. 1. Energy diagram of a dye-sensitized photocell ⟨n-type semiconductor | dye solution | metal⟩. The electron energy in the bulk of the semiconductor shifts upward as shown by the broken lines when the photocurrent flows through an external load; ▬ , electron donating levels of an excited dye and a redox couple; ▭ , electron accepting levels of an excited (or oxidized) dye and a redox couple.

to the cathodic region when the ilght was turned off (chapter 2). On the other hand, the photocurrent of the photocell $\langle$ ZnO | dye solution | Pt $\rangle$ was found to decay even when the solution contained reducing agents, showing overshoot to the cathodic region when the light was turned off as shown in Fig. 2. The decay and overshoot of the photocell system could be prevented by addition of a redox couple into the solution. In Fig. 2, the results for the addition of the KI / I_2 redox couple is given.

When the concentration of the electron acceptor such as iodine was low, the potential of the counter electrode of the above photocell shifted cathodically by the illumination, approaching the flat band potential of the ZnO electrode (Fig. 3). Therefore, the decrease of the photocurrent in the absence of the redox couple (Fig. 2) is attributable to the disappearance of the potential gradient in the semiconductor. The relatively large photocurrent observed for the first several seconds in the absence of the oxidizing agent is due to the charging current by the capacity at the electrode-electrolyte interface. On the other hand, in the presence of the redox couple at high concentrations, the potential of the counter electrode was practically fixed at the potential of the redox couple, maintaining the potential gradient to produce high photocurrent.

The current-potential characteristics of the platinum

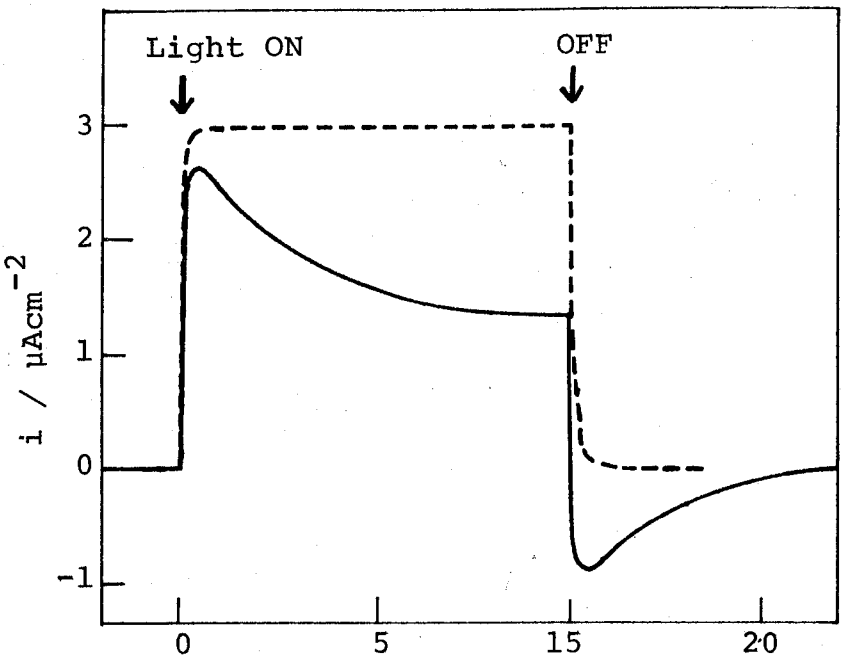

Fig. 2. The change of the short-circuit photocurrent of the dye-sensitized photocell vs. time: rose bengal, 2 x 10^{-6} M; KI, 0.1 M; I_2, 0 M (———) and 10^{-4} M (- - - -).

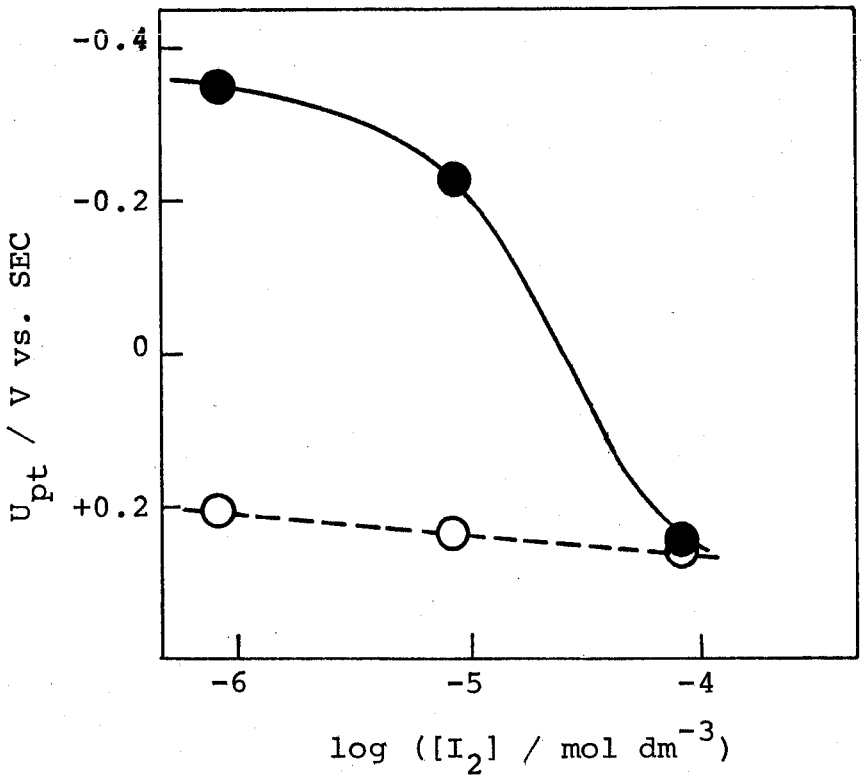

Fig. 3. The potential of the platinum counter electrode of the dye-sensitized photocell: ○, in dark; ●, under illumination; rose bengal, 2 x 10^{-6} M, KI, 0.1 M.

electrode used as a counter electrode in the solutions with and without the KI / I_2 redox couple are shown in Fig. 4.

The photocurrent, i_{dye}, and the photovoltage, U_{ph}, obtained from the photocell changed with the magnitude of the load resistance. The relations between the i_{dye} and U_{ph} after 30 s illumination are plotted in Fig. 5 for the photocells containing rose bengal and the KI / I_2 couple at various concentrations. The open circuit photovoltage observed in the presence of 0.1 M KI and 1×10^{-5} M I_2 was 0.59 V, which was 0.24 V smaller than the value of $U_{redox} - U_{fb}$. This difference is ascribable to the increase of the recombination rate of the electron-hole pair as the electrode potential reaches near the U_{fb} value, and possibly the back electron transfer from the conduction band to the solution phase across the energy barrier at the semiconductor-electrolyte interface.

The power output of the photocell is given by $i_{dye} \times U_{ph}$, and the maximum output obtained in the presence of the KI / I_2 couple is represented by the hatched area in Fig. 5, which corresponds to the energy conversion efficiency of ca. 0.1 %. The efficiency of the photocell increased with the concentration of I_2. This is attributable to the increase of U_{redox} and the fixation of the potential of the counter electrode. When the concentration of I_2 was high (curve d), however, a small decrease of the U_{ph} value was observed. This is probably due to the enhanced

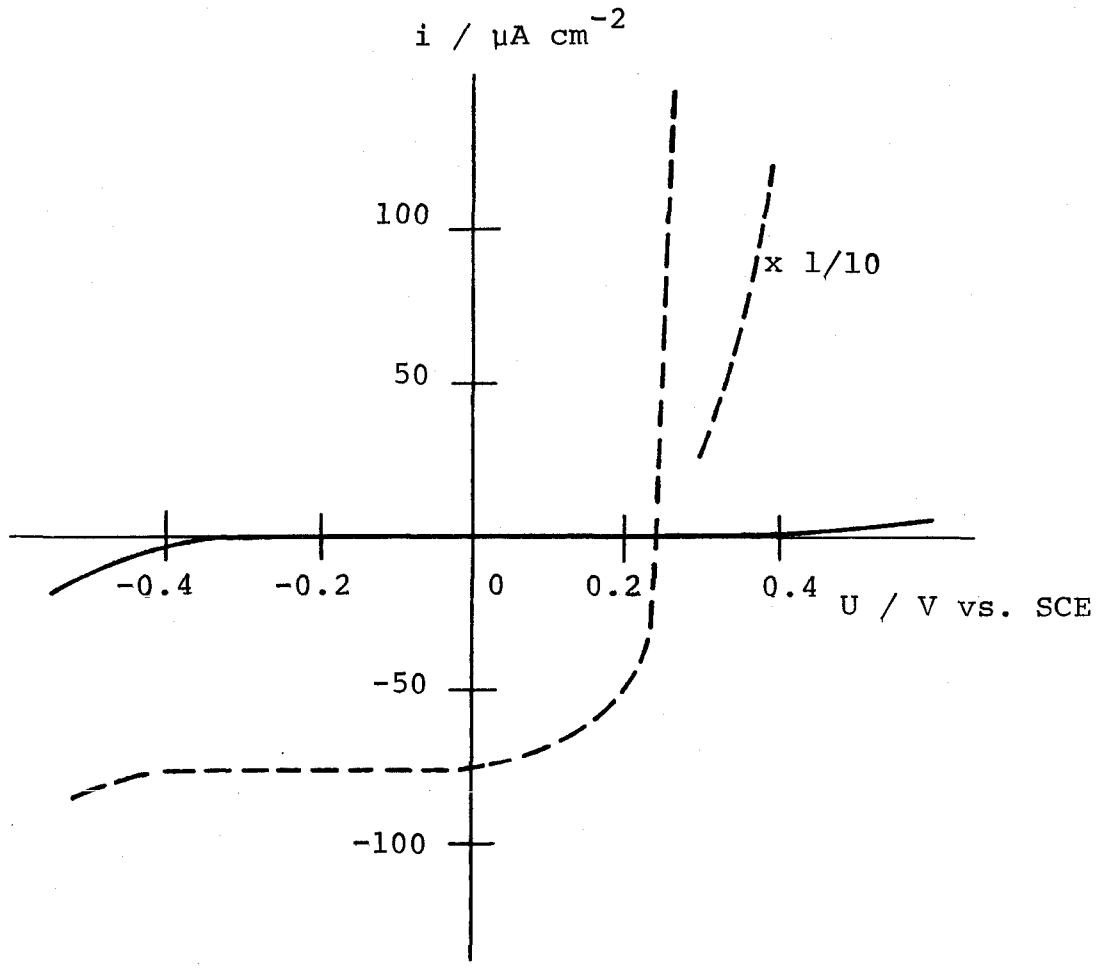

Fig. 4. Current-potential curves of a platinum electrode in aqueous solutions; ———, 0.2 M Na_2SO_4;- - - - , 0.1 M KI + 3 x 10^{-4} M I_2.

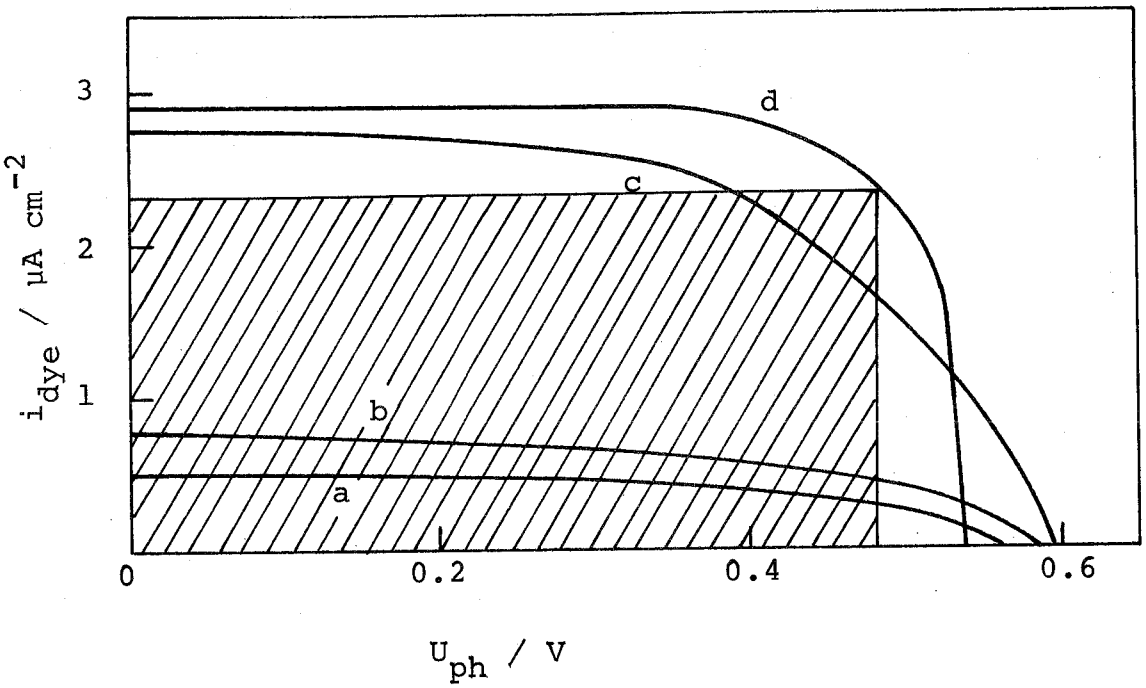

Fig. 5. Photocurrent-photovoltage curves for the photocell ⟨ZnO| rose bengal (3×10^{-5} M) + KI (0.1 M)/I_2 | Pt⟩. $[I_2]$ = 0 M (a), 1×10^{-6} M (b), 1×10^{-5} M (c), 1×10^{-4} M (d).

back electron transfer from the conduction band to the solution, in which iodine acts as the electron acceptor.

The effects of other redox couples were also studied. The results for hydroquinone / p-benzoquinone were similar to those for KI / I_2, with the U_{ph} somewhat smaller than that observed in the latter case. This is probably due to the lower (negative) value of the redox potential of hydroquinone / p-benzoquinone than that of KI / I_2. In the case of $Fe(CN)_6^{3-/4-}$, the i_{dye} was quite low, probably due to the inhibition of the adsorption of the dye by the $Fe(CN)_6^{3-}$ and $Fe(CN)_6^{4-}$ ions (chapter 3). By addition of Fe^{2+} / Fe^{3+} redox couple, a cathodic current was observed in the dark, showing the existence of a chemical reaction between the redox couple and the electrode. Consequently, the KI /I_2 couple was concluded to be most suitable for the ZnO photocell sensitized by rose bengal in the redox couples studied so far.

2. The Porous ZnO Electrodes.

One of the most important factors for achieving a high efficiency of the photocell is to increase the photoabsorption by the dye on the semiconductor electrode. The absorption of light by a dye mono-layer on a flat surface is expected

to be ca. 3 % at maximum. Trials to increase the photocurrent by using semiconductor electrodes coated thickly with various insoluble dyes were unsuccessful, mostly because these dye films formed electrical insulating layers, when they became sufficiently thick to absorb light appreciably. It was then thought that an efficient photocell can be constructed by using porous ZnO sinter as an electrode, because with such an electrode the overall quantity of the dye adsorbed on the surface can be made fairly large, with the thickness of the dye layer on the electrode surface kept rather small.

At the initial stage of our experiments, we tried to make ZnO sinter from ZnO powder obtained from many different sources, and found that the dye-adsorbing capability of the sinter depended largely on the material. The sinter produced from the ZnO powder (Kadox 15), which had been kept in our laboratory for a few years, showed strong adsorptivity for the dye, causing efficient photocurrent.[4] By the electron-microscopic observation, it was found that the strong adsorptivity of the sinter was due to the porous structure of the specimen, which was caused by a small amount of impurities included in the material, e.g., $ZnCO_3$. In order to get a sufficiently porous specimen reproducibly, further investigations have been made. As the result, we have found that the porous sinter could be obtained from any ZnO material by the following methods.

1. Sintering the ZnO powder at low temperatures. The degree of sintering, defined as the ratio of the density of the sinter to that of a single crystal, reaches nearly one for the specimen obtained from pure (99.99 %) ZnO powder by heating at 1300 °C for 1 hour. On the other hand, those for the specimens sintered at lower temperatures decreased with lowering the sintering temperature as shown in Table 1.
2. Sintering the ZnO powder, after washing the powder in dilute hydrochloric acid.
3. Sintering the ZnO powder containing zinc salts being thermally decomposed, such as $ZnCO_3$.
4. Sintering the ZnO powder by adding dopants such as aluminum oxide.[1)]

The scanning electron micrographs of the ZnO sinter made by the different methods are shown in Fig. 6. The porous specimens (b, c, and d) are dyed easily by immersing them into the dye solution, whereas the well-sintered specimen (a) is dyed scarcely by the same method. The reflectance spectrum of the well-sintered specimen and that of a porous sinter after immersing into the dye solution are shown in Fig. 7.

The electric resistivity of the sinter usually increases as the specimen becomes more porous. The relation between the electric resistivity of the sinter and the degree of the

Table 1. The degree of sintering of the ZnO specimens sintered at various temperatures for 1 or 5 hours.

Dopant	Temperature (°C)	Period (hour)	Degree of Sintering (%)
Free	700	1	69
	900	1	94
	1050	1	96
	1300	1	98
Al_2O_3, 0.5 mol%	1000	5	56
	1200	5	75
	1300	5	77
Al_2O_3, 2.0 mol%	1000	5	50
	1200	5	59
	1300	5	65
Li_2O, 1.0 mol%	700	5	92

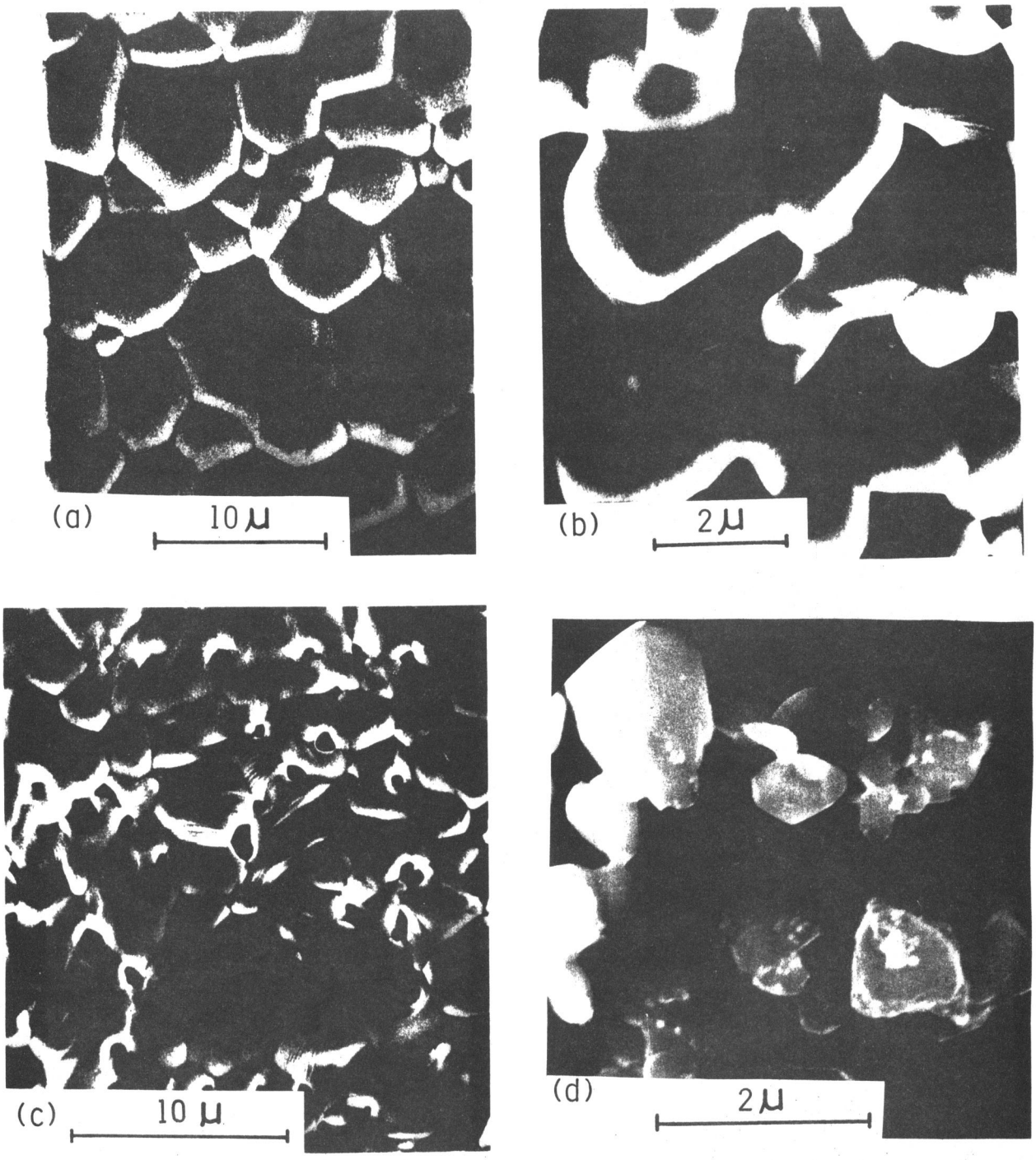

Fig. 6. Scanning electron micrographs of the ZnO sinter obtained by sintering various ZnO powder materials at 1300 °C for 1 hour: (a) pure ZnO, (b) ZnO powder washed with 2 N HCl for ca. 1 min., (c) ZnO powder containing $ZnCO_3$ (25 % by weight), (d) ZnO doped with 0.5 mol% Al_2O_3.

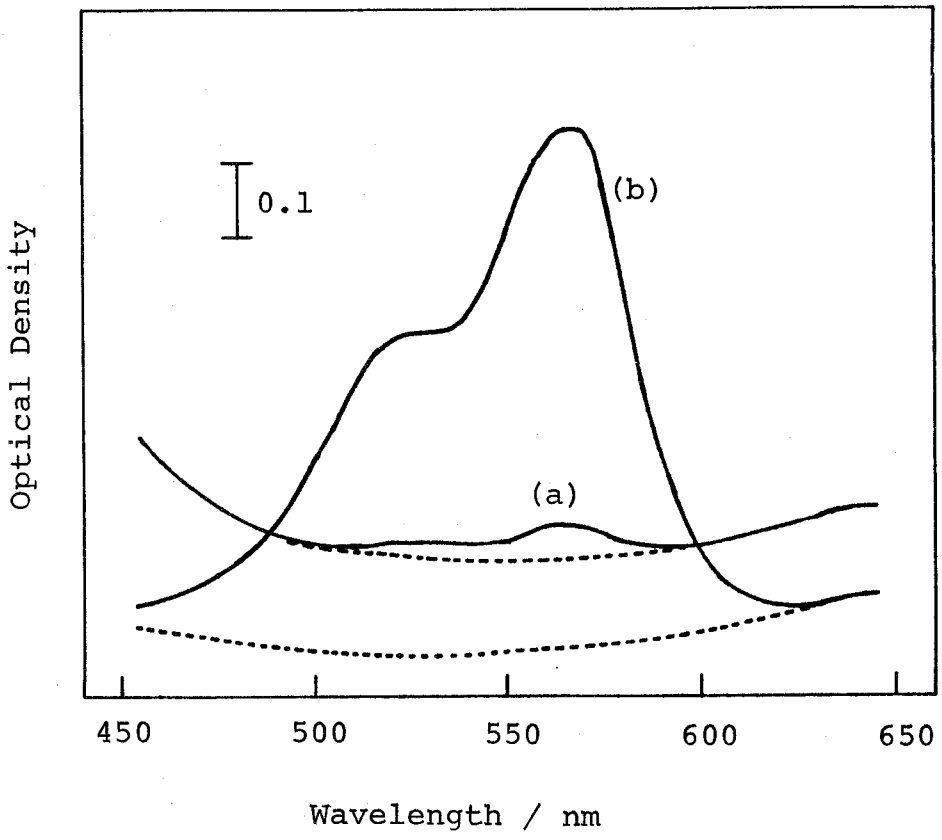

Fig. 7. Diffuse reflectance spectra of ZnO sinter after immersing in an aqueous solution of rose bengal (1×10^{-4} M), the residual solution on the sinter being soaked with filter paper: (a) well-sintered ZnO (degree of sintering 98 %); (b) porous ZnO (degree of sintering 70 %).

sintering is shown in Fig. 8. The specimens of various sintering degrees were obtained by sintering at different temperatures and for different periods. As can be seen from Fig. 8, the aluminum doped (Al-doped) sinter shows electric resistivity 2 to 3 orders lower than that of undoped ZnO sinter, whereas the lithium doped (Li-doped) sinter shows a higher resistivity. These results are qualitatively explained by the principle of controlled valency.[2] The density of the free electrons in ZnO is determined by the equilibria and the doping processes as,

$$Zn^{2+}_{(Zn)} + O^{2-}_{(O)} \rightleftharpoons Zn_{(i)} + 1/2\ O_2 \quad (1)$$

$$Zn_{(i)} \rightleftharpoons Zn^{+}_{(i)} + e \quad (2)$$

$$Zn^{+}_{(i)} \rightleftharpoons Zn^{2+}_{(i)} + e \quad (3)$$

$$Al_2O_3 \longrightarrow 2\ Al^{3+}_{(Zn)} + 2\ O^{2-}_{(O)} + 1/2\ O_2 + 2\ e \quad (4)$$

$$Li_2O + 1/2\ O_2 + 2\ e \longrightarrow 2\ Li^{+}_{(Zn)} + 2\ O^{2-}_{(O)} \quad (5)$$

where the subscripts, i, Zn, and O represent the interstitial, zinc, and oxygen positions in the crystal, respectively. The resistivity of the porous sinter is mostly determined by the high resistivity at the grain boundary in the sinter. The decrease in the resistivity of the Al-doped ZnO may be ascribable to a decrease of the depth of space charge layer, due to the generation of the high density donor states. On the other hand, the high resistivity of the Li-doped ZnO sinter is attributable to the decrease of the

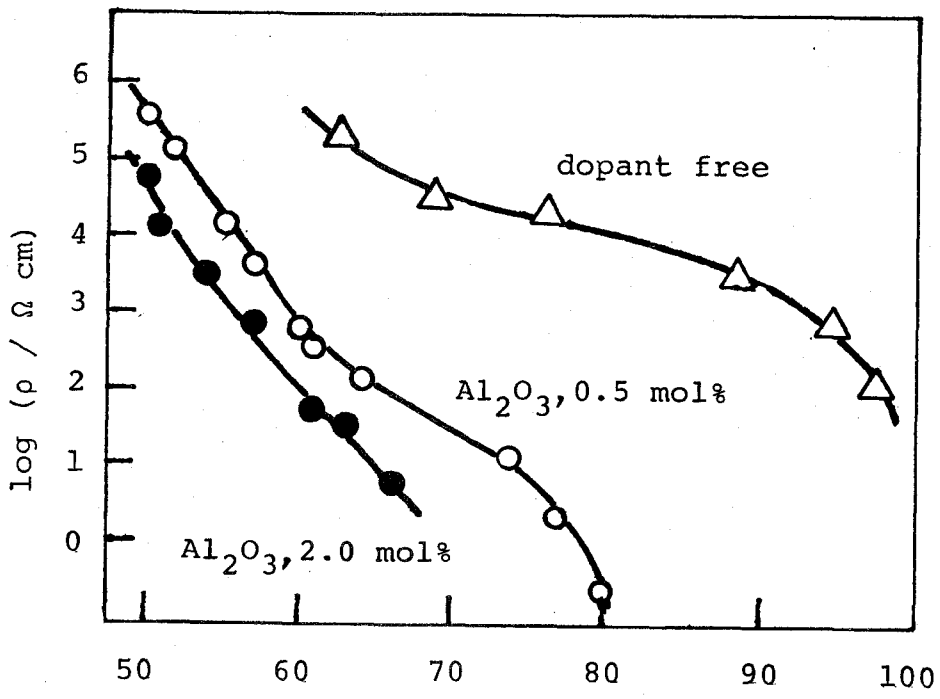

Fig. 8. Resistivity of the ZnO sinter against the degree of sintering; △ dopant free, ○ doped with 0.5 mol% Al_2O_3, ● doped with 2.0 mol% Al_2O_3.

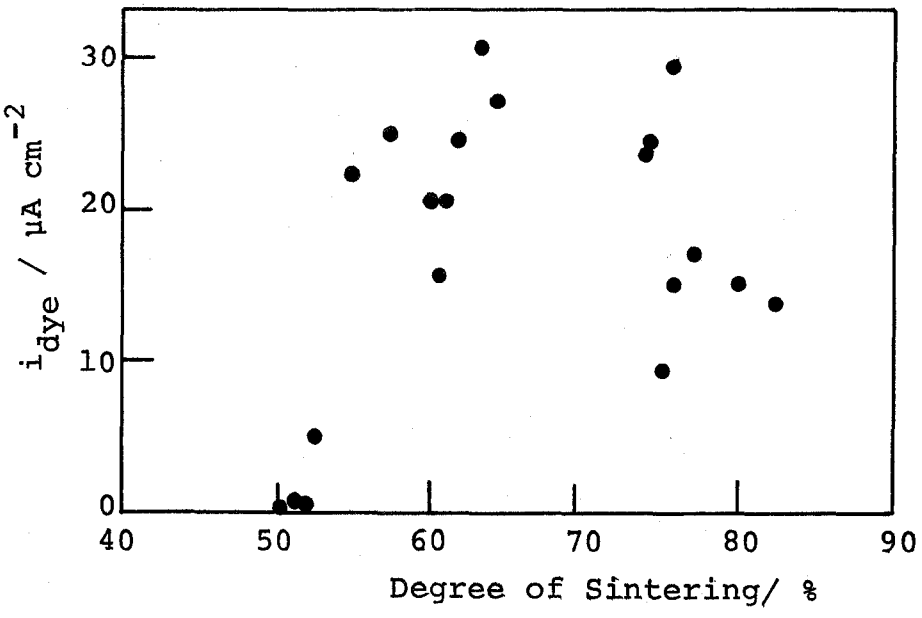

Fig. 9. Dye-sensitized photocurrent against the degree of sintering of the ZnO electrodes doped with 0.5 mol% Al_2O_3.

donor density as shown by Eq. 5, the effect being opposite to that of the Al-doped sinter.

The change of the sintering degree by the dopants can also be understood on the basis of Eqs. 1 - 5, since the velocity of the sintering of ZnO is controlled by the diffusion of the interstitial zinc ion.[3] The addition of the aluminum ion in ZnO shifts the Eqs. 2 and 3 to left hand sides, leading to a low sintering degree. The effect of the lithium ion is opposite to that of the aluminum ion (Eq. 5).

The photocurrent sensitized by rose bengal is plotted in Fig. 9 against the sintering degree of the ZnO sinter doped with 0.5 mol % Al_2O_3. The photocurrent shows a maximum at the sintering degree of 65 - 75 %. The decrease of the photocurrent at the lower sintering degree is attributable to a high inner resistance of the electrode, while that at the higher sintering degree is attributed to a decrease of the amount of the adsorbed dye on the electrode.

By doping Al_2O_3 at a concentration higher than 2 mol %, the dye-sensitized photocurrent became smaller. In this case, the photocurrent caused by the larger-than-band-gap illumination of ZnO also decreased.

Finally, the energy conversion efficiency, ϕ, and the apparent quantum efficiency of the photocurrent, η_{app}, the latter being defined as the number of flowing electrons divided by the number of incident photons, for the dye-sensitized

photocells provided with undoped or Al-doped porous ZnO electrodes will be discussed.

In the case of the photocells with undoped porous ZnO[4] electrodes prepared by the afore-mentioned several methods, the ϕ and η_{app} values attained for monochromatic light (λ 562 nm) were 1.0 to 1.5 % and 15 to 20 % at maxima, respectively, with little difference by the preparation methods of the sinter. On the other hand, the ϕ and η_{app} values for the photocells with the Al-doped ZnO electrode reached to 2.5 % and 22 %, respectively, using 0.1 M KI and 10^{-3} M I_2 as a redox couple. These values are considerably higher than the best results obtained from the undoped ZnO electrodes, due probably to the higher electric conductivity of the Al-doped ZnO electrodes (Fig. 8).

The above results were obtained under weak illumination of the order of 1 mW cm^{-2}. The difference in the ϕ and η_{app} values between undoped and Al-doped ZnO electrodes will become greater in a case of strong illumination, e.g., under ordinary solar radiance, since the ohmic loss in the electrode increases with the current density. The energy conversion efficiency under the solar radiance is estimated to be ca. 1 %, for a photocell containing an Al-doped ZnO electrode, from the degree of the overlap of the action spectrum of the photocurrent and the solar spectrum (Fig. 10). Further improvement of the photocell can be expected by the choice of semiconductor

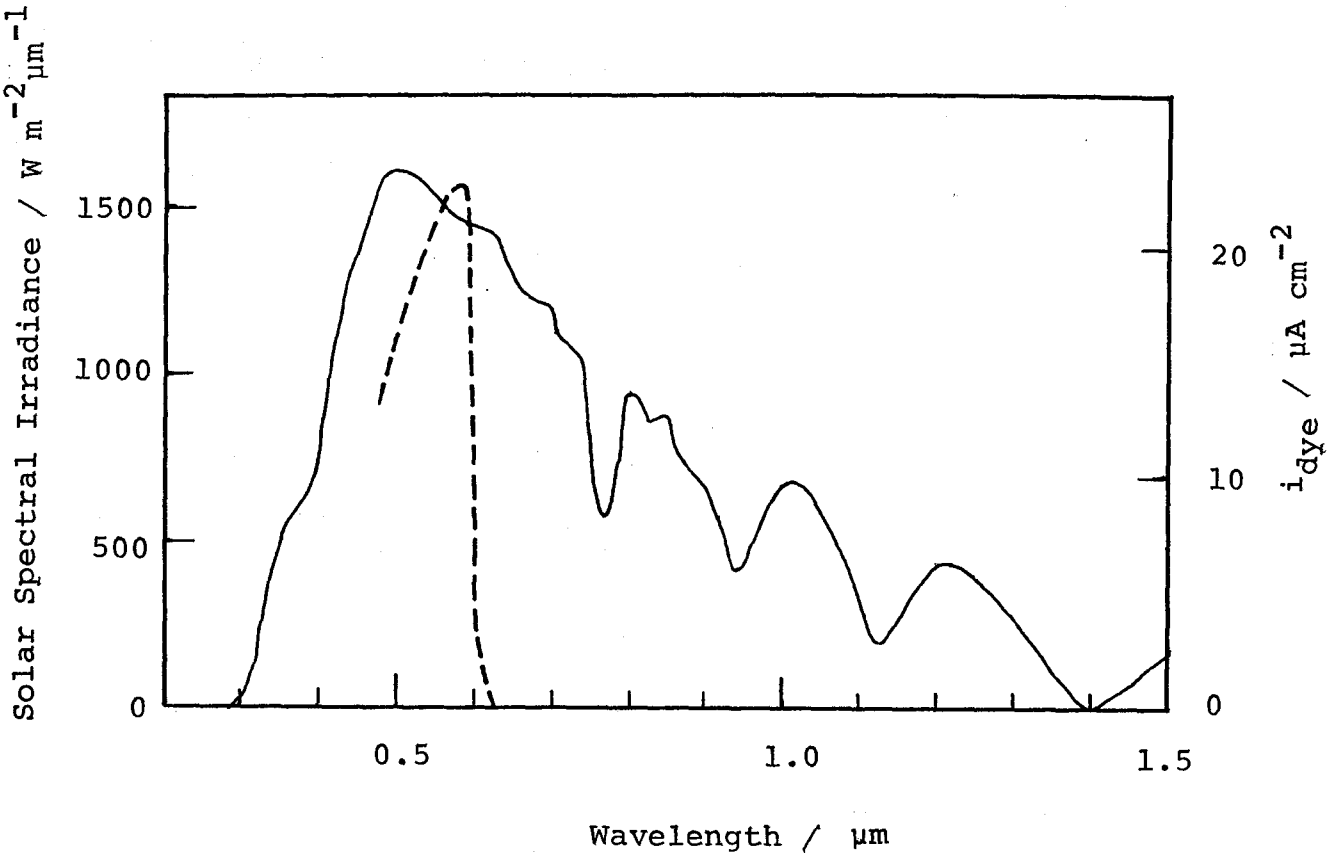

Fig. 10. The action spectrum of the photocurrent sensitized by rose bengal at the porous ZnO electrode (----), and the AM 1 solar spectrum (——). The solar energy in the wavelength region above 1.5 μm is less than 10 % of the total.

electrodes, redox couples, and sensitizing dyes.

References

1). M. Takata, D. Tsubone, and H. Yanagida, J Am. Ceramic Soc., 59, 4 (1976).

2). W. Komatsu, M. Miyamoto, S. Hujita, and Y. Moriyoshi, Yogyo-Kyokai-Shi (J. Ceramic Soc. Jpn.), 76, 407 (1968).

3). K. Hauffe and A. L. Vierk, Z. phys. Chem., 196, 160 (1950).

4). H. Tsubomura, M. Matsumura, Y. Nomura, and T. Amamiya, Nature, 261, 402 (1976).

Conclusion

Fundamental features and mechanism of the dye-sensitization of semiconductor photoelectrodes have been investigated. From the results, it has been found that the dye-sensitized photocell has the advantages as a solar energy converter: (1) the dye-sensitized photocurrent is insensitive to impurities included in the semiconductor, (2) the photo-dissolution of the semiconductor electrodes is trivial in the case of dye-sensitized photocurrent.

The highest energy conversion efficiency for the solar irradiance obtained with our photocells reached ca. 1 %, which is about one-tenth that of the solid-state solar cells, and nearly equal to that attained photosynthetically by cane or sugar beet. The efficiency of the dye-sensitized photocell is expected to increase further, possibly to the degree of the solid-state solar cells in future, by search for the optimal conditions for the method of preparation of the semiconductor electrodes, and the choice of the dyes, redox cuples, and semiconductors.

Acknowledgments

I would like to express my sincerest gratitude to Professor H. Tsubomura for the continuing encouragement and suggestion throughout this work. My thanks are also due to Dr. N. Yamamoto and Dr. Y. Nakato for valuable discussions.

I am grateful to Professor H. Yanagida (The University of Tokyo) and Dr. M. Takata (The Technological University of Nagaoka) for their help in preparing the aluminum-doped and lithium-doped ZnO sinter.

I wish to thank the former and present students of our laboratory for their active collaboration. Especially, thanks are due to Dr. K. Nakatani (chapter 1), Mr. K. Yamamoto (chapter 1), Mr. S. Matsudaira (chapter 3), Mr. K. Mitsuda, (chapter 3), Mr. Y. Nomura (chapter 4), and Mr. T. Amamiya (chapter 6). Thanks are also due to Miss M. Mizushima for typing the manuscript.

List of Published Papers

1) "Thermoluminescence from the UV-Irradiated Solution of Triphenylmethane at Low Temperature"
N. Yamamoto, M. Matsumura, and H. Tsubomura.
Bull. Chem. Soc. Jpn., 46, 2307 (1973).

2) "The Photovoltaic Effect in Naphthacene-Gold Layers"
M. Matsumura, H. Uohashi, M. Furusawa, N. Yamamoto, and H. Tsubomura.
Bull. Chem. Soc. Jpn., 48, 1965 (1975).

3) "Dye Sensitized Photocurrent in Aqueous Electrochemical Systems with the ZnO Sintered Electrode"
M. Matsumura, K. Yamamoto, and H. Tsubomura.
Nippon Kagaku Kaishi (J. Chem. Soc. Jpn.), 1976, 399.

4) "Chelation Effect of Alizarin Dyes on the Semiconductor-Aqueous Solution Systems"
M. Matsumura, Y. Nomura, and H. Tsubomura.
Bull. Chem. Soc. Jpn., 49, 1409 (1976).

5) "Dye Sensitized Zinc Oxide : Aqueous Electrolyte : Platinum Photocell"
H. Tsubomura, M. Matsumura, Y. Nomura, and T. Amamiya.

Nature, 261, 402 (1976).

6) "Dye-sensitization on the Photocurrent at Zinc Oxide Electrode in Aqueous Electrolyte Solution"
M. Matsumura, Y. Nomura, H. Tsubomura.
Bull. Chem. Soc. Jpn., 50, 2533 (1977).

7) "Wet-type Solar Cells with Semiconductor Electrodes"
H. Tsubomura, M. Matsumura, K. Nakatani, K. Yamamoto, and K. Maeda.
Solar Energy, 21, 93 (1978).

8) "Effect of Etching on Intrinsic and Dye-sensitized Photocurrents in Zinc Oxide Electrodes"
M. Matsumura, Y. Nomura, and H. Tsubomura.
Bull. Chem. Soc. Jpn., 52, 1599 (1979).

9) "Sintered ZnO Electrode for Dye-sensitized Photocell"
M. Matsumura, S. Matsudaira, H. Tsubomura, M. Takata, and H. Yanagida.
Yogyo-Kyokai-Shi (J. Ceramics Soc. Jpn.), 87, 169 (1979).